UNIVERSIDADE DE LISBOA

Faculdade de Medicina

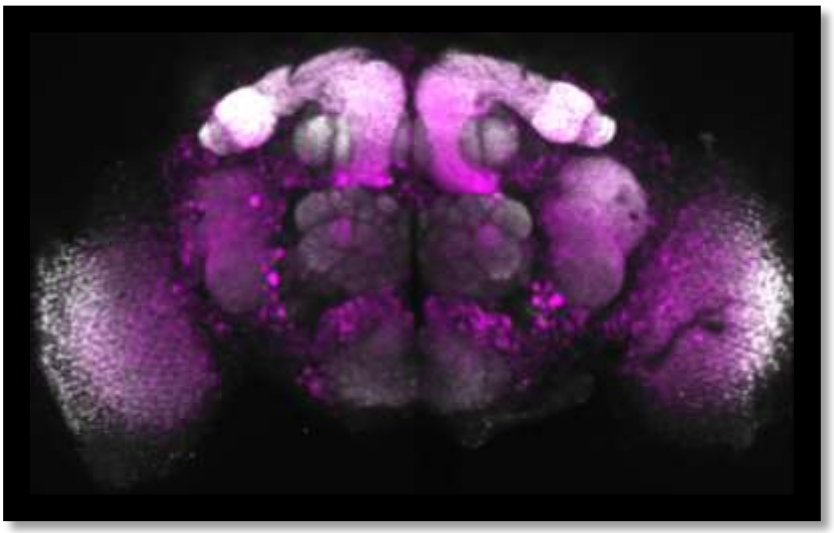

pERK as a neuronal activity marker in *Drosophila melanogaster*

Sofia Alexandra Goulão da Silva

Supervisor: Marta Moita, *PhD*
Behavioural Neuroscience Lab - Champalimaud Foundation
Co-Supervisor: Domingos Henrique, *PhD*
Stem Cells & Neurogenesis – IMM

Dissertação especialmente elaborada para obtenção do grau de Mestre em Neurociências

2020

UNIVERSIDADE DE LISBOA

Faculdade de Medicina

pERK as a neuronal activity marker in *Drosophila melanogaster*

Sofia Alexandra Goulão da Silva

Supervisor: Marta Moita, *PhD*
Behavioural Neuroscience Lab - Champalimaud Foundation
Co-Supervisor: Domingos Henrique, *PhD*
Stem Cells & Neurogenesis – IMM

Dissertação especialmente elaborada para obtenção do grau de Mestre em Neurociências

2020

“A impressão desta dissertação foi aprovada pelo Conselho Científico da Faculdade de Medicina de Lisboa em reunião de 30 de junho de 2020.”

Agradecimentos

Gostaria de agradecer primeiramente à Fundação Champalimaud, um instituto inigualável que me acolheu enquanto profissional, e ao Moita *Lab* - Anna Hobbiss (toda a ajuda, apoio, discussões imprescindíveis e gratificantes), Andreia Cruz, Anh Nguyen, Catarina Mendes (a força e apoio indescritíveis), Clara Ferreira (a motivação e ajuda), Marta Moita, Matheus Farias (todo o apoio logístico, tecnológico e impressionante conhecimento partilhado), Mirjam Heinemans, Natalia Barrios, Ricardo Silva (toda a ajuda, apoio, revisão, correcção, força e motivação transcendentais) Ricardo Zacarias, Rui Gonçalves (todo o apoio e força, bem como a alegria e amizade que me mantiveram positiva e sã) e Violetta La Franca - construído por pessoas extraordinárias e cientistas exímios, que me acolheram e apoiaram durante este processo de aprendizagem e desenvolvimento científico e pessoal.

À Marta Moita, a minha orientadora principal, por me ter permitido integrar neste grupo e explorar um projecto quase protótipo e pioneiro no *lab*. Agradeço o apoio, as discussões construtivas e os conhecimentos partilhados, que certamente me permitirão traçar as minhas passadas futuras. Obrigada pelo vislumbre científico e despertar de espírito crítico. Agradeço ainda pela revisão e correcção do presente manuscrito. Obrigada pela oportunidade, pelo desafio e pela experiência vivida.

À Isabel Campos, a minha chefe e também uma verdadeira mentora, por todas as discussões frutíferas, partilhas de informação, linhas de pensamento e observações construtivas. Agradeço profundamente, e em primeiro lugar, por me ter permitido frequentar o mestrado sem reservas, depositando confiança na minha capacidade de gerir os desafios profissionais e a exigência curricular. Agradeço todo o apoio neste período mais áspero, mas igualmente positivo, evolutivo e desafiante. Obrigada pela atenção e disponibilidade, bem como pela compreensão, pelos gestos de confiança e segurança. Obrigada por me fazer sentir capaz de conquistar os objectivos, com trabalho e perseverança. É um privilégio fazer parte da sua equipa.

À Luísa Vasconcelos, Investigadora Principal na Fundação, por todo o conhecimento partilhado e ajuda na interpretação dos dados. Agradeço igualmente à Cristina e Eliane, membros do Vasconcelos *Lab*, pelo apoio e força sempre presentes durante este processo.

À Catarina Pereira, *Postdoctoral Researcher* no Moreno *Lab* e grande amiga, por todos os conselhos preciosos, discussões construtivas e dinâmicas, ajuda, apoio e força durante este período. Todos os conhecimentos e sugestões foram fulcrais para o planeamento e elaboração deste projecto. Obrigada pela coragem e confiança que me deste. Agradeço igualmente à Dina Coelho, *Postdoctoral Researcher* no Moreno *Lab*, pela ajuda e apoio na análise dos resultados. Obrigada pelos esclarecimentos e conselhos valiosos, que me permitiram evoluir e analisar condignamente os dados recolhidos. Deixo ainda um especial agradecimento aos colegas e

amigos Joana Couceiro e Pedro Durão, também membros do Moreno *Lab*, pelo apoio e ajuda durante este projecto. A Joana foi simplesmente incansável, destemida e uma verdadeira heroína durante este processo. À Carolina Rodrigues, a pessoa mais forte e corajosa que conheço, que nunca me deixou ficar para trás. Obrigada por me manterem sã e apaziguarem os meus estados de ansiedade mais difíceis.

Uma palavra de agradecimento à Célia, à Patrícia Francisco, à Rita Figueiredo e ao Ibo, membros do Ribeiro *Lab*, pelo apoio, ajuda e troca de ideias positivas e relevantes. Agradeço ainda à Ece Sönmez (Chiappe *Lab*) pelo apoio e força incondicional durante todo este desafio.

À Christa Rhiner, Investigadora Principal na Fundação, pela partilha de informação e ajuda no início deste projecto. Agradeço igualmente à Ruth Corral, *Research Associate*, pelo apoio, partilha de informação e reagentes no início deste projecto, permitindo a execução das primeiras experiências e abordagens.

A toda a equipa da *Fly Platform* – Ana Reis, Catarina Craveiro, Carina Monteiro, Isabel Campos, Liliana Costa, Patrícia Valentim e Zichiena Zovo – por tudo aquilo que são enquanto colegas, amigas e seres humanos. Quero deixar um especial agradecimento à Liliana Costa, por ser uma mulher naturalmente iluminada, radiante, positiva e uma força da natureza. Obrigada pelo teu apoio e ajuda, que na verdade são impagáveis e indescritíveis. Agradeço-vos a todas pelo apoio incondicional, pela força sobre-humana, pelo incentivo diário e incansável, pela coragem inesgotável (sim, eu sei que não sou fácil de lidar sob pressão) e sobretudo pela vossa paciência durante este período mais conturbado. Trabalhar convosco é um privilégio gigantesco e agradeço-vos muito por me fazerem sentir tão completa. São parte integrante da minha família.

A toda a equipa da ABBE *Platform* – Anna Pezarossa, Davide Accardi e Leonor Morgado – pelo apoio, ajuda e incentivo no processamento das imagens e dados a incluir neste projecto. Agradeço particularmente à Anna, pelas discussões produtivas, sugestões fundamentais e conhecimentos do programa Fiji, bem como a ajuda na manipulação do sistema do microscópio confocal. Obrigada pelo tempo tão apreciado e essencial, para que a análise dos resultados fosse possível.

À Sandra Crisóstomo, uma amiga já de sempre, pelo apoio sobre-humano e absoluto em todas as fases difíceis e pesadas, estridentes e felizes, ao longo desta jornada. Obrigada pelos conselhos sábios, pelo positivismo a cada passo, por nunca me deixares desistir e principalmente por este laço de amizade tão forte e bonito que construímos. Já és de sempre e para sempre.

A todos os meus colegas de mestrado, em particular ao Daniel Correia, ao João Santos e à Renata Cruz, pela força incondicional e indescritível neste caminho tão longo, nem sempre fácil e directo. Vocês foram uma fonte de luz e bem-estar, nunca me deixaram desistir e sempre

apoiaram cada pequena conquista. Obrigada pelos momentos fulcrais de boa disposição, à vontade e descontracção. Vocês são pessoas incríveis.

Aos meus amigos mais próximos, não pela distância, mas sim pela ligação – ao Bruno Brito e respectiva família (grandes impulsionadores deste caminho, amigos queridos, e uma segunda família para mim), à Ana Vicente (uma amiga extraordinária, forte e insubstituível), ao Gérard Siegel (um verdadeiro amigo, que sempre acreditou em mim e nas minhas capacidades), à Aurélia e ao Jorge (amigos queridos, que sempre me deram força e que são uma família presente em mim) e à Rita Pereira (uma amiga maravilhosa e confidente, que acreditou em cada passo cambaleado). A Rita marcou a diferença pelas palavras positivas, pelo carinho, por me deixar gritar a plenos pulmões, mas também por recolher a insegurança. É linda, no verdadeiro sentido da palavra.

Agradeço igualmente à Teresa Gomes (uma mulher poderosa, que apoiou cada passo) e à Liliana Vieira, amiga e companheira de casa, que suportou com bravura os altos e baixos deste processo e incentivou diariamente para a subida de cada degrau. Obrigada por apoiares os meus devaneios. Obrigada pelas refeições partilhadas, pelos risos tão apreciados, por não me deixares enlouquecer sozinha e pelo pouco que enlouquecemos juntas. Obrigada pela ajuda e amizade, pois não há de facto como agradecer pela família que adquirimos ao longo da vida.

Aos meus amigos de sempre, residentes na minha saudosa cidade de Évora e espalhados pelo mundo, pelo carinho e apoio nos dias mais cinzentos e pelo humor peculiar que se aviva pelo convívio. Obrigada pela motivação e força, pois são factores impagáveis em qualquer trajecto que assumamos. Ao Adrian, pela pessoa especial e importante que é, pelo apoio transcendente e motivação diária. Obrigada por acreditares em mim, por não duvidares da minha força e contribuíres incansavelmente para o sucesso deste projecto.

À Marcia Matos e à partilha do yoga, cuja prática me permitiu alcançar a calma, a coragem e o foco exigidos neste processo. Agradeço profundamente à Marcia, pelo carinho e amizade, por me fazer acreditar em mim, nas minhas capacidades e força interior. O yoga passou a ser uma parte integrante em mim, e mais do que um estado, já se tornou uma forma de ser. Esse conhecimento e partilha são inesgotáveis e inestimáveis. Obrigada por tudo isso e pelo resto, que num riso se resume.

À minha família maravilhosa, aos meus pais, à minha irmã e aos meus sobrinhos, que simplesmente não consigo descrever por palavras o verdadeiro agradecimento e admiração que lhes tenho. Os meus pais são responsáveis pela vida e iluminação que trago comigo, são indescritíveis e sagrados em toda a sua complexidade. Obrigada por me ajudarem a crescer, pela orientação e apoio, pela educação, valores e formação pessoais. Obrigada por me apoiarem sempre, em tudo. É inestimável o vosso papel na minha vida. A minha irmã é a minha melhor parte, a verdadeira alma gémea, se nisso acreditarmos. A melhor amiga, a melhor pessoa, o melhor ser humano. Devo-lhe a sanidade mental, a alegria, a força e motivação inesgotáveis. Os

meus sobrinhos são parte dela, e portanto, parte nossa. Por vocês não há caminho que seja difícil. Agradeço igualmente ao Nuno, por ser o verdadeiro pai dos meus sobrinhos. Obrigada a vocês, pela vossa pura existência.

Resumo

Um dos principais desafios para os neurocientistas é compreender de que forma o cérebro dá origem a comportamentos observáveis, sendo fulcral mapear a actividade neuronal em circuitos conhecidos e bem definidos. Devido à simplicidade e rastreabilidade genética da mosca da fruta, os neurónios e respectivos circuitos são identificáveis entre animais, com um amplo conjunto de linhas transgénicas disponíveis para regular a actividade neuronal. Todavia, apesar de existir um *kit* experimental bastante sofisticado, os investigadores que utilizam a *Drosophila melanogaster* como modelo animal, não têm à sua disposição um bom marcador endógeno de actividade neuronal. Actualmente existem algumas técnicas para medir a actividade dos neurónios (e.g. electrofisiologia e influxo de cálcio), mas relativamente aos organismos invertebrados, as ferramentas disponíveis são escassas e com limitações muito concretas no estudo de comportamentos inatos e não confinados. É fundamental desenvolver uma ferramenta que nos permita aceder e monitorizar a actividade neuronal, a título rigoroso e preciso, em animais que se movem livremente e com uma expressão robusta e identificável no cérebro da mosca.

Neste projecto, testámos a detecção imuno-histoquímica da proteína ERK (*Extracellular signal-Regulated Kinase)* fosforilada, pERK - uma molécula-chave para a regulação dos eventos de plasticidade sináptica - como marcador de actividade neuronal no cérebro da *Drosophila*. A actividade dinâmica de ERK tem sido utilizada em diversos estudos com mamíferos e outros vertebrados (e.g. peixe-zebra), e foi comprovada a sua eficácia na marcação de neurónios activos, aquando da presença de um estímulo externo.

No nosso paradigma, as moscas experimentais foram expostas durante 1 minuto a um odor atractivo, o farnesol, um composto presente em citrinos. As moscas do grupo controlo foram expostas durante 1 minuto a água destilada. 20 minutos após a exposição ao estímulo e controlo, os cérebros das moscas foram dissecados e rapidamente fixados. Em seguida, procedemos a uma avaliação qualitativa e imparcial de 3 observadores (modelo aplicado a todas experiências realizadas), que atribuíram pontuações para a ausência (0) ou presença (1) da expressão de pERK nos lóbulos das antenas das moscas. Os 3 observadores concluíram que havia uma maior percentagem de cérebros com expressão de pERK na condição experimental (88.9%), comparativamente com os cérebros controlo expostos a água destilada (15.1%). Estas primeiras observações sugeriram que o estímulo de farnesol aumenta a expressão de pERK nos lóbulos das antenas, o que suporta a nossa hipótese inicial de utilização de pERK como marcador de actividade neuronal, na sequência de um estímulo. Todavia, as classificações atribuídas pelos investigadores não foram concordantes para cada cérebro transversalmente, nas diferentes condições. Por essa razão, pareceu-nos fundamental uma abordagem alternativa de

quantificação automatizada da fluorescência de pERK, que nos permitisse verificar as observações iniciais.

Criámos então um método de quantificação automatizado, considerando como região de interesse o sinal de pERK obtido nos cérebros experimentais, expostos a farnesol. Foi estabelecido um sistema de coordenadas para aplicarmos a região de interesse, que apresentava expressão de pERK, e duas regiões *background* (adjacentes à região de interesse) aos cérebros das duas condições, garantindo assim a consistência entre todas as amostras analisados. Como resultado desta análise, verificámos níveis significativamente mais elevados de pERK na condição experimental, em comparação com o grupo controlo. Estes resultados encorajaram e motivaram uma investigação mais detalhada da activação neuronal nos lóbulos das antenas, em resposta ao estímulo de farnesol.

Considerámos neste caso que seria importante verificar se esta activação neuronal nos lóbulos das antenas correspondia aos neurónios que expressam os receptores olfactivos 83c no glomérulo DC3, anteriormente identificados como sendo sensíveis ao farnesol. Para tal, recorremos ao sistema binário Gal4-UAS, anteriormente desenvolvido para induzir a expressão de genes, com a devida precisão em células específicas. Cruzámos então machos Or83c-Gal4 com fémeas virgens UAS-CD8::GFP. CD8 é uma proteína transmembranar e, por isso, a superfície dos neurónios Or83c vai estar marcada a verde, devido à fusão desta proteína com a *green fluorescence protein* (GFP). Desta forma, podemos facilmente identificar os neurónios 83c e medir a expressão de pERK em simultâneo. A análise qualitativa dos observadores mostrou um aumento dos níveis de expressão de pERK nos cérebros experimentais, comparativamente aos controlos. Relativamente à quantificação automatizada, a região de interesse e respectivos *backgrounds* foram obtidos com base na anatomia do glomérulo DC3. A análise estatística mostrou uma expressão elevada e significativa de pERK no glomérulo DC3, depois da estimulação com farnesol. Assim, os nossos resultados suportam a hipótese colocada inicialmente, e que sugere o aumento da expressão de pERK nos neurónios Or83c activos, na presença de farnesol.

De acordo com as observações anteriores, considerámos que seria interessante perceber se a inibição ou activação artificial dos neurónios Or83c afectaria os níveis de expressão de pERK no glomérulo DC3. Para investigarmos estas questões, resolvemos silenciar e activar directamente os neurónios Or83c, com recurso a um canal hiperpolarizado de potássio, Kir2.1, e a uma proteína fotossensível constituinte de um canal de catiões, CsChrimson, respectivamente. A expressão de Kir2.1 e de CsChrimson está igualmente acoplada à proteína GFP, o que nos permitiu visualizar os neurónios Or83c e medir a expressão de pERK nestas células, à semelhança da experiência anterior.

No protocolo de inibição dos neurónios 83c, verificámos inicialmente que não havia expressão de pERK nos cérebros controlo, expostos ao farnesol. Com base nos resultados das experiências anteriores seria expectável que os cérebros controlo, que correspondiam às gerações parentais (Or83c-Gal4 e 10xUAS-Kir2.1::eGFP), apresentassem expressão de pERK na presença do estímulo, o que não se verificou. A análise quantitativa revelou ainda resultados não significativos entre os cérebros experimentais e controlos.

Para o protocolo de activação dos neurónios 83c, com recurso à proteína fotossensível CcChrimson, e considerando as possíveis variações da actividade neuronal em resposta à duração e dinâmicas da estimulação luminosa, estabelecemos primeiramente 2 protocolos distintos: luz pulsada (1 min, 2 Hz) e luz contínua (1 min). Foi ainda testado um terceiro protocolo, que consistia num estímulo mais longo (5 estímulos, 30 seg de luz, espaçados por 90 seg sem luz). Este último protocolo de activação foi estabelecido com base em estudos anteriores, que reportaram a capacidade de treinos espaçados para activar importantes cascatas de sinalização intracelulares, como a *Mitogen-Activated Protein Kinase* (MAPK). O ERK é uma molécula-chave desta cascata, e portanto questionámos se existiria uma expressão aumentada de pERK em função da resposta dos neurónios Or83c aos estímulos espaçados. Os resultados que obtivemos com as 3 manipulações artificiais não foram significativos entre moscas experimentais e controlos, sugerindo assim que os protocolos de activação não foram eficientes para activar os neurónios Or83 e aumentar a expressão de pERK no glomérulo DC3.

Em suma, os nossos resultados mostram uma expressão aumentada de pERK, na presença de um estímulo externo, em neurónios olfactivos. No entanto, no seguimento das experiências de manipulação artificial de actividade neuronal, não foi possível confirmar a robustez da utilização de pERK como marcador de actividade neuronal na *Drosophila*. Não obstante, as nossas observações poderão abrir novos caminhos para estudar a actividade neuronal no cérebro da *Drosophila* e medir a actividade em neurónios específicos, envolvidos em diferentes comportamentos inatos e em contextos mais naturalistas.
A identificação de neurónios envolvidos em diferentes condições pode ser crucial no estudo de outros paradigmas de função e actividade neuronal no cérebro das moscas, bem como permitir que se estabeleçam ligações com outros organismos. Acreditamos que este trabalho possa ser um passo firme nessa direcção.

Todos os detalhes de execução experimental e análise foram partilhados com Dr.ª Marta Moita (e respectivo laboratório), e com a Dr.ª Isabel Campos. O total desenvolvimento experimental, recolha e processamento dos dados foi realizado por mim.

Palavras-chave: Actividade neuronal, fosforilação de ERK, glomérulo DC3, cérebro de *Drosophila*.

Abstract

In order to understand how the brain generates behavior, we need to map neural activity onto defined neuronal circuitry. Due to the simplicity and genetic tractability of the fruit fly, neurons and circuits are identifiable across animals, with a large and established set of transgenic lines. Although vast, the *Drosophila* experimental tool kit does not yet include a good endogenous marker of neuronal activity.

In this project, we used immunohistochemical detection of phosphorylated Extracellular signal-Regulated Kinase (pERK) - a key molecule for synaptic plasticity regulation - as readout of neuronal activity in the *Drosophila* brain. Flies exposed to farnesol (an attractive citrus fruit compound) showed higher levels of pERK expression in the antennal lobes. Furthermore, pERK levels in Or83c-expressing neurons, which were previously implicated in processing the farnesol stimulus, were significantly increased after stimulation.

We next exposed flies to farnesol, while expressing the inward rectifier potassium channel Kir 2.1 to silence Or83c neurons in the DC3 glomerulus. Additionally, we used a genetically encoded neuronal activator – CsChrimson – to artificially trigger those same neurons in the DC3 glomerulus. Our results from these manipulations were inconclusive and further analysis is required to explore pERK dynamics when we induced changes in Or83c-expressing neurons.

In this study we show that, at least in some paradigms, pERK expression can be used as a marker of neuronal activity and, thereby, can increase our understanding about *Drosophila* circuits connectivity in the context of unrestrained behaviors. This tool can be quickly tested after stimulation to highlight the active neurons and brain regions involved in different behavioral responses. In the future, it will be interesting to see whether this endogenous marker can be applied to other paradigms, which should prove very useful as another tool to help map behavior onto neurons in the *Drosophila* brain. We hope this work encourages such future studies.

Keywords: Neuronal activity, ERK phosphorylation, DC3 glomerulus, *Drosophila* brain

Index

Figures Index

Tables Index

Appendix I - Index

Appendix II - Index

List of Abbreviations

(v/v) – (volume/volume)

°C – Celsius degrees

ALs – Antennal Lobe(s)

B1 – Background 1

B2 – Background 2

CD8 – transmembrane protein

c-fos –Immediate Early Gene (proto-oncogene)

ChRs – Channelrhodopsins

CREB – cAMP (cyclic adenosine monophosphate) - response element binding protein

d – day

DC3 – farnesol-sensitive olfactory glomerulus

DNp09 - Descending neurons P9

ERK – Extracellular signal-Regulated Kinase

g – grams

GAL4 – Gal4 regulatory protein (*Saccharomyces cerevisiae*)

GEGI/GCaMP - Genetically encoded calcium indicators

GFP – Green Fluorescent Protein

hr – hour

Hr38 – Immediate Early Gene (Hormone receptor-like)

IEGs – Immediate Early Genes

Inv. – Investigator

LC11 - Lobula Columnar visual projection neurons

MAPK - Mitogen-Activated Protein Kinase

MB – Mushroom bodies

min – minute(s)

mL – milliLitre

mM – milliMolar

NGS – Normal Goat Serum

nm - nanometer

NMJ - larval neuromuscular junction

Or83c – Olfactory receptor 83c

ORs – Olfactory receptor(s)

PBS - Phosphate Buffered Saline

PBT - phosphate buffered saline with 5% Triton X--100

pERK – phosphorylated ERK

PNs – Projection Neurons

ROIs – Region(s) Of Interest

rolled, rl – *Drosophila* homologue of ERK

rpm – rotations per minute

RT – Room Temperature

TRIP – Transcriptional reporter of intracellular Ca^{2+}

UAS – Upstream activating sequence

µL – microLitre

µM – microMolar

Introduction

1. Brain activity, classic tools and limitations

A typical brain uses neural circuits to collect and process information from the internal biological and external environmental worlds and generates motor commands for observable behaviors[1]. Understanding the mechanisms of how a nervous system develops from single progenitor cells to a functional unit integrating responses and how the brain orchestrates behaviors have always been central areas of interest in modern neuroscience. Brain activity includes all the sensory ways in which animals take in information, process, retain and decide to act on it. The activity of neurons has been shown to be vital for the accurate formation of neuronal circuits, as it ensures normal brain development and function. The synaptic plasticity[2] is one of the most important and absorbing properties of the brain and comprises cellular mechanisms that underlie the ability to sense the environment and preserve the long-term behavioral experience (see molecular processes in **Fig. 1**). Therefore, monitoring neural activity is crucial in understanding the underlying mechanisms of animal behavior.

There has been recent progress in understanding the flow of information in the brain from experiments using techniques of molecular genetics, electrophysiology and optical imaging (e.g. optogenetic tools and calcium imaging). However, the full knowledge of the assembly and function of neural circuits is still incomplete. In humans, there are a few methods to monitor and measure brain activity, using a combined set of tools and also multimodal acquisition systems, such as non-invasive fMRI (functional magnetic resonance imaging) and EEG (electroencephalography). fMRI presents a high spatial resolution, but does not provide suitable temporal resolution, due to the slow blood oxygen level response (in order of seconds). On the other hand, EEG ensures a millisecond temporal resolution that gives accuracy in recording the dynamics of electrical changes in neuronal population. Conversely, this technique offers a poor localization of signal sources[3,4]. Unlike measuring brain activity in humans, the techniques used to record brain activity in other animals provide much greater detail, working in a controlled and smaller neuronal environment, with an invasive methodology. For several years, the main technique for monitoring the dynamics of individual neurons in freely behaving animals has been extracellular electrophysiological recording, which has provided important and diverse advances in our knowledge of brain function[5,6]. However, and even though electrophysiology still retains unique advantages (e.g. temporal resolution), some limitations persist regarding the obstacles of achieving stable long-term recordings, targeting cells by genetic type or connectivity and even difficulties in identifying cells with spaced periods of activity. Furthermore, it has been truly challenging to sample a dense population of cells and record from different projections (e.g. dendrites or axons), in addition to the invasive profile of this methodology.

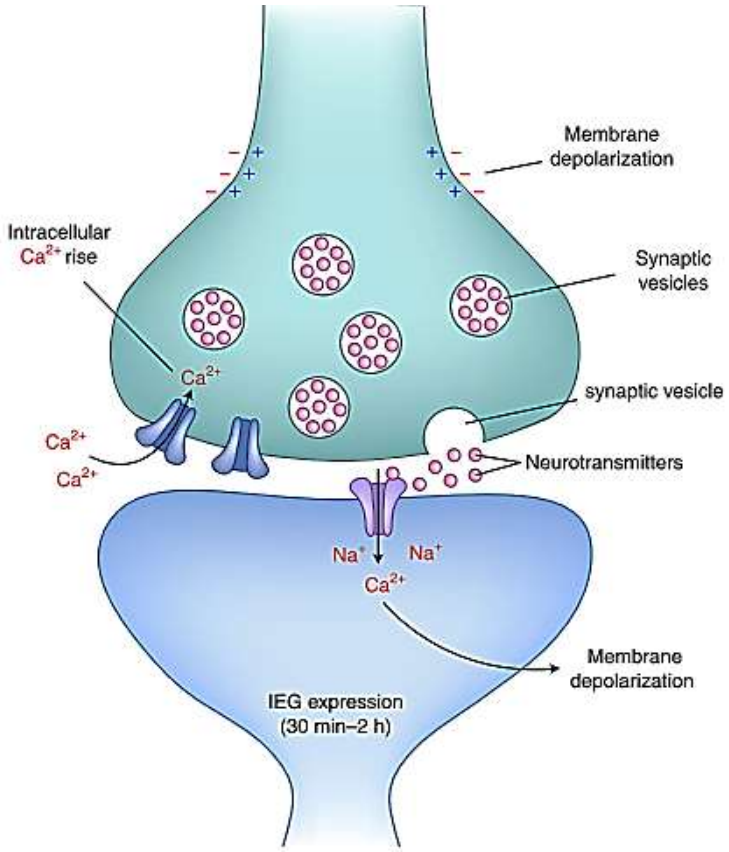

Fig. 1: Schematic of molecular processes underlying neuronal activation.
Membrane depolarization leads to a transient rise in intracellular Ca^{2+} followed by synaptic vesicle release of neurotransmitters, which activate the receptors on the postsynaptic side. During periods of prolonged excitatory activity, transcription of IEGs (immediate early genes) is activated. Adapted from "Molecular tools for imaging and recording neuronal activity", Nature Chemical Biology | Vol. 15, 101-110. Wenjing Wang, Christina K. Kim and Alice Y. Ting, February 2019.

2. Calcium Imaging – a worldwide measure of neuronal activity

In recent years, to overcome some of the previous limitations, Calcium Imaging of cytoplasmic free calcium (Ca^{2+}) ions has been rapidly improving, either combined with electrophysiology or as an isolated technique, covering both temporal and spatial resolutions requirements. Ca^{2+} is a second messenger for neurotransmitter signaling and membrane depolarization. In most cell types, action potentials (APs) are tightly attached to the opening of voltage-gated Ca^{2+} channels, which cause large and rapid increase in Ca^{2+} concentration[7]. There are two complementary paradigms for optical brain imaging studies in behaving animals: those involving head-fixed animals and those allowing unconstrained behavior. Both methods can be a benefit or a disadvantage, depending on the scientific purpose, but these approaches play an important and continuous role in the study of cellular and neural circuit dynamics during active animal behavior.

2.1. Head-fixed methods

- **Genetically Encoded Ca^{2+} Indicators (GECIs)**

The latest progress in Ca^{2+} imaging has been largely driven by the development of progressively more sensitive GECIs[8], which are based on fusions of fluorescent proteins and Ca^{2+}-binding proteins. This imaging technique is now regularly used to measure activity of large populations of neurons in behaving flies[9], fish[10], and rodents[11,12] and has also been verified in non-human primates[13]. The GCaMP family of GECIs are dominant in calcium imaging and have been extensively used. GCaMPs are based on a calmodulin (calcium-binding protein) domain that is inserted into a circularly permuted green fluorescent protein (GFP)[14]. High intracellular Ca^{2+} concentration induces structural rearrangement of this fused complex and results in an increase in fluorescence emission intensity. Nevertheless, the main limitations of GECI imaging derive from the magnitude and kinetics of calcium entry and extrusion, with low temporal precision (in order of milliseconds), and so raising questionable ability for single APs detection. Inefficient tracking of hyperpolarizations and subthreshold depolarizations[15] are also pointed out as important limitations of GECI imaging. Additionally, with the exception of a few examples (such as the bioluminescent Ca^{2+} indicator GFP-aequorin system in freely behaving fish[16] and flies[17]), most work with Calcium imaging is also limited to either immobilized preparations or partially dissected ones, which is a major disadvantage for experiments with small freely behaving animals (e.g. *Drosophila melanogaster*, the fruit fly).

2.2. Freeling behaving method

- **Calcium-dependent markers**

An important advantage of this method is the non-invasive approach using transgenic animals, such as calcium-dependent transcription factors, Calcium-dependent nuclear import of LexA (CaLexA[18]) and Transcriptional Reporter of Intracellular Ca^{2+} (TRIC[19]) in fruit flies. The use of transgenic animals provides a stable and reproducible labeling of neurons. Moreover, recent research reported the strengths of the Gal4-UAS binary expression system combine with bioluminescent Ca^{2+} indicator GFP-aequorin to record the activity of specific neurons in freely behaving flies[17]. However, Ca^{2+} signaling can be accumulated over time, even after the behavior of interest has ended and, therefore, potentially labeling irrelevant neurons.

3. Optogenetic tools to track neuronal activity

Although much can be learned by simply observing molecular markers (e.g. fluorescent proteins) or reporting physiological parameters of neurons (e.g. membrane depolarization, synaptic activity), other methodologies can also be used to simultaneously manipulate labeled

cells and gene function, which allow clarifying the molecular mechanisms that underlie specific neuronal properties and to establish causal relationships between neural activity and behavior.

The last decade has seen great advances in optical imaging methods, as well as the development of optogenetic proteins that allows direct stimulation or inhibition of action potential firing of neurons using light, permitting cellular level recordings in behaving animals and also manipulating complex neuronal function[20,21]. Channelrhodopsins (ChRs) are classically nonspecific cation channels that depolarize neurons in response to light. Several studies have used different types of opsins, with diverse peak wavelength sensitivity to address distinct and independent cell populations. Chrimson[22] - an opsin type particularly popular amongst *Drosophila* behavioral neuroscientists - is a red light–drivable channelrhodopsin with a peak absorption at 600 nm, which means that it is more easily excited across larger tissue volumes. In flies, longer wavelengths of light penetrate the cuticle better, allowing activation of deep-brain neurons in freely moving adult flies. This privileged access permits the identification of neural circuits controlling fly behavior and actually contributes to our understanding about nervous system development, function and context of disease[23,24]. One of the challenges for optogenetics and functional imaging is that light itself can affect the experiment, and so can be a potential source of a behavioral phenotype or change in neural activity.

4. Immediate early genes (IEGs), as neuronal activity markers

In fact, the optogenetic tool offers improved access to the control of neuronal activity, but this technique implies a considerable number of transgenes and it may be difficult to use in combination with genetic manipulation of neuronal activity. Thus, IEGs could be very useful in overcoming this practical constraint. These genes are quickly induced after a certain behavior, therefore allowing a privileged access to the neuronal circuit implicit to that behavior.

Biochemical events that occur naturally in response to neural activity can also be used to detect active neurons in freely behaving animals. In mammals, IEGs, such as *c-Fos* and *Arc*, whose expression is transiently and rapidly upregulated upon neural activity, have allowed the identification of many neurons associated with several behaviors, such as memory, sleep, fear, mating and drug addiction[25]. IEG promoters have also been used for more than a decade by the scientific community to drive transgene expression in upregulated activity neurons[26,27] and several studies have shown their role as activity markers for mapping neuronal circuits involved in specific behaviors in many different species. In flies, only one IEG has been described so far (Hr38[28], a transcription factor conserved among insects and up to humans) and its expression used as a neural activity marker[29] to label active neurons in the male fly brain, related to courtship behavior. As mentioned above, immediate early genes are rapidly induced inside nerve cells by extracellular stimuli without the need of intermediate proteins. Their expression

can be detected on an entire brain scale and at single cell resolution. Despite these advantages, IEGs have relatively poor temporal resolution (15-30 min for *cFos* activation and 1–2 hours for mRNA and protein responses respectively, in both mammalian and teleost neurons[12,30,31]) and display low sensitivity and specificity.

5. Extracellular signal-Regulated Kinase (ERK) as readout of neuronal activity

In an attempt to overcome some of the IEGs limitations mentioned previously, ERK (Extracellular signal-Regulated Kinase) phosphorylation, an endogenous sensor, has been used to track neuronal activity in vertebrates and also in invertebrate models. ERK is a member of the mitogen-activated protein kinase (MAPK) family (see illustration in **Fig. 2**). ERK is activated via phosphorylation by its upstream kinase MEK (MAP kinase or ERK kinase)[32,33,34] and its activation requires a cascade that involves sequential activation of Ras, Raf, and MEK[35]. Early studies indicated a critical role of ERK in regulating mitosis, proliferation, differentiation, and survival of mammalian cells during development[36]. Upon activation, phosphorylated ERK (pERK) can be translocated into the nucleus to activate several transcriptional factors, such as cAMP-response element binding protein (CREB[37]) that is required for the transcription of many neuronal genes and long-term synaptic plasticity[38]. ERK is abundant in the vertebrate adult brain, and its activation can play several roles in the activity-dependent regulation of neuronal function[39]. ERK1 and 2 are also involved in neuroinflammation and neural death, and have been described as necessary for learning and memory formation in rodents[40], including conditioned place preference[41], fear conditioning[42] and spatial learning[43]. In zebrafish, pERK has been used as a reporter of neural activity[44,45], through development of a technique to map neural activity in freely swimming fish. In flies, recent research has shown that sleep deprivation and social enrichment independently increase ERK phosphorylation in wild-type flies, suggesting that ERK phosphorylation may be a mechanism for sleep and plasticity regulation[46]. The *Drosophila* homologue of ERK (*rolled*, rl) has been shown to regulate synaptic bouton number at the larval neuromuscular junction (NMJ)[47,48] and also CREB[49,50].

The usage of ERK activation as a readout to measure neural activity offers advantages when compared with IEGs (such as *c-fos*)[51], beyond all the common features of robust activation pattern, easily detected and quantified by immunohistochemistry. pERK has an improved temporal resolution, a more dynamic expression pattern with rapid induction, several cellular and subcellular locations and close connections to identify regions of interest involved in particular behaviors[45].

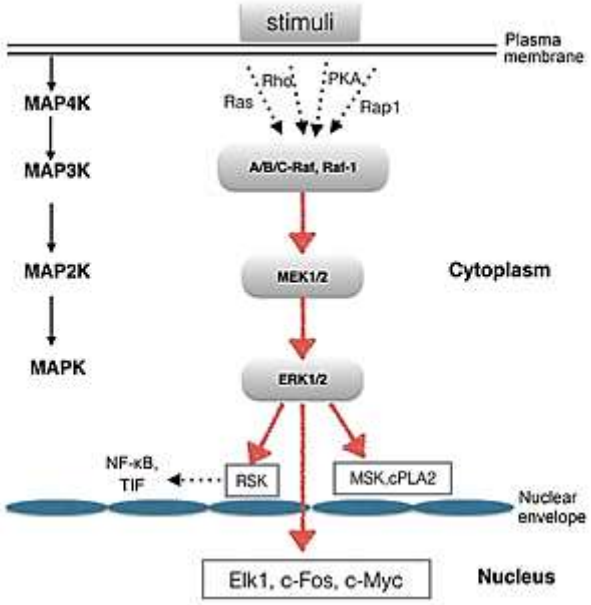

Fig. 2: Extracellular signal-regulated kinase 1/2 (ERK1/2) mitogen-activated protein (MAP) kinase cascade. The phosphorylation of ERK1/2 MAP kinase occur in the cytoplasm and can be translated into the nucleus and catalyze the phosphorylation of many proteins and transcription factors, such as c-Myc. Adapted from "The extracellular signal-regulated kinase 1/2 pathway in neurological diseases: A potential therapeutic target (Review)", International Journal of Molecular Medicine 39: 1338-1346. Jing Sun and Guangxian Nan, April 2017.

6. *Drosophila melanogaster* as a model organism to study neuronal activation

The fly brain is an attractive system to explore both computations and mechanisms underlying behavior at levels spanning from genes through neurons to circuits[52]. The brain architecture, the relatively small number of neurons (~100.000) and the molecular, genetic, cellular and behavioral approaches available to dissect brain development and processing in *Drosophila melanogaster*, show us that the fly brain could be the place to find some valuable cues[53]. Due to the simplicity and genetic tractability of the fruit fly, neurons and circuits are identifiable across animals. Moreover, a large set of transgenic lines has been developed with the aim of specifically labeling small subsets of neurons and manipulating them in sophisticated ways[54,55]. Taking into account the combination of these unique molecular and genetic techniques and recent advances in recording neural activity, *Drosophila* has become a powerful system for studying the neural circuit basis of behavior[56]. Neuronal studies in *Drosophila* often rely on genetic tools to manipulate and monitor activity of neuronal subsets. However, to identify the relevant neuronal subsets for a given behavior, the approach is often the laborious and time-consuming screening strategy of testing the same behavioral paradigm in the context of many different genetic manipulations. The field would therefore benefit greatly from being able to rely on a neuronal marker that could be quickly tested after a given behavior to highlight the

neuronal networks or brain regions involved in such behavior, and thereby guide other manipulations in a more educated way.

- **6.1. Olfactory system**

As outlined above, pERK activity is induced by neuronal activity and has been used to report neuron responsiveness, including in the mammalian olfactory system[57]. In flies, the olfactory system has been widely explored due to the uniquely comprehensive description of the sensory apparatus, including complete molecular descriptions of identified olfactory receptor neurons, their projection to higher brain regions and detailed information about their physiology[58]. The antenna is the major substrate for detection of volatile pheromones and food odorants[59,60]. There are approximately 500 hair-like sensilla, each covering the dendrites of one to four olfactory neurons[61]. The sensilla are classified into four morphological groups: trichoid, basiconic, coeloconic and intermediate sensilla[61,62]. Most olfactory neurons in *Drosophila* have been characterized according to the sensillum class in which they are located, by the odorant receptor (OR) they express and also by which odorants they detect. The olfactory receptor neurons in the antennae send axons to specific glomeruli in the antennal lobe, and thus these neurons are also characterized by the glomerular targets they innervate in the antennal lobes[58,63,64]. Many efforts have been done to characterize these ORs in their endogenous sensilla and most neurons express one type of odorant receptor. Therefore, different neurons that express the same receptor will converge at a given glomerulus. However, several studies have described the co-expression of two different receptors in the same neuron and also events of co-convergence between two different types of receptor neuron at a single glomerulus[65,66] (see illustrations in **Fig.3**). Consequently, it may not be possible to correlate odor-evoked activity with individual neurons or ORs and many *Drosophila* olfactory receptors remain orphans with unknown chemical specificity or function.

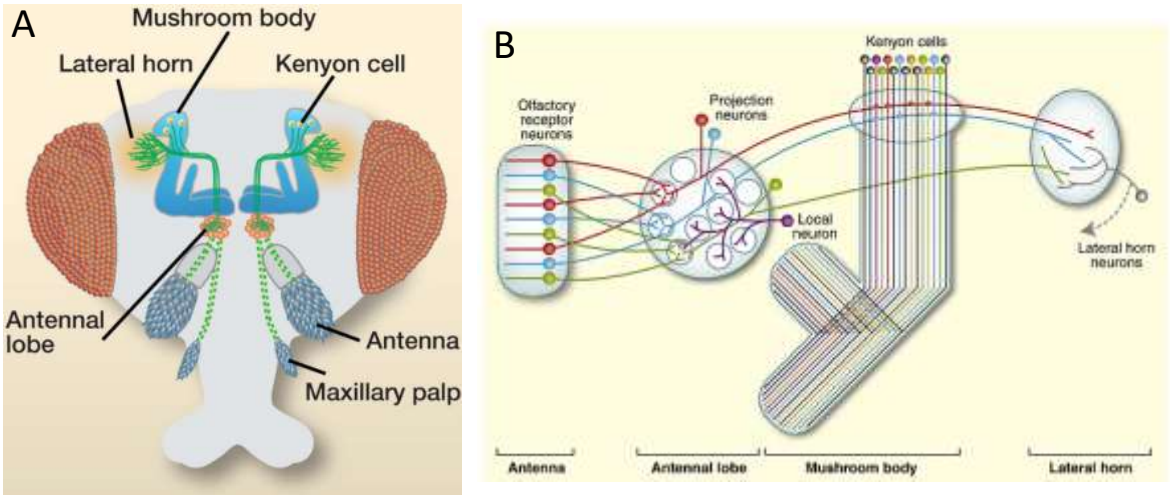

Fig. 3: (A) Frontal view of a Drosophila head.
There are two pairs of olfactory organs: antennal segments and maxillary palps. Olfactory information is first relayed to the antennal lobe, which contains multiple glomeruli. Subsequent processing takes place at the lateral horn of the protocerebrum and Kenyon cells in the mushroom body. Adapted from "Olfactory Perception: Receptors, Cells, and Circuits", Cell 139(1): 45–59. Chih-Ying Su, Karen Menuz and John R. Carlson, October 2009. **(B) Schematic representation of the olfactory system of Drosophila**. Olfactory receptor neurons in the antennae send axons to specific glomeruli in the antennal lobe. All olfactory receptor neurons expressing the same odorant receptor (same colour) converge at the same glomerulus. There they form synaptic contacts with projection neurons and local neurons. Projection neurons send axons either directly to the lateral horn (green projection neuron) or indirectly to the mushroom bodies (red and blue projection neurons), where they form synapses with Kenyon cells. Adapted from "Olfactory Information Processing in Drosophila Review", Current Biology R700–R713. Nicolas Y. Masse, Glenn C. Turner and Gregory S.X.E. Jefferis, August 2009.

7. Laboratory context and thesis motivation

In the laboratory, we are focused on social interactions in different contexts, specifically when fruit flies perceive a threat. We have been studying how the social context modulates defensive behaviors, more particularly freezing behavior, in response to a threatening visual stimulus. More recently, our lab characterized a subset of descending neurons, one of which DNp09, when silenced were found to be a key element in the circuit mediating freezing, a defensive response in flies[67]. In addition, we found that freezing behavior is modulated by the social environment and that LC11 neurons (a type of lobula columnar visual projection neurons) are involved in the propensity for freezing flies to resume moving in response to the movement of others[68]. The puzzling question that remains unanswered is whether these and other neurons involved are active during the behavior performed by the animal. We actually managed to genetically manipulate DNp09 and LC11 neurons, but we lack a tool to measure the activity of these neurons in unrestrained flies when freezing behavior is displayed and also understand how this neuronal activity can be modulated by different factors, such as the social context.

8. Goals of present work

The aim of this project is to test whether ERK phosphorylation is a potentially good tool for monitoring neuronal activity in the *Drosophila* brain, given the scarcity of activity

measurement tools in invertebrate freely behaving animals. In our paradigm, we decided to assay for neural activity in the *Drosophila* olfactory system through ERK phosphorylation, after an external odor stimulus. As previously mentioned, pERK has been recurrently used to identify active neurons in different model organisms, considering the improved temporal resolution and robust activation pattern. As a proof of principle, we chose a very specific and attractive odor stimulus, Farnesol. This volatile compound is an intermediate in juvenile hormone biosynthesis, but is also produced by ripe citrus fruit peels, and it was also described as a potent and specific activator for the orphan odorant receptor 83c[69]. Or83c was previously identified in a subset of poorly characterized intermediate sensilla and suggested as a narrowly tuned receptor that contributes to localize citrus fruit substrates[69]. Therefore, we will confirm whether ERK is activated in the DC3 glomerulus, which is innervated by Or83c-expressing neurons in the antennal lobes (see **Fig. 4**). The PNs (Projection Neurons) relaying information from the DC3 glomerulus to higher brain areas target a region of the lateral horn, previously associated with pheromone perception. We also aim to artificially manipulate neuronal activity in these neurons and observe concordant changes in pERK expression, in relation to the inhibition or activation protocols. As a result, we anticipate that Or83c neurons will be active upon farnesol stimulation, which supports our hypothesis that ERK phosphorylation can be used as a neuronal activity marker in *Drosophila* brain. This endogenous tool can be very useful for future research in our laboratory (and also for the *Drosophila* scientific community), allowing us to label recent active neurons in a particular behavior and monitor neuronal activity in different contexts, such as freezing behavior.

Understanding the mechanisms of neural communication is a key advantage to interpret behavior. The identification of the neurons involved in different conditions can be useful to reveal some detailed mechanisms to further studies on mammalian brain function.

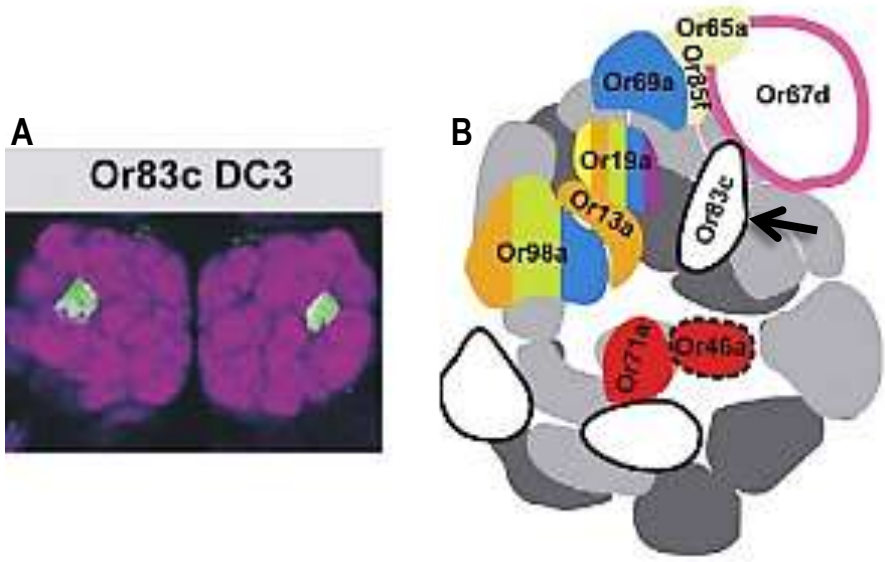

Fig. 4: Or83c-expressing neurons in the DC3 glomerulus in the antennal lobes.
(A) The neuronal expression pattern shows stereotypy and bilateral symmetry in the antennal lobes (stained with anti-nc82 in magenta and anti-GFP in green). **(B)** Three-dimensional representation of different odorant receptors in the antennal lobe. The black arrow is pointing to our region of interest, DC3 glomerulus, which is innervated by the Or83c neurons. Adapted from "Genetic and Functional Subdivision of the Drosophila Antennal Lobe", Current Biology Vol. 15, 1548–1553. Elane Fishilevich and Leslie B. Vosshall, September 2005.

Materials and Methods

1. Animal husbandry and fly strains

In all experiments, *Drosophila melanogaster* virgin males 4-6 d after eclosion were used for stimulation. Flies were raised at 25°C and 70% humidity, in a 12h:12h dark:light cycle. Newly eclosed adult flies were collected from polypropylene medium culture vials (Semadeni, 28x85 mm #10405) daily under CO2 anesthesia. Flies were maintained on standard fly medium, until the experimental protocols. Strains and sources are described in **Table 1**.

Table 1: Fly stocks and sources.

STRAINS	SOURCES
Canton S (Wild-type)	Bloomington Drosophila Stock Center (#64349)
w[*]; P{w[+mC]=Or83c-GAL4.F}73.4A	Bloomington Drosophila Stock Center (#23132)
y,w/Yhs-hid; UAS-CD8::GFP;;	"virginized" stock from Fly Facility, Champalimaud Foundation
$w^{[*]}$; DL; 10xUAS-Kir2.1::eGFP	Rubin Laboratory, Janelia Research Campus, Fly Light Split-GAL4 Driver Collection
$w^{[*]}$;; UAS-Chrimson::mVenus/ $TM3.Sb^{[1]}$	"virginized" stock from Fly Facility, Champalimaud Foundation

2. Fly food recipes

Standard fly medium: Experimental and control flies were reared on a yeast-based medium (per liter of water: 8 g agar [NZYTech, PT], 80 g barley malt syrup [Próvida, PT], 22 g sugar beet syrup [Grafschafter, DE], 80 g corn flour [Próvida, PT], 10 g soya flour [A. Centazi, PT], 18 g instant yeast [Saf-instant, Lesaffre], 8 ml propionic acid [Argos], and 12 ml 10% nipagin [10g methyl 4-hydroxybenzoate in 100 mL ethanol 96%]). Retinal-free culture medium: Control flies were transferred to yeast medium for 3 days before the optogenetic activation protocol (per liter of water: 90 g sugar, 20 g yeast extract [Próvida, PT], 20 g peptone [Acros Organics], 10 g agar [NZYTech, PT], 0.6 g magnesium sulfate heptahydrate [Acros Organics], 0.6 g calcium chloride dihydrate [Acros Organics], 80 g instant yeast [Saf-instant, Lesaffre], 10 ml propionic acid [Argos], and 10 ml nipagin (10g methyl 4-hydroxybenzoate [VWR] in 100 mL ethanol 96%).

3. GAL4/UAS System.

The GAL4-UAS system is designed for targeted gene expression that allows spatial and temporal selective expression of genes of interest[70]. This tool comprises the expression of a

certain gene to specific cells where both the transcription activator protein, encoded by the *GAL4* gene (GAL4), and the UAS enhancer sequence are present. After being translated, GAL4 protein binds to the UAS sequences thereby promoting the expression of a desired gene of interest in those cells (see **Fig. 5A**). In this manner, the Gal4/UAS system works as a switch for gene expression that depends on the presence of both elements. In order to get these two parts of the system together, we decided to cross a Gal4 driver fly line with a line containing the UAS sequences upstream of the gene of interest to ectopically express it (see scheme in **Fig. 5B**). The UAS enhancer sequences will be present in every cell, but the GAL4 protein will only be present in our specific set of neuronal cells. In our paradigm, we used the Or83c-Gal4 fly strain that expresses GAL4 in the pattern of the *Odorant receptor 83c* gene. This Gal4 driver line was crossed with different UAS sequences, promoting the gene expression in our particular set of intermediate sensilla neurons. Regarding the UAS fly lines, we chose 3 different stock lines to address our initial question and genetically manipulate these olfactory neurons: UAS-CD8::GFP (CD8 is a transmembrane protein and therefore the cell surface was labeled with GFP[71]), UAS-Chrimson::mVenus (red-shifted channelrhodopsin[22], fused with a fluorescence protein) and 10xUAS-kir2.1::eGFP (kir is hyperpolarizing potassium channel[72], fused with GFP). By using this binary system, we were able to analyze the Or83c-expressing pattern and also activate or silence these cells in neuronal manipulation experiments.

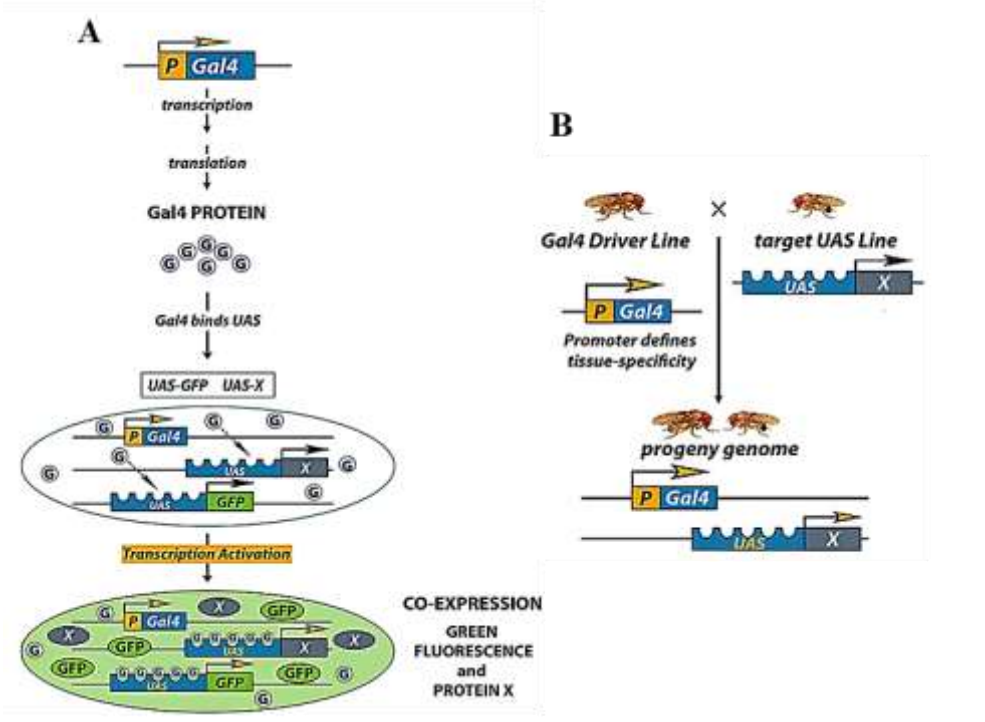

Fig. 5: Schematic of the Gal4-UAS system and its targeted gene expression in flies.
(A) The yeast Gal4 promoter determines the time and cell specificity of transcription. After translation, Gal4 protein binds to UAS sequences placed upstream of any and all gene-coding sequence, causing their co-expression. Therefore, a single UAS-marker reveals the specific expression pattern of all UAS-linked sequences. **(B)** Cross between two distinct transgenic flies (Gal4 driver x target UAS sequence) in order to drive the transgene expression in a particular set of neurons. Adapted from "Genetic odyssey to generate marked clones in Drosophila mosaics" by R. Griffin, R. Binari, and N. Perrimon, 214, vol. 111, no. 13.

On experimental days, all flies were manipulated without CO2 anesthesia.

4. Farnesol stimulation and experiment design (Canton S and Or83c-Gal4xUAS-CD8::GFP flies).

We used an odor stimulus for neuronal activation, farnesol, which is a potent and specific activator of Or83c-expressing olfactory neurons. These neurons innervate the DC3 glomerulus in the antennal lobe and mediate attraction behavior to low concentrations of farnesol[69]. We prepared a stimulation vial with a 300 uL of a 10% (v/v) farnesol solution (30 uL of farnesol solution [Sigma-Aldrich, R2500] in distilled water) on a paper tissue soaked inside an empty vial. 5-7 virgin-male flies were transferred to this vial for 1 minute. Immediately after stimulation, flies were changed to an empty vial for 20 minutes before dissection. As a control, flies were exposed to a paper tissue soaked in distilled water for 1 minute and then transferred, as previously described. Canton S strain was used to confirm pERK expression pattern in the *Drosophila* brain (more particularly in the antennal lobe). To confirm whether pERK signal was colocalized with the olfactory neurons (GFP labeling) in the DC3 glomerulus, we crossed Or83c-Gal4 male flies with UAS-CD8::GFP virgin females and the male progeny was exposed to the stimulus or distilled water (control), as mentioned earlier.

5. Silencing/Inactivation of Or83c-expressing neurons (Or83c-Gal4x10xUASKir2.1::eGFP).

Experimental virgin-male flies were transferred to a stimulation vial (300 uL of 10% farnesol solution) for 1 minute. Next, flies were changed to an empty vial for 20 minutes before dissection. To inactivate the olfactory neurons and confirm whether we have an effect on pERK expression in the DC3 glomerulus, we crossed Or83c-Gal4 male flies with 10xUAS-Kir2.1::eGFP females. As a control, parental males were exposed to farnesol solution, as previously described. Co-localization of pERK and GFP expressions was analyzed upon stimulation.

6. Optogenetic activation (Or83c-Gal4xUAS-Chrimson::mVenus).

We expressed a red-shifted channelrhodopsin, CsChrimson, to artificially manipulate Or83c-expressing neurons in the DC3 glomerulus. Co-localization of pERK and GFP expressions was analyzed after stimulation under 3 different light-delivery protocols. All flies were collected and kept in the dark (covered in foil) for 3 days until the experimental days. Male flies from the first and second experimental protocols were aspirated into a chamber and placed on the optogenetic stage set-up, while in the third experimental condition, flies were kept in an empty vial during the entire stimulation. In the first two protocols, flies were kept in standard fly food, in which we added 0.2mmol/L *all-trans-retinal* ([Sigma-Aldrich, #R2500], using a stock solution of 0.2 mM all-*trans*-retinal in ethanol 100%). We established two different stimulation protocols, in which all flies (handled with a “mouthpiece” and gently placed in the arenas) were allowed to

explore the acrylic arena (30 mm in diameter and 4 mm in height) for 30 seconds and then stimulated for 1 minute with pulsed light (pulse frequency 2 Hz, 250 ms each pulse, duty cycle 50%) or continuous light. Between the arenas and the high-powered 627 nm LEDs, a diffuser plate insured homogeneous lighting for a total radiance of 15 mW/cm^2 for light pulses and 7.5 mW/cm^2 for continuous light. The total radiation differences between the stimulation protocols were given due to the 50% duty cycle and ensure that the average intensity of continuous and pulsed light (half the time, twice the intensity) is the same. Flies in standard fly food were used as control groups (one group was exposed to the stimuli and the other group was kept in the dark throughout the experiment, as a negative control to the light). In a third assay, experimental flies were kept in retinal-free fly food, in which we added 0.4 mmol/L *all-trans-retinal* ([Sigma-Aldrich, #R2500], using a stock solution of 0.2 mM all-*trans*-retinal in ethanol 100%). Controls were kept in retinal-free fly food. For this assay, we established a different stimulation protocol, in which flies were allowed to explore the vial (avoiding restrictions on handling and decreasing stress effects) for 30 seconds and then stimulated with continuous light (5 stimuli of 30 seconds light on and 90 seconds light off, intensity 7.5 mW/cm^2). All fly food cultures and experimental activation protocols are summarized in the following **Table 2** and **Fig. 6**:

Table 2: Fly food recipes for control and experimental flies in all different optogenetic activation protocols. All flies were kept in the dark for 3 days before the experimental days.

Optogenetic activation	**Stimulation Protocol**	**Culture medium [Control flies]**	**Culture medium [Experimental flies]**
1	Light pulses [1 min]	Vienna	Vienna + 0.2 mmol/L retinal
2	Continuous light [1min]	Vienna	Vienna + 0.2 mmol/L retinal
3	5x continuous light [30secON-90secOFF]	Retinal-free	Retinal-free + 0.4 mmol/L retinal

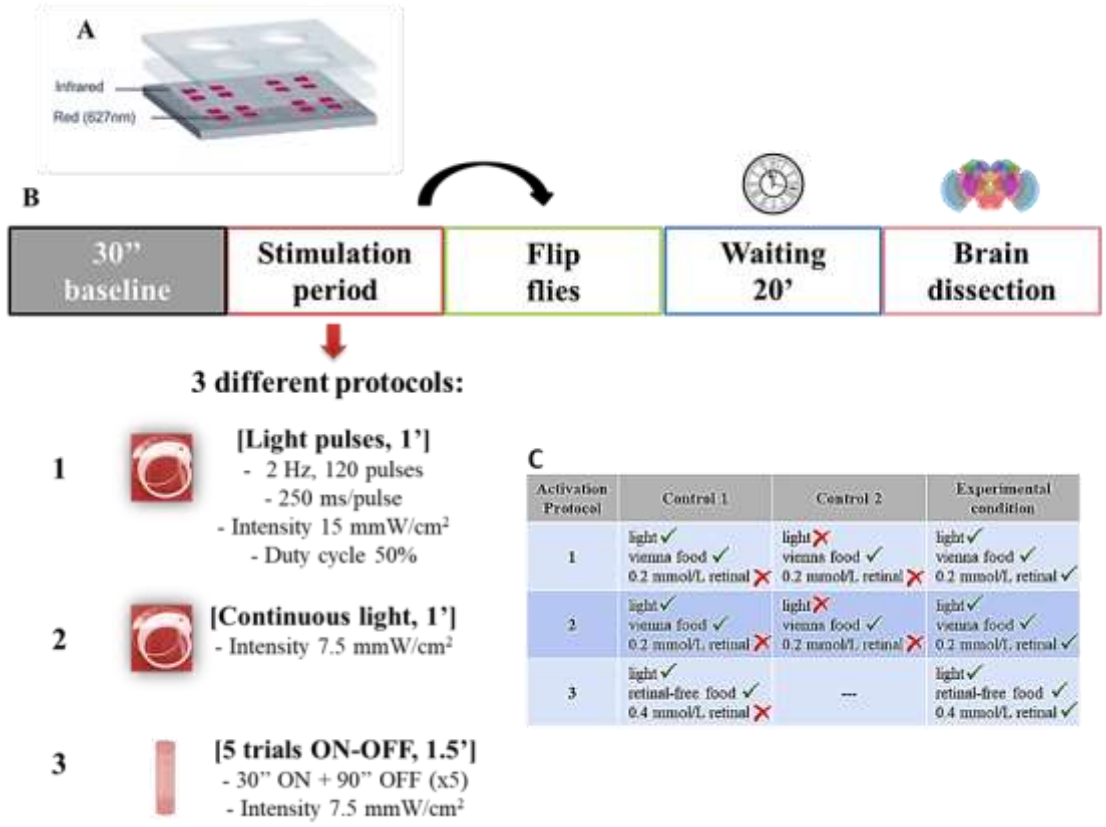

Fig. 6: Experimental protocol for three different optogenetic activations.
(A) Schematic of experimental set-up for CsChrimson stimulation. **(B)** Experimental protocol for artificial activation, in which male flies (4-6 days old) were allow to explore for 30 seconds, followed by 3 different stimulation periods. After stimulation, flies were transferred to a new vial for 20 minutes before dissection. **(C)** Optogenetic activation protocols for both 1 and 2 controls and experimental condition.

7. Dissection and immunohistochemistry protocols.

All animals were anesthetized on ice during ≈1 min before dissection and heads were cut off. Fly brains were dissected in 4°C PBS and then transferred to formaldehyde solution (4% paraformaldehyde in PBS) and incubated for 30 min at RT. Brains were washed 3x10 min in 0.5% PBT and blocked in 10% NGS [Normal Goat Serum, #G9023-0010 Sigma] in 0.5% PBT for 15 min at RT. Samples were incubated in primary antibody solution (chicken anti-GFP [Abcam, ab13970] at 1:1000, rabbit anti-pERK [Cell Signaling, #4370] at 1:1000 and mouse anti-NC82 [DSHB, Developmental Studies Hybridoma Bank] at 1:10 in 10% NGS in 0.5% PBT). Primary antibody incubations were performed during 3 days at 4°C with rocking. Brains were then washed in PBT 3x10 minutes at room temperature. The secondary antibodies were applied (anti-chicken Alexa 488 [Abcam, ab150173] and anti-rabbit Alexa 488 [Invitrogen, A11034], anti-mouse Alexa 594 [Invitrogen, A11032] and anti-rabbit A594 [Invitrogen, A11012] in 10% NGS in 0.5% PBT), covered in foil. Secondary antibody incubations and washes were the same as for primary antibodies. Fly brains were mounted in Vectashield [Vector Laboratories (USA)]. Images were captured on a Zeiss LSM 710 using 25 x objective (glycerol solution).

8. Sample mounting, image acquisition and treatment

Fly brains were mounted in Vectashield [Vector Laboratories (USA)] and mounted onto glass coverslips. Imaging of stained brain tissue was performed using an upright confocal microscope (Zeiss LSM710), using a 25× gycerol dipping objective. To cover the entire brain, two imaging tiles were acquired and stitched together using the Zeiss ZEN Imaging Software. Both experimental and control brain images from artificial manipulation were acquired on the same day and imaged in one run (positions selection) to ensure they were imaged with near-identical imaging conditions. Images were then processed with ImageJ.

9. Data and statistical analysis.

Flies from each cross were randomly assigned intro treatment groups, where possible. The odor stimulation and dissection protocols were performed by the same investigator and confocal imaging was performed blindly by the researcher. For all the genetic manipulation assays and visual scoring, all samples were numbered and the investigators were blinded. Each experiment was successfully reproduced at least two times and performed on multiple days. The quantification method for pERK fluorescence is explained in detail in results section. Briefly, we used a region of interest previously obtained in experimental brains exposed to farnesol. A coordinate system was established to apply the region of interest, which presents pERK expression, and two background regions (B1 and B2, adjacent to the region of interest) to all tested brains, being consistent among all analyzed samples. All statistical tests used are specified in the results section. Samples' distributions assumed non-normal and non-parametric statistical tests were used. To quantify group differences we used Mann-Whitney and Kruskal-Wallis nonparametric test analysis. All statistical analyzes were performed using GraphPad Prism 8.3.1 (GraphPad Software, San Diego, CA, USA).

Results

pERK expression in the antennal lobes upon farnesol stimulation

Several studies have analyzed ERK activation, since it is part of activity-dependent signaling pathways and have shown that pERK can be used to localize active neurons[33,46,73] and offers improved temporal resolution over IEGs. In our paradigm, we used an olfactory stimulus (farnesol, an attractive odor for flies) to induce neuronal activity in the *Drosophila* antennal lobe. Consequently, we hypothesized that ERK phosphorylation in the olfactory neurons could be used as readout of neuronal response to farnesol. To confirm this hypothesis, we first exposed WT flies to distilled water (control) or farnesol solution (**Fig. 7**). After the stimulation protocol, male flies were dissected, fixed and followed by immunostaining with nc82 (neuropil marker, bruchpilot protein) and pERK antibodies (**Fig. 8**), as previously described in Methods section **7**. WT flies revealed enrichment of pERK labeling in the nervous system in both control and experimental brains (**Fig. 8A'' and 8B''**). Punctate pERK staining of individual cells was seen throughout the brain, with strongest staining in the antennal lobes upon farnesol stimulus (**Fig. 8B',** zoomed-in) when compared to the control (**Fig. 8A',** zoomed-in).

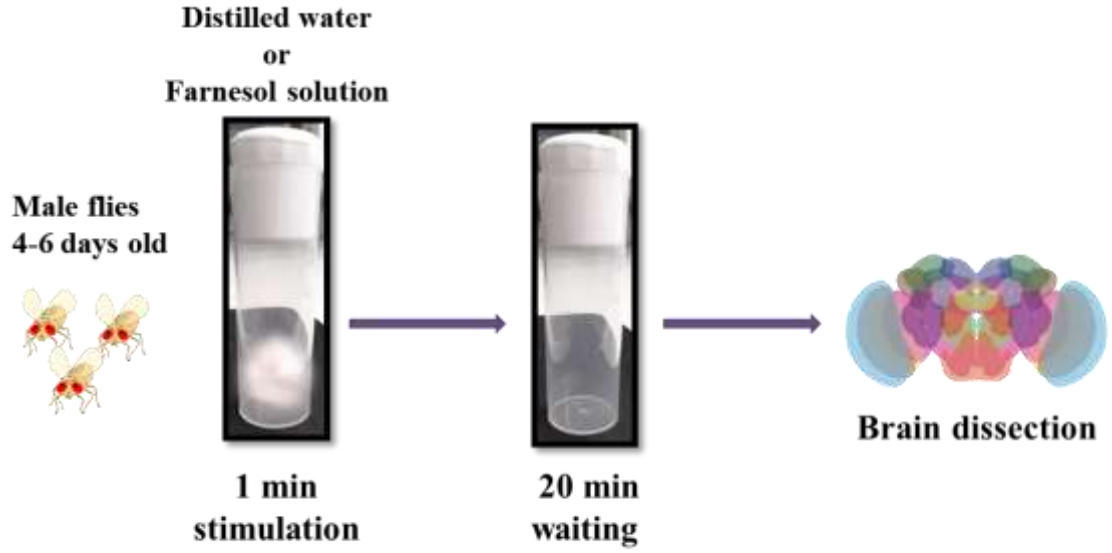

Fig. 7: Experimental odor stimulation protocol.
Male flies were transferred to a vial with distilled water (control flies) or a solution of farnesol soaked in paper for 1 minute. After the stimulation period, flies were changed to an empty vial for 20 minutes before dissection.

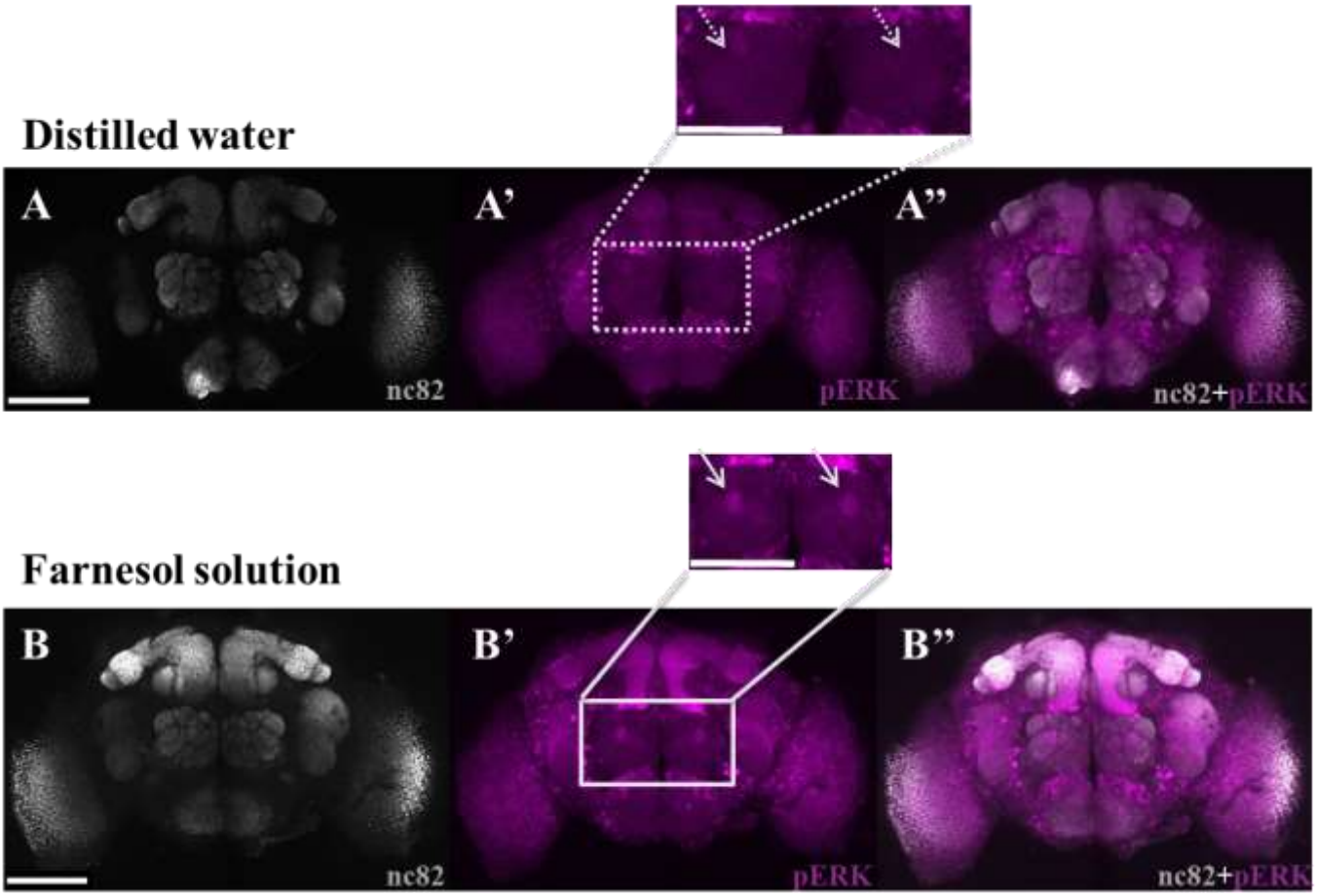

Fig. 8: pERK is a neural activity sensor in *Drosophila* brain.

WT males were exposed to distilled water (**A-A''** controls, n=7) and farnesol solution (**B-B''**, n=9) for 1 minute and dissected after 20 minutes (see protocol **Fig. 7**). All images are confocal ZProjections (8 slices, as maximum intensity projections) of fly brains stained for a neuropil marker nc82 (**A** and **B**, in grey) and phosphorylated-ERK (**A'** and **B'**, in magenta). **A''** and **B''** images show the merge channels for both control and experimental brains, respectively. (**A'**) (**B'**) The antennal lobes are outlined (light gray boxes) to highlight pERK expression in this area, which is the primary olfactory center of the *Drosophila* brain and also the region of interest in this study. Dashed (**A'** zoomed-in) and solid (**B'** zoomed-in) light gray arrows are pointed to the absence (control) or presence (farnesol) of pERK expression in the antennal lobes. Scale bars represent 70 µm (**A-A''**, **B-B''**) and 26 µm (**A'** and **B'** zoomed-in images).

Our first observations were consistent with the initial hypothesis, since we observed pERK expression in the olfactory area in response to the external odor stimulus. To properly validate these results and also increase confidence between visual assumptions with unbiased quantification, we decided to perform a blinded visual scoring from 3 impartial investigators for the absence (scored as 0) or presence (scored as 1) of pERK expression in the ALs (**Fig. 9, Tables A** and **B**). According to the observers, 15.1% of control brains show pERK expression in the antennal lobe (**Fig. 9, Table A1**) after distilled water exposure (**see Fig. 7**). In contrast, 88.9% of farnesol-exposed brains have pERK expression in the ALs (**Fig. 9, Table B1**). We show the percentage of brains with pERK expression in the antennal lobe for each observer in

both conditions to better illustrate the differences between all scored brains in **Fig. 9C**. Furthermore, we analyzed the ratio of agreement among investigators to confirm the robustness of the scores within conditions (**Fig. 9D**). All investigators agree on more than half of the scored brains for both control (57.1%) and experimental (77.8%) conditions, as depicted in the Venn diagrams of **Fig. 9D**. Although there was some coherence between the researchers' observations, there were enough disagreements that required automated quantification to verify these results.

A

Distilled water	Investigator 1 (pERK expression)	Investigator 2 (pERK expression)	Investigator 3 (pERK expression)
Brain #1	0	0	0
Brain #2	0	1	1
Brain #3	0	0	1
Brain #4	0	0	0
Brain #5	0	0	0
Brain #6	0	0	0
Brain #7	0	NA	0
0 = no			
1 = yes			

B

Farnesol stimulation	Investigator 1 (pERK expression)	Investigator 2 (pERK expression)	Investigator 3 (pERK expression)
Brain #1	1	1	1
Brain #2	1	1	1
Brain #3	1	1	1
Brain #4	1	1	1
Brain #5	1	1	1
Brain #6	0	1	1
Brain #7	1	1	1
Brain #8	0	1	0
Brain #9	1	1	1
0 = no			
1 = yes			

A1

WT male brains (4-6 days old) Control	% of positive brains for pERK expression (ALs)
Investigator 1	0%
Investigator 2	16.7%
Investigator 3	28.6%
Mean	**15.1%**

B1

WT male brains (4-6 days old) Farnesol	% of positive brains for pERK expression (ALs)
Investigator 1	77.8%
Investigator 2	100%
Investigator 3	88.9%
Mean	**88.9%**

C

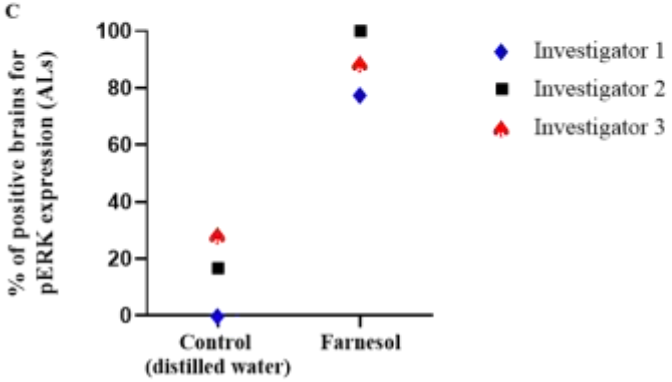

D

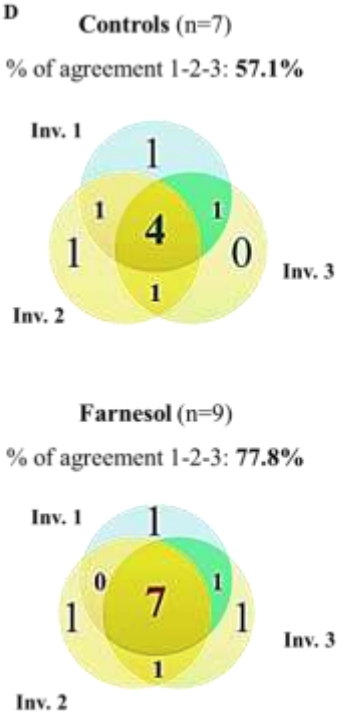

Fig. 9: Farnesol stimulus increases pERK expression in the antennal lobes.
Blinded visual scoring from 3 impartial investigators for the absence (scored as 0) or presence (scored as 1) of pERK expression in the antennal lobes (**Tables A and B**). **Tables A1 and B1** show the percentage of brains scored as having expression of pERK in the antennal lobes by each individual observer, in both control and experimental situations, respectively. Control flies (n=7) were exposed to distilled water, as previously described (**Fig. 1**) and 15.1% of the brains were considered to have pERK in the antennal lobes (**Table A1**). Experimental flies (n=9) were exposed to farnesol solution (see **Fig. 1**) and 88.9% of the brains presented pERK expression in the ALs, according to the investigators (**Table B1**). (**C**) Percentage of positive brains for pERK expression in the ALs in both control and farnesol experimental conditions, scored by the investigators. The brain classified as NA (non-applicable, **Table A**) was removed from the statistical analysis. Brain numbers highlighted in red (**Tables A and B**) were used to distinguish brains with different scores. (**D**) Illustrative Venn Diagrams show the relationship between all investigators in control and farnesol conditions. All investigators show 57.1% of agreement in control brains and 77.8% of agreement in farnesol condition. NA-scored brain (**Fig. 3A**) was included in the ratio of agreement analysis.

In order to define a region of interest in the antennal lobes and automatically quantify the expression of pERK, we established a specific method, considering the observable pERK staining in the experimental brains. As outlined above, male flies exposed to farnesol show a stronger pERK labeling in the antennal lobes, when compared to the control flies (see **Fig. 8**). Therefore, we draw two ellipses around the areas with increased pERK expression, and used them as regions of interest in left and right antennal lobes (ROIs1L and ROIs2R, respectively). In order to apply the same ROI in control brains, where weak or no pERK expression was present, we devised a coordinate system. Briefly, we defined two orthogonal axis (x,y) that spanned the height and width of each AL. We then used these axis to define the coordinates of the center of the ROI by measuring the distance (x,y) from the center of the ROI to the axis (performing the same operation on each side of the brain). This method was applied to all experimental brains. We next computed an average ROI, based on the average coordinates (x,y) values, for each AL. To test whether an average ROI capture most ROIs, we applied the average ROI to each experimental brain and compared fluorescence within the average ROI to that of the originally defined ROI (drawn for each brain). Since we found similar values for average and original ROIs, we proceeded to apply the average ROI to control brains mapped onto the AL coordinate axis drawn for each brain. In addition, since differences in fluorescence within the ROI may be due to general changes in fluorescence in the rest of the AL (or even the whole brain), we compared fluorescence in the ROI to neighboring regions defined as background. We used the same ellipse area, using the same coordinate system explained above, to define two background regions (background 1, B1 and background 2, B2). We used two background regions to test whether the region chosen for background within AL mattered, i.e. to check whether our analysis was robust and independent of background region used. pERK fluorescence within the ROI was normalized to each background separately.

As shown in **Fig. 10**, we tested whether the ROIs and backgrounds were consistently positioned in the ALs (**see Fig. 10B** with the average ROIs and backgrounds) and the pERK fluorescence was measured in both situations. Since the average pixel intensity was not significantly different between ROIs in both left and right antennal lobes, when compared to that of average ROIs (Mann-Whitney U test, p=0.9314 and p=0.8633, respectively), we applied the average ROIs and backgrounds to control brains (see **Fig. 10C**), as shown in **Fig. 10F** and **G**. The fluorescence intensity values were normalized to the backgrounds 1 and 2 (see appendix I, **Fig. 1** for absolute values). The normalized pixel intensity was significantly higher for flies exposed to farnesol relative to controls, regardless of which background was used for normalization (Mann-Whitney U test, ** denotes p=0.0012, *** denotes p=0.0007, respectively). These results clearly show a significantly higher pERK expression in a specific glomerulus area, which is expected to be activated by farnesol stimulus.

This finding was a very encouraging result and motivated us to further investigate this neuronal activation in the antennal lobe. We needed to verify whether this specific region, with increased pERK expression was in fact the glomerulus known to respond to farnesol.

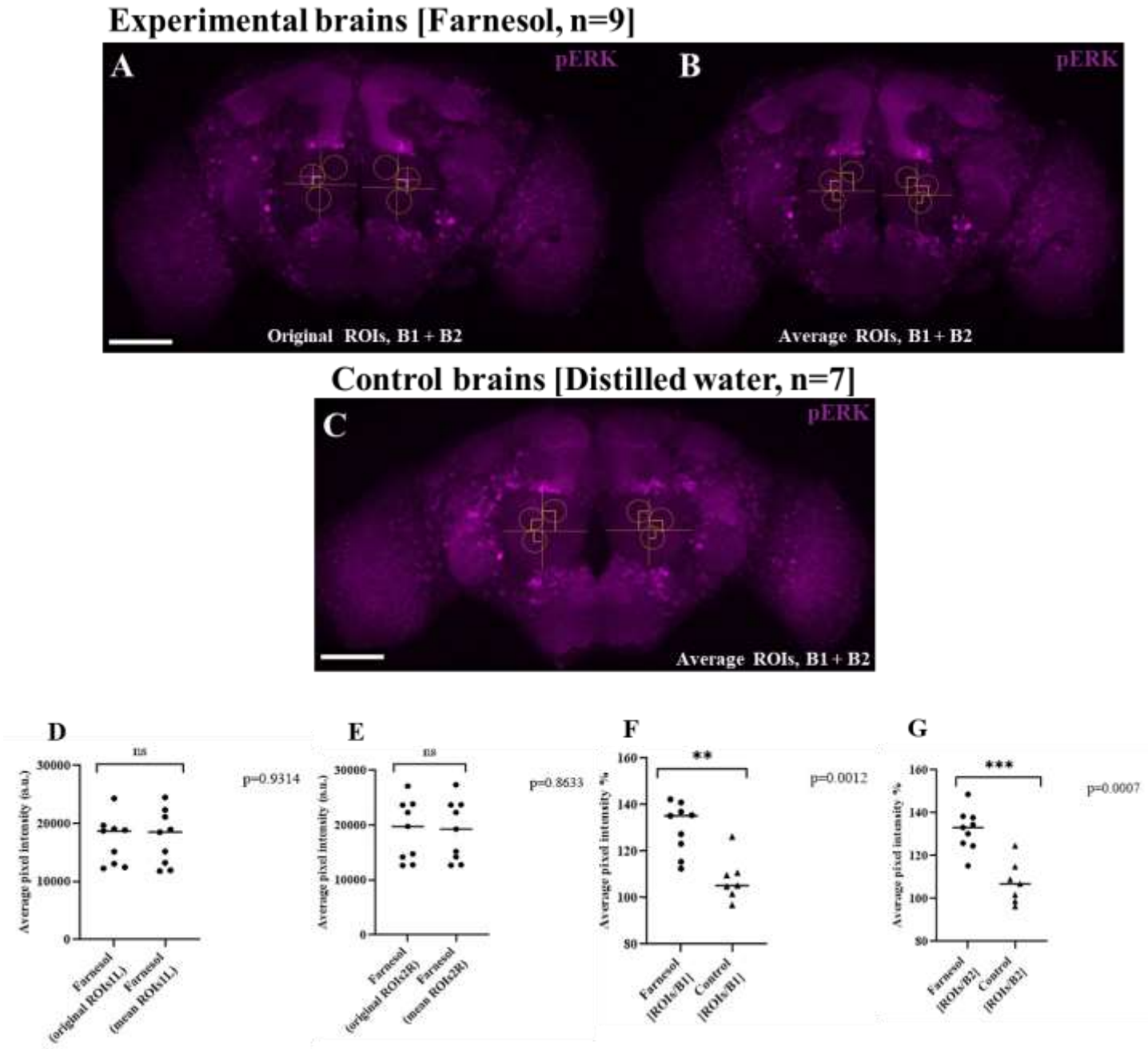

Fig. 10: WT brains show a higher pERK expression in the antennal lobes upon farnesol stimulation.
(A) Experimental fly brains were used to draw the original ROIs (yellow ellipse) around the area with stronger pERK staining in the left (ROIs1L) and right (ROIs2R) antennal lobes. Axes x (horizontal) and y (vertical) were drawn inside each of the ALs as a reference to calculate the distance (coordinates x,y) between the center of each area of interest (white highlighted in **A**) and the respective axes. The two yellow ellipses in the upper (background 1, B1) and bottom (background 2, B2) positions in the antennal lobes were used as background areas for each ROI and all coordinate values were also noted. (**B**) Experimental fly brains were tested with the mean size (area 456.8 μm, width 24.18 μm and height 22.97 μm) and the mean coordinate values of the ROIs1L (-11 μm, 10 um) and ROIs2R (10 μm, 13 um). (**C**) Control brains were tested with the average ROIs from the experimental condition. All images are confocal ZProjections (4-8 slices, as maximum intensity projections) of fly brains stained for anti-pERK (**A-C**, in magenta) for experimental and control brains. Scale bars represent 53 μm (**A-C**). (**D-E)** Average pixel intensity (a.u) of the original ROIs and mean ROIs for left and right ALs in experimental brains, respectively. (**F-G)** Ratio of pERK fluorescence intensity in experimental and control brains, normalized to the B1 and B2, respectively. P-values result from Mann-Whitney statistical analysis. ** denotes p= 0.0012, *** denotes p= 0.0007, ns not significant.

pERK as a reporter of neural activity in Or83c-expressing neurons

Farnesol was previously identified as a potent and specific activator for the orphan odorant receptor Or83c[69], which is expressed in the olfactory neurons that innervate the DC3 glomerulus in the antennal lobes. To confirm whether pERK expression in WT brains (see **Fig. 8**) was in fact a response of those neurons when stimulated, we crossed Or83c-Gal4 males with UAS-CD8::GFP female flies. CD8 is a transmembrane protein and therefore the Or83c neurons surface was labeled with CD8-GFP fusion protein. The progeny of this cross will allow us to specifically localize these neurons and confirm our hypothesis for co-localization with pERK after farnesol stimulation. Male flies were exposed to distilled water (control) or farnesol solution (experimental protocol in **Fig. 7**), as mentioned before. After the stimulation protocol, male flies were dissected, fixed and stained for both GFP and pERK antibodies (**Fig. 11**). Or83c-expressing neurons are labeled in green (**Fig. 11**, **A** and **D**), whereas pERK labeling is represented in magenta **(Fig. 11**, **B** and **E)** in both control and experimental conditions. To confirm whether we have GFP and pERK co-labeling, which indicates that our olfactory neurons were active upon stimulation (pERK labeling), we defined a contour around the DC3 glomerulus in the green channel and kept the obtained ROI to quantify fluorescence in the magenta channel (**Fig. 11**, **A'-B' zoomed-in**, **D'** and **E'' zoomed-in**). In this approach, according to a qualitative evaluation of the brain images, we have increased pERK activity in the Or83 glomerular expression region in experimental condition (**Fig. 11**, **E'-E''** and **F')** when compared to control (**Fig. 11**, **B'-C'**), and so suggesting that pERK activity in the AL is in fact a response to the odor stimulus. As previously performed, we asked the 3 impartial investigators to blindly score all the brains in both control and experimental condition (see Appendix II, **Fig. 1, Tables A and B)**. Additionally, the same analysis parameters were considered for co-localization between GFP and pERK expressions in the DC3 glomerulus and also the percentage of agreement between the researchers (see Appendix II, **Fig. 1C and D**, respectively).

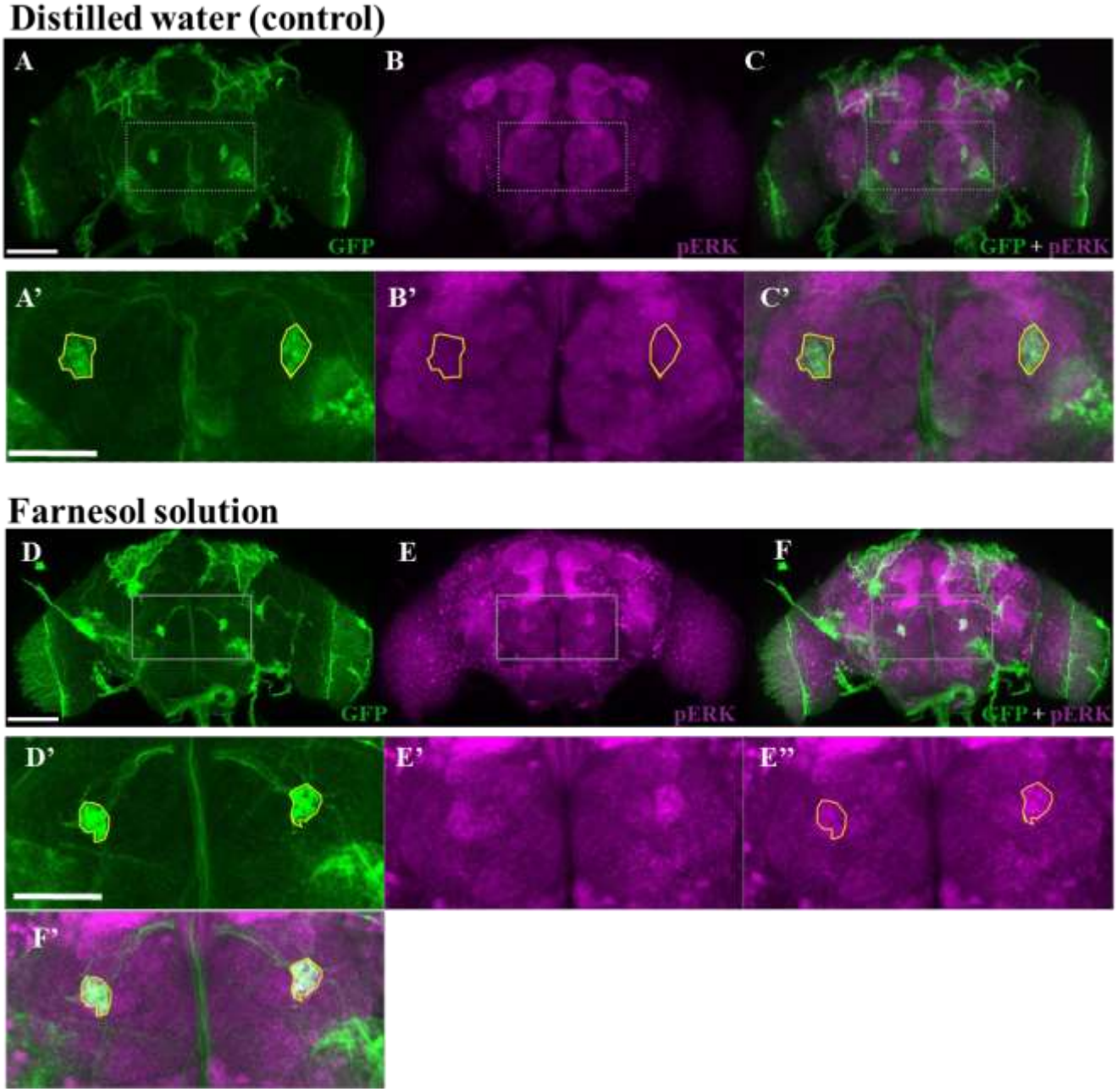

Fig. 11: pERK is a reporter of neural activity in Or83c-expressing neurons.
Or83c-Gal4;UAS-CD8::GFP flies were exposed to distilled water (**A-C** controls, n=15) and farnesol solution (**D-F**, n=17) for 1 minute and dissected after 20 minutes (see protocol **Fig. 7**). All images are confocal ZProjections (6-8 slices, as maximum intensity projections) of fly brains stained for anti-GFP (**A** and **D**, in green) and phosphorylated-ERK (**B** and **E**, in magenta). **C** and **F** images show the merge channels for both control and experimental brains, respectively. **A'-C'** are zoomed-in images of **A-C,** with a contour around the DC3 glomerulus in control brains. **D'**, **E''** and **F'** are zoomed-in images of **D-F,** with a contour around the DC3 glomerulus in experimental brains. **(E')** Zoomed-in of **E** without the contour to clearly identify pERK expression in this area. Scale bars represent 70 µm (**A-F**) and 26 µm (**A'-F'** and **E''** zoomed-in images).

To further investigate these observations and test whether we actually have a higher pERK fluorescence in the Or83c neurons, we decided to automatically quantify the pERK fluorescence in a similar way to the previous experiment. We took advantage of the DC3 glomeruli anatomy in the green channel and defined a contour around each glomerulus to quantify the pERK fluorescence in experimental (**Fig. 12A and B**) and control brains (**Fig. 12C** and **D**). Furthermore, we identified two other regions as backgrounds (B1 and B2), as in the previous experiment. As shown in **Fig. 12E** and **F**, the fluorescence intensity values were normalized to the backgrounds 1 and 2 (see appendix I, **Fig. 2** for absolute values). The average pixel intensity was significantly higher for flies exposed to odor stimulus in relation to controls (Mann-Whitney U test, ** denotes $p=0.0010$, *** denotes $p<0.0001$, respectively). Altogether, these results show a significantly higher average intensity of pERK expression in the DC3 glomerulus after the odor stimulus, which in fact supports our hypothesis of pERK increased expression as a readout of neuronal activity.

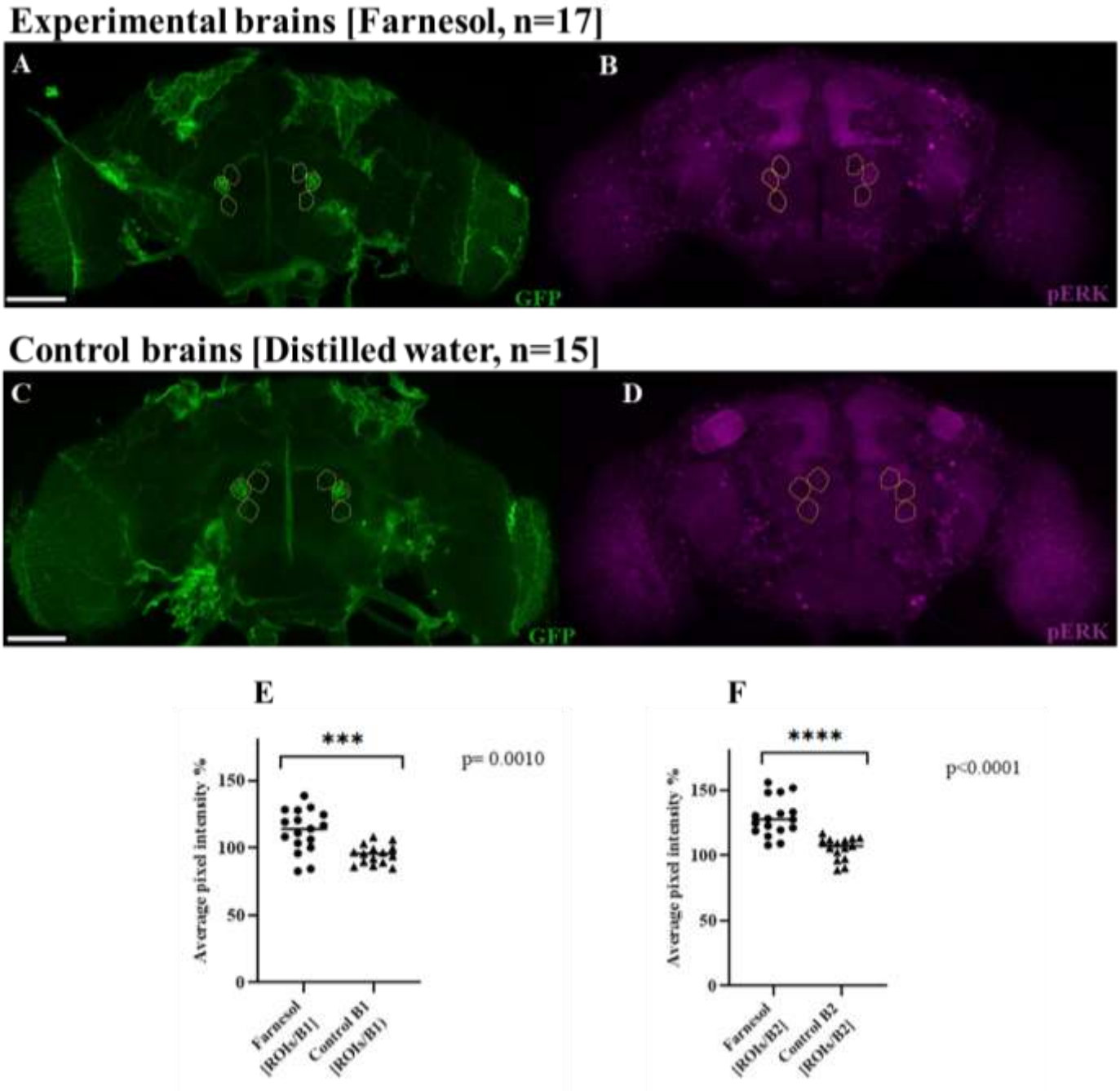

Fig. 12: Or83c-Gal4;UAS-CD8::GFP fly brains show a significant higher pERK expression in DC3 glomerulus upon farnesol stimulation.

(A-B) We defined a contour around the DC3 glomerulus in the green channel (**A**) and kept the obtained ROI to the magenta channel (**B**) in both left and right antennal lobes of the experimental flies. The same ROI area for each glomeruli was used as a reference to the backgrounds 1 (upper B1) and 2 (bottom B2). (**C-D**) Control brains were also tested with a contour around the DC3 glomerulus, first obtained in the green channel. All images are confocal ZProjections (6-8 slices, as maximum intensity projections) of fly brains stained for anti-GFP (**A-C**, in green) and anti-pERK (**B-D**, in magenta) for experimental and control brains. Scale bars represent 70 μm. (**E-F)** Ratio of pERK fluorescence intensity in experimental and control brains, normalized to the B1 and B2, respectively. P-values result from Mann-Whitney statistical analysis. *** denotes p= 0.0010, **** denotes p< 0.0001.

Silencing Or83c neurons and pERK expression in the DC3 glomerulus

Taken together, our previous results showed that pERK expression is increased in the Or83c neurons after farnesol exposure. Therefore, we decided to investigate whether we could artificially silence DC3 neurons and directly reduce pERK expression in those neurons.

Since ion channels are important and determinant molecules of excitability, manipulation of their levels and properties allows neuronal modulation and affects the function of the circuits. In flies, there are many ways to suppress neuronal activity by overexpression of potassium channels, such as the inward rectifier K^+ channel (Kir 2.1)[74]. This electrical activity suppression leads to an increased potassium efflux and membrane hyperpolarization. Therefore, the resting membrane potential remains below the threshold required to fire action potentials (APs). To confirm whether pERK expression is affected when we silence Or83c-expressing neurons triggered by the presentation of farnesol, we first crossed Or83c-Gal4 males with 10xUAS-Kir2.1::eGFP female flies. Kir2.1 is fused with an enhanced green fluorescent protein (eGFP), so we will be able to drive the expression of Kir2.1 tagged with eGFP in the DC3 glomerulus. The progeny of this cross will allow us to accurately localize the Or83c neurons and confirm whether we have an effect on pERK expression in these neurons. As a control for this experiment, we chose individual male flies from each parental line (Or83c-Gal4 and 10xUAS-Kir2.1::eGFP flies). Both control and experimental male flies were exposed to farnesol solution (experimental protocol in **Fig. 7**). After the stimulation protocol, male flies were dissected, fixed and stained for both GFP and pERK antibodies (**Fig. 13**). Or83c neurons are only green labeled in the experimental condition (**Fig. 13E**), since parental controls are missing either the UAS-sequence (control 1) or the promoter region (control 2) to drive GFP expression in these neurons. The expression of pERK is labeled in magenta (**Fig. 13B**, **D** and **F**) in both control and experimental conditions. Merge channels are shown to confirm whether we have co-staining between GFP and pERK in experimental condition (**Fig. 13G** and **G'** zoomed-in). The experimental brain images show no apparent pERK expression upon farnesol stimulus (**Fig. 13G-G'**), which supports the inactivation possibility of the Or83c neurons, as previously expected. Nevertheless, control brains also lack pERK expression in the antennal lobes, which indicates that the stimulation protocol may not have worked properly.

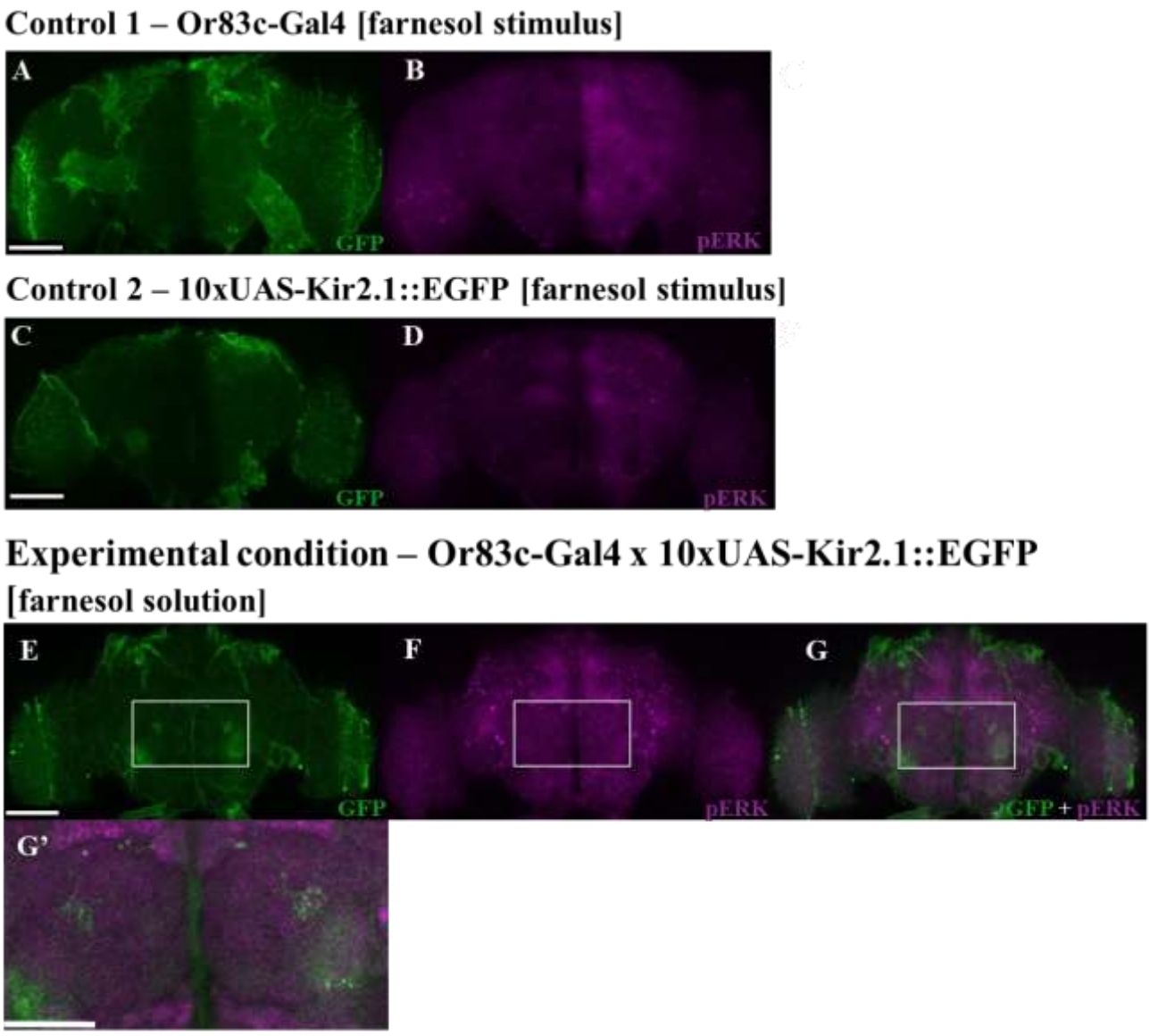

Fig. 13: Silencing Or83c neurons with Kir2.1 in the DC3 glomerulus.
(**A-D**) Parental controls 1 (n=7) and 2 (n=7) were exposed to farnesol solution for 1 minute and dissected after 20 minutes (see protocol **Fig. 7**). (**E-G**) Experimental flies (n=10) were also exposed to farnesol solution, as mentioned above. (**G'**) Zoomed-in of **G** to clearly identify the DC3 glomerulus and co-staining possibility. All images are confocal ZProjections (4-10 slices, as maximum intensity projections) of fly brains stained for anti-GFP (**A**, **C** and **E**, in green), anti-pERK (**B**, **D and F**, in magenta) and merge channels (**G**) for control and experimental brains, respectively. Scale bars represent 53 µm (**A-G**) and 26 µm (**G'** zoomed-in image).

To further investigate these observations, we performed the blinded visual scoring and the percentage of agreement from 3 impartial investigators, as described earlier (see appendix II, **Fig. 2, Tables A** and **B**). Finally, as previously shown in WT brains (see **Fig. 10**), we applied a similar strategy to quantify pERK fluorescence in control and experimental brains. We defined two regions of interest in left and right antennal lobes in the experimental condition, as shown in **Fig. 14A** and **B**. To confirm whether these ROIs were consistently positioned in the ALs (see **Fig. 14C** and **D** with the average ROIs), we compared the average pERK fluorescence in the original ROIs with the average ROIs (**Fig. 14E** and **F**). Since the average pixel intensity was not

significantly different between ROIs in both left and right antennal lobes when compared to that of average ROIs (Mann-Whitney U test, $p=0.9705$ and $p> 0.9999$, respectively), we applied the average values of ROIs to control brains (see **Fig. 14E and F**), as shown in **Fig. 14G** and **H**. The fluorescence intensity values were normalized to the backgrounds 1 and 2 (see appendix I, **Fig. 3** for absolute values) in **Fig. 14I and J**. The average pixel intensity was not significantly different between experimental condition and control flies relative to B1 and B2 (Kruskal-Wallis test, $p\approx0.8920$ and $p\approx0.1286$, respectively). The statistical result revealed a non-significant difference between controls and experimental conditions. Altogether, these results show that this genetic manipulation to silence the Or83c neurons was not efficient, as we have no visible pERK expression in control brains, which we expected to see based on previous results with WT brains. Therefore, we consider that this experiment didn't work properly to further evaluate the results.

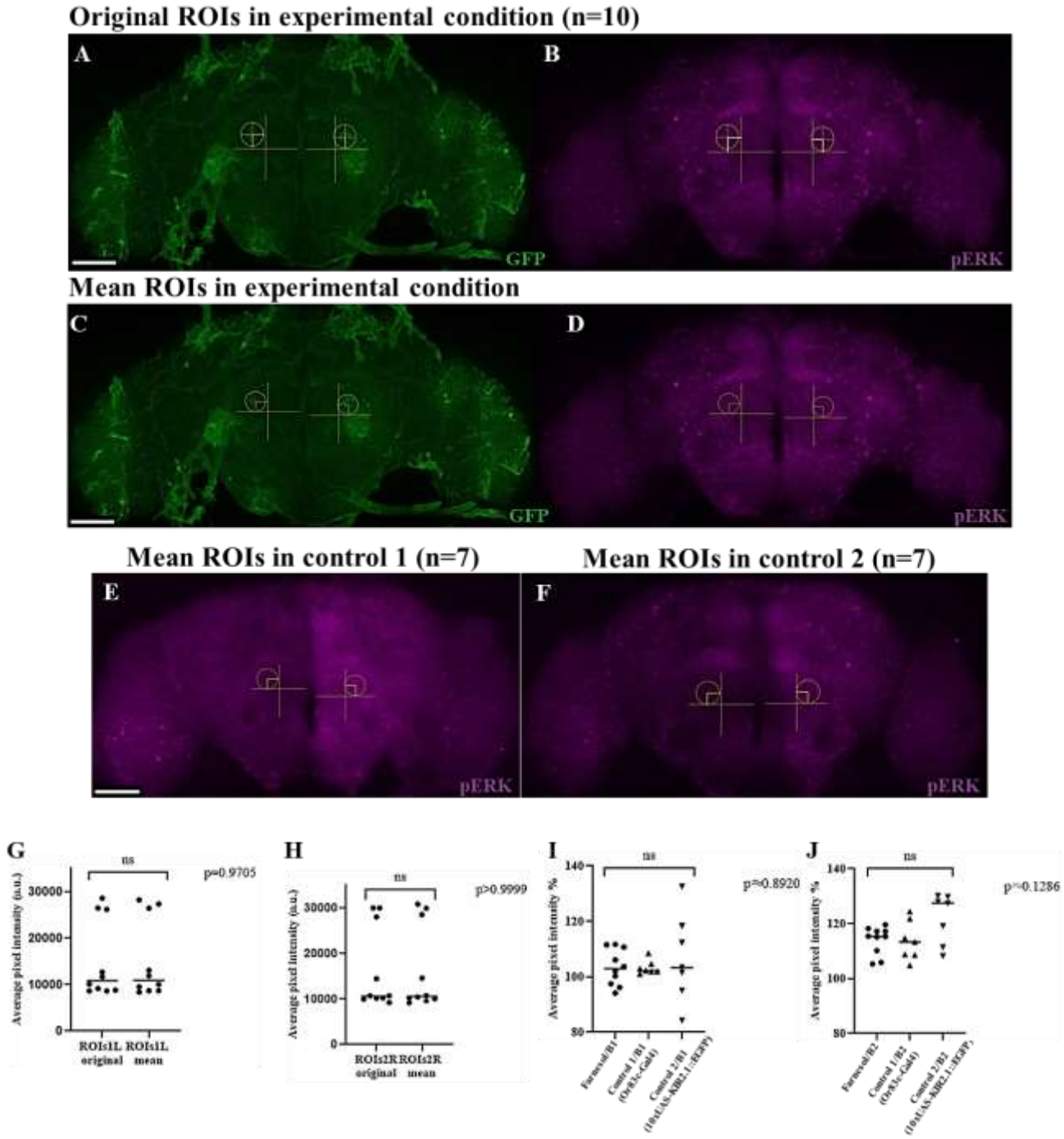

Fig. 14: Inactivation of Or83c-expressing neurons shows no significant difference between conditions.
(A-B) Experimental fly brains were used to draw the original ROIs (yellow ellipse) around the DC3 glomeruli in the left (ROIs1L) and right (ROIs2R) antennal lobes. Axes x (horizontal) and y (vertical) were drawn inside each of the ALs as a reference to calculate the distance (coordinates x,y) between the center of each glomeruli (white highlighted in **B**) and the respective axes. (**C-D**) Experimental fly brains were tested with the average ROIs (for each: area 518.519 µm, width 25.24 µm and height 25.14 µm) and the average coordinates x,y for each AL in relation to the axes (left AL -11 µm, 14 µm and right AL 12 µm, 11 µm). (**E-F**) Average ROIs were tested in control brains. All images are confocal ZProjections (4-10 slices, as maximum intensity projections) of fly brains stained for anti-GFP (**A** and **C**, in green) and anti-pERK (**B** and **D** for experimental condition and **E-F** for controls, in magenta). Scale bars represent 53 µm. (**G-H)** Average pixel intensity (a.u) of the original ROIs and mean ROIs for left and right ALs in experimental brains, respectively. (**I-J)** Ratio of pERK fluorescence intensity of experimental condition (Or83c-Gal4; 10xUAS-Kir2.1::eGFP), control 1 (Or83c-Gal4) and control 2 (10xUAS-Kir2.1::eGFP), normalized to the B1 and B2, respectively. P-values result from Mann-Whitney U test (**G-H**) and Kruskal-Wallis (**I-J**) statistical analysis. ns not significant.

Artificial activation of Or83c neurons and pERK expression in the DC3 glomerulus

Based on our previous results with the natural odor, we knew that pERK expression is increased in the DC3 glomerulus upon farnesol exposure. Next, we asked whether we could artificially activate DC3 neurons and directly increase pERK expression in those neurons.

"Optogenetics" allows light-controlled manipulation of a specific set of neurons, to activate or silence them[14]. In recent years, all the progress in this sophisticated technique has allowed more guided access to neuronal activity with improved sensitivity and spatiotemporal resolution. CsChrimson is a red light (590 nm)-activated cation channel from the red alga *C. subdivisa* and has been shown to effectively lead to neuronal activation in freely behaving flies.[75,76] To confirm whether pERK expression can be affected by direct activation of the Or83c neurons in the DC3 glomerulus, we crossed Or83c-Gal4 male flies with UAS-Chrimson::mVenus female flies. Venus is an artificial derivative of the naturally occurring fluorescent protein encoded by the *Aequorea victoria GFP* gene, so we also labeled Or83c neurons in green, as in the odor experiments. We established 3 different optogenetic activation protocols (**Table 2** and **Fig. 6** in methods). Commonly, the odor information is recognized by one or multiple ORs and sent to different higher brain areas, leading to innate behavioral outputs (e.g. attraction or aversion). Regarding this project, we already knew that farnesol was an attractive odor for flies, but we were not able to identify a behavioral phenotype when we triggered the Or83c neurons with light. For that reason, we chose different protocols to test possible variations in neuronal activity, in response to duration and dynamics of light stimulation. To begin with, we defined a 30 seconds baseline period for exploration (common to all activation protocols) and then a pulsed light protocol (1min, frequency 2 Hz) or 2 continuous light exposures (1min of stimulation or 5 stimuli with 30 seconds ON + 90 seconds OFF), followed by 20 minutes of waiting period before dissection (see **Table 2** and **Fig. 6** in materials and methods section).

Pulsed light stimulation

CsChrimson requires retinal to function and so experimental flies were kept in food containing retinal for 3 days, whereas control animals were raised in vienna food (see **Table 2** in methods section). We chose two control conditions for this protocol, given that control 2 was a negative control for light. After the stimulation protocol (**Table 2** and **Fig. 6**, protocol 1 in methods), flies were dissected and stained for GFP and pERK antibodies (**Fig. 15**). Or83c-expressing neurons are labeled in green (**Fig. 15**, **A**, **D** and **G**), while pERK labeling is presented in magenta (**Fig. 15**, **B**, **E** and **H**) in both controls 1 and 2. In this activation protocol, we can confirm by visual observation that control brains (**Fig. 15**, **B'-C'** and **E'-F'**) have no

obvious co-labeling between GFP and pERK signals, while experimental brains have a gentle expression in the DC3 glomerulus (**Fig. 15, H'-I'** and **H'').** These first observations suggest that we can slightly induce the activation of ERK in the DC3 glomerulus, after pulsed light. In an attempt to validate these observations, we again performed a blinded visual scoring from 3 impartial investigators (see Appendix II, **Fig. 3, Tables A and B)**. The co-localization between GFP and pERK expressions in the DC3 glomerulus were also considered, as well as the percentage of agreement between the researchers (see Appendix II, **Fig. 3C** and **D**, respectively).

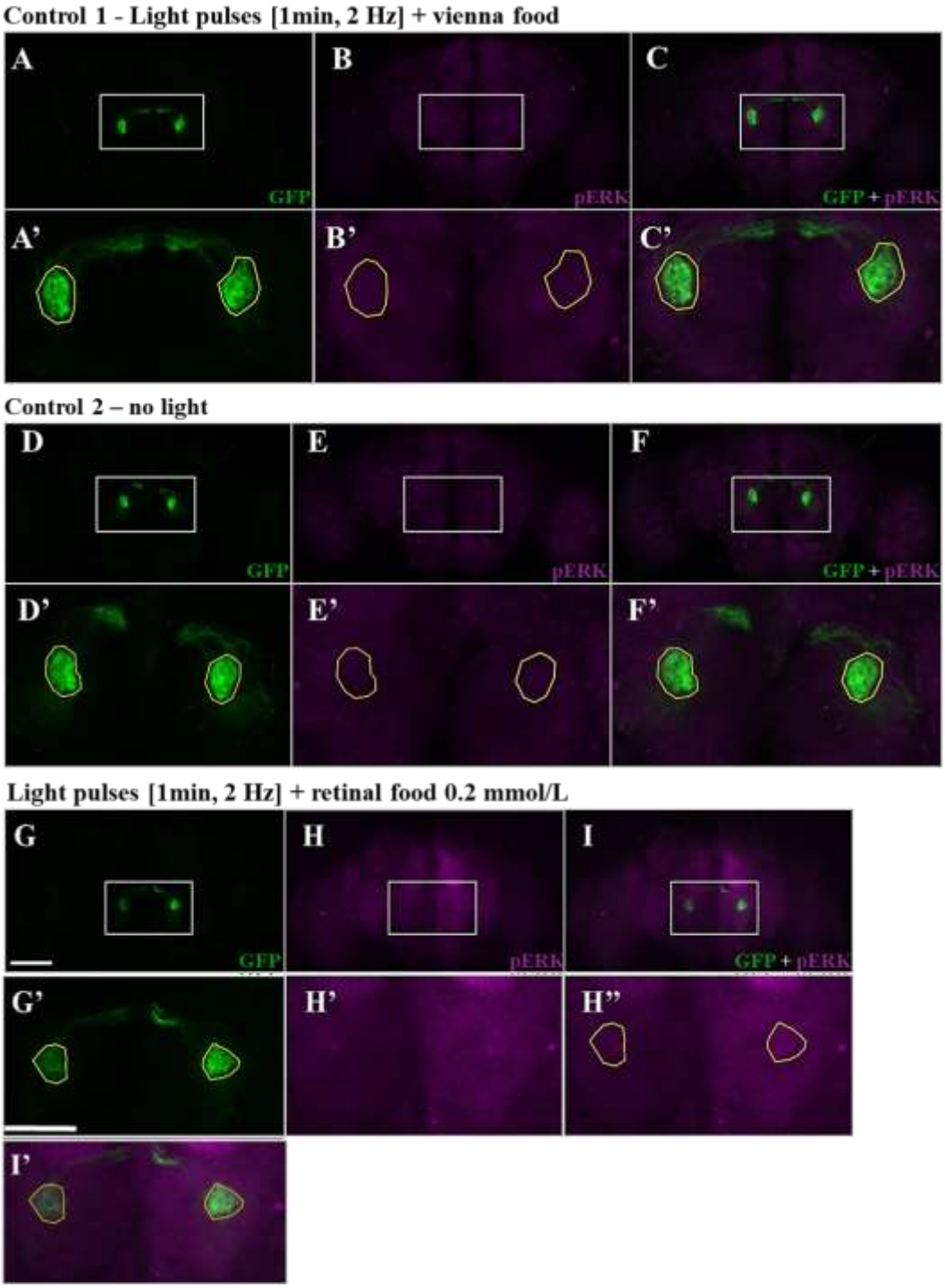

Fig. 15: Optogenetic activation of Or83c neurons in the DC3 glomerulus by pulsed light.
(**A-C**) Control 1 flies (n=4) were kept in vienna food and then exposed to light pulses for 1 minute (see **Table 2** and **Fig. 6** in materials and methods section). (**A'-C'**) Zoomed-in images of **A-C** with a contour around the DC3 glomerulus. (**D-F**) Control 2 flies (n=3) were kept in vienna food and no light stimulus was performed (negative control to the light). (**D'-F'**) Zoomed-in images of **D-F** with a contour around the DC3 glomerulus. (**G-I**) Experimental flies (n=5) were supplemented with retinal 0.2 mmol/L for 3 days and then exposed to pulsed light for 1 minute, as previously described. (**G', H'' and I'**) Zoomed-in images of **G-I** with a contour around the DC3 glomerulus All images are confocal ZProjections (6-8 slices, as maximum intensity projections) of fly brains stained for anti-GFP (**A-A'**, **D-D'** and **G-G'**, in green), anti-pERK (**B-B'**, **E-E'**, **H-H' and H''**, in magenta) and merge channels (**C-C'**, **F-F'** and **I-I'**) for control and experimental brains, respectively. **(H')** Zoomed-in of **H** without the contour to clearly identify pERK expression in this area. Scale bars represent 70 µm (**A-I**) and 26 µm (**A'-I'** and **H''** zoomed-in images).

As previously performed for pERK fluorescence analysis, we used the DC3 glomeruli anatomy to draw our ROIs (see **Fig. 16 A'-B', D'-E'** and **G'-H'' zoomed-in**) and added two other regions as backgrounds (B1 and B2) for both conditions (**Fig. 16**). Experimental brains are shown in **Fig. 16 A-B**, control 1 in **C-D** and control 2 in **E-F** images. The fluorescence intensity values were normalized to the backgrounds 1 and 2 (see Appendix I, **Fig. 4** for absolute values) in **Fig. 16G** and **H**. The average pixel intensity was not significantly different for flies exposed to pulsed light in relation to control 1 and 2 in both left and right antennal lobes (Kruskal-Wallis test, p=0.9172, p=0.3429, ns not significant). These results show that pulsed light stimulation did not lead to reliable Or83c neurons activation in the DC3 glomerulus, since we have no differences between experimental and both control conditions.

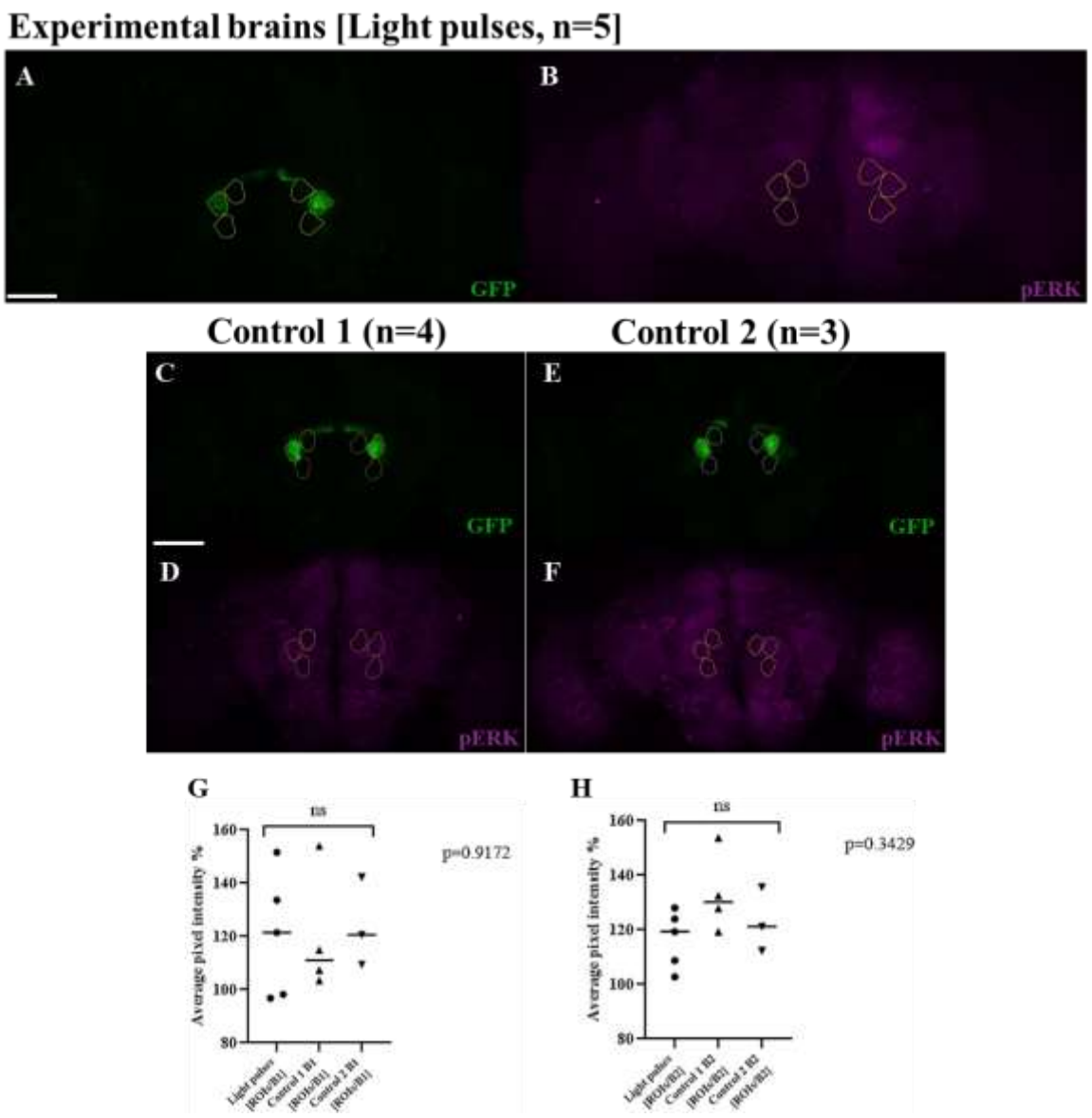

Fig. 16: Pulsed light stimulation does not induce significant expression of pERK in the DC3 glomerulus.
We drew a contour around the DC3 glomerulus in the green channel (**A, C and E**) and kept the obtained ROI to the magenta channel (**B, D and F**) in both left and right antennal lobes of the experimental (**A-B**) and control (**C-F**) flies, respectively. The same ROI area for each glomeruli was used as a reference to the backgrounds 1 (upper B1) and 2 (bottom B2). All images are confocal ZProjections (6-8 slices, as maximum intensity projections) of fly brains stained for anti-GFP (**A, C** and **E**, in green) and anti-pERK (**B**, **D and F**, in magenta) for experimental and control brains. Scale bars represent 70 µm. (**G-H)** Ratio of pERK fluorescence intensity in experimental and control brains, normalized to the B1 and B2, respectively. P-values result from Kruskal-Wallis statistical analysis. ns not significant.

Continuous light stimulation

In this second activation protocol (see **Table 2** and **Fig. 6,** protocol 2 in methods), all experimental and control brains were stained for GFP and pERK antibodies and analyzed as previously described. **In Fig. 17**, we showed control 1 (**A-C**, **A'-C' zoomed-in**), control 2 (**D-F**, **D'-F' zoomed-in**) and experimental (**G-I**, **G'-I'** and **H'' zoomed-in**) brain images. We can visually verify that control brains (**Fig. 17**, **B'-C'** and **E'-F'**) have no prominent co-labeling between GFP and pERK signals, although they are more doubtful when compared to the control brains in pulsed light stimulation (see **Fig. 15 B'-C'**). The experimental brains have a smooth expression in the DC3 glomerulus (**Fig. 17, H'-I' and H''),** similar to the previous experimental protocol**.** As previously performed to corroborate these observations, a blinded visual scoring from 3 impartial investigators was created (see Appendix II, **Fig. 4**).

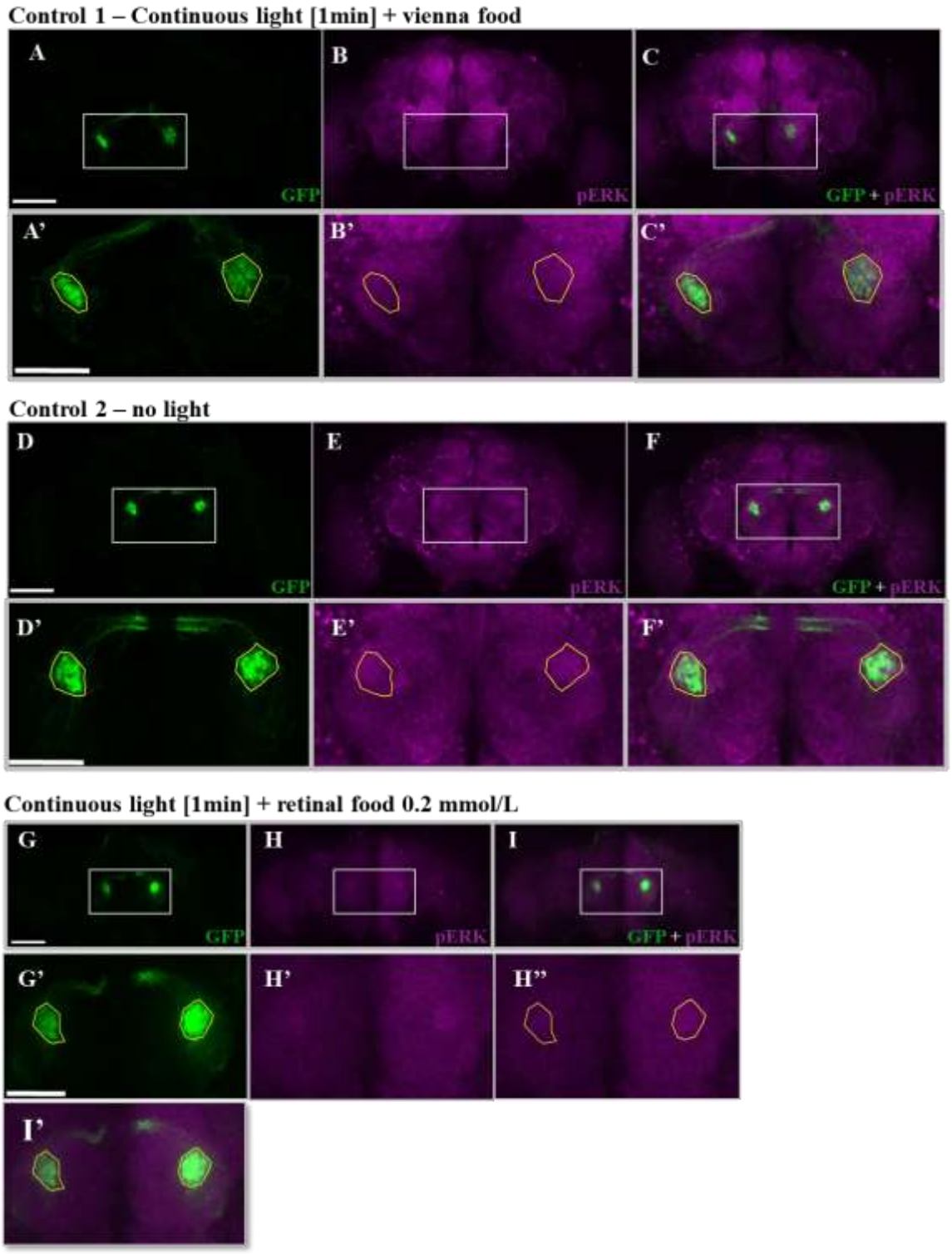

Fig. 17: Continuous optogenetic activation of Or83c neurons in the DC3 glomerulus.
(**A-C**) Control 1 flies (n=3) were kept in vienna food and then exposed to light pulses for 1 minute (see **Table 2** and **Fig. 2** in methods section). (**A'-C'**) Zoomed-in images of **A-C** with a contour around the DC3 glomerulus. (**D-F**) Control 2 flies (n=4) were kept in vienna food and no light stimulus was performed (negative control to the light). (**D'-F'**) Zoomed-in images of **D-F** with a contour around the DC3 glomerulus. (**G-I**) Experimental flies (n=6) were supplemented with retinal 0.2 mmol/L for 3 days and then exposed to pulsed light for 1 minute, as mentioned before. (**G', H'' and I'**) Zoomed-in images of **G-I** with a contour around the DC3 glomerulus All images are confocal ZProjections (6-8 slices, as maximum intensity projections) of fly brains stained for anti-GFP (**A-A'**, **D-D'** and **G-G'**, in green), anti-pERK (**B-B'**, **E-E' H-H' and H''**, in magenta) and merge channels (**C-C'**, **F-F'** and **I-I'**) for control and experimental brains, respectively. (**H'**) Zoomed-in of **H** without the contour to clearly identify pERK expression in the glomerulus. Scale bars represent 70 µm (**A-I**) and 26 µm (**A'-I'** and **H''** zoomed-in images).

To properly supplement the qualitative analysis, we proceed with the pERK fluorescence analysis and used the DC3 glomerulus to draw our ROIs and add two other regions as B1 and B2. In **Fig. 18**, we show the results for the continuous light stimulation protocol in experimental condition (**Fig.18A** and **B**), control 1 (**Fig. 18C** and **D**) and control 2 (**Fig. 18E** and **F**). Similar as before, the fluorescence intensity values were normalized to the backgrounds 1 and 2 (see **appendix I, Fig. 5** for absolute values) in **Fig. 18G** and **H**. The average pixel intensity was not significantly different for flies exposed to continuous light in relation to control 1 and 2 flies (Kruskal-Wallis test, p=0.8782, p=0.9429, ns not significant). As a result of the statistical analysis, we can assume that continuous light stimulation was also not effective to activate our neurons in the DC3 glomerulus.

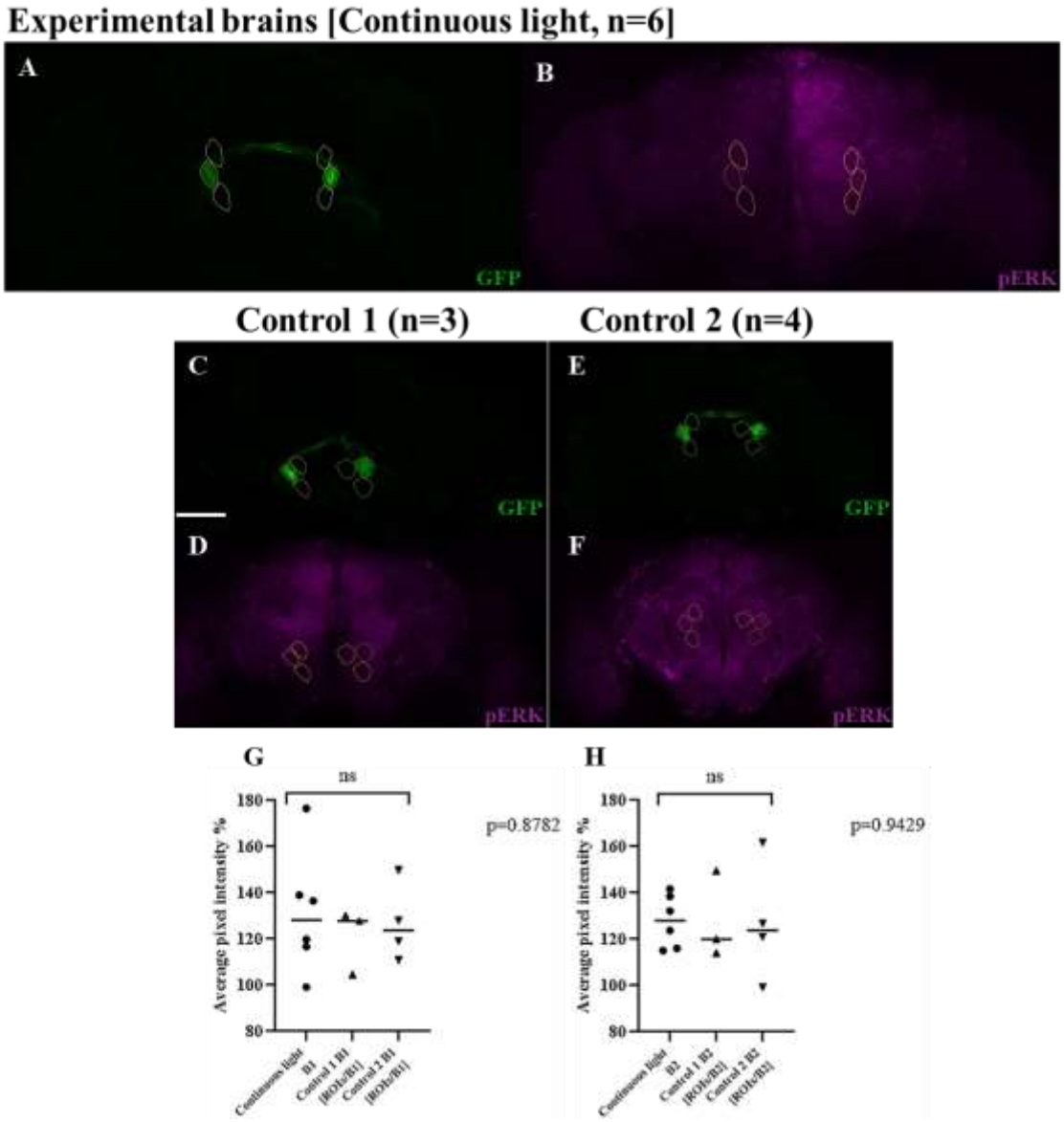

Fig. 18: Continuous light stimulation does not show significant expression of pERK in the DC3 glomerulus.
We drew a contour around the DC3 glomerulus in the green channel (**A, C and E**) and kept the obtained ROI to the magenta channel (**B, D and F**) in both left and right antennal lobes of the experimental (**A-B**) and control (**C-F**) flies, respectively. The same ROI area for each glomeruli was used as a reference to the backgrounds 1 (upper B1) and 2 (bottom B2). All images are confocal ZProjections (6-8 slices, as maximum intensity projections) of fly brains stained for anti-GFP (**A, C** and **E**, in green) and anti-pERK (**B**, **D and F**, in magenta) for experimental and control brains. Scale bars represent 70 µm. (**G-H)** Ratio of pERK fluorescence intensity in experimental and control brains, normalized to the B1 and B2, respectively. P-values result from Kruskal-Wallis statistical analysis. ns not significant.

5 stimuli of continuous light (30sec ON + 90sec OFF)

This last activation protocol (see **Table 2** and **Fig. 6**, protocol 3 in methods) was established to overcome previous inconclusive results with pulsed and continuous light stimulation. Several studies have shown the increased ability of spaced trials to activate important molecular pathways for memory formation, in both invertebrate[77] and vertebrate models[78,79]. At the cellular level, spaced training is characterized by synaptic plasticity generated from spaced stimulations. As noted earlier, the MAPK/ERK signaling cascade is powerfully involved in synaptic plasticity events and also regulates the activity of many transcription factors, such as CREB. Considering this knowledge, we hypothesized that MAPK/ERK signaling cascade could be upregulated during the spaced light stimulation, and in this case, increase pERK levels in the DC3 neurons. For that reason, we performed a longer stimulation protocol, which consisted of 5 stimuli of light during 30 seconds spaced with 90 seconds without light (see **Table 2** and **Fig. 6** in methods section). Experimental male flies were kept for 3 days in retinal-free food, previously supplemented with 0.4 mmol/L of retinal. In contrast, control flies were kept in retinal-free food. After the stimulation period, all experimental and control brains were stained for GFP and pERK antibodies and analyzed, as mentioned above. In **Fig. 19**, we showed control (**A-C**) and experimental condition (**D-F**) brain images. Control brains (**Fig. 19**, **A'-C'**) have no substantial co-labeling between GFP and pERK expressions, according to a qualitative observation of the brains. On the other hand, experimental brains show a slight increase of pERK expression in the DC3 glomerulus (**Fig. 19**, **D'-F'** and **E''**), even though we have some control brains working as confounders in this visual inspection (see **Fig. 6**, appendix II). The blinded visual scoring and the percentage of agreement between the researchers was also noted (Appendix II, **Fig. 5**, **Tables A** and **B**).

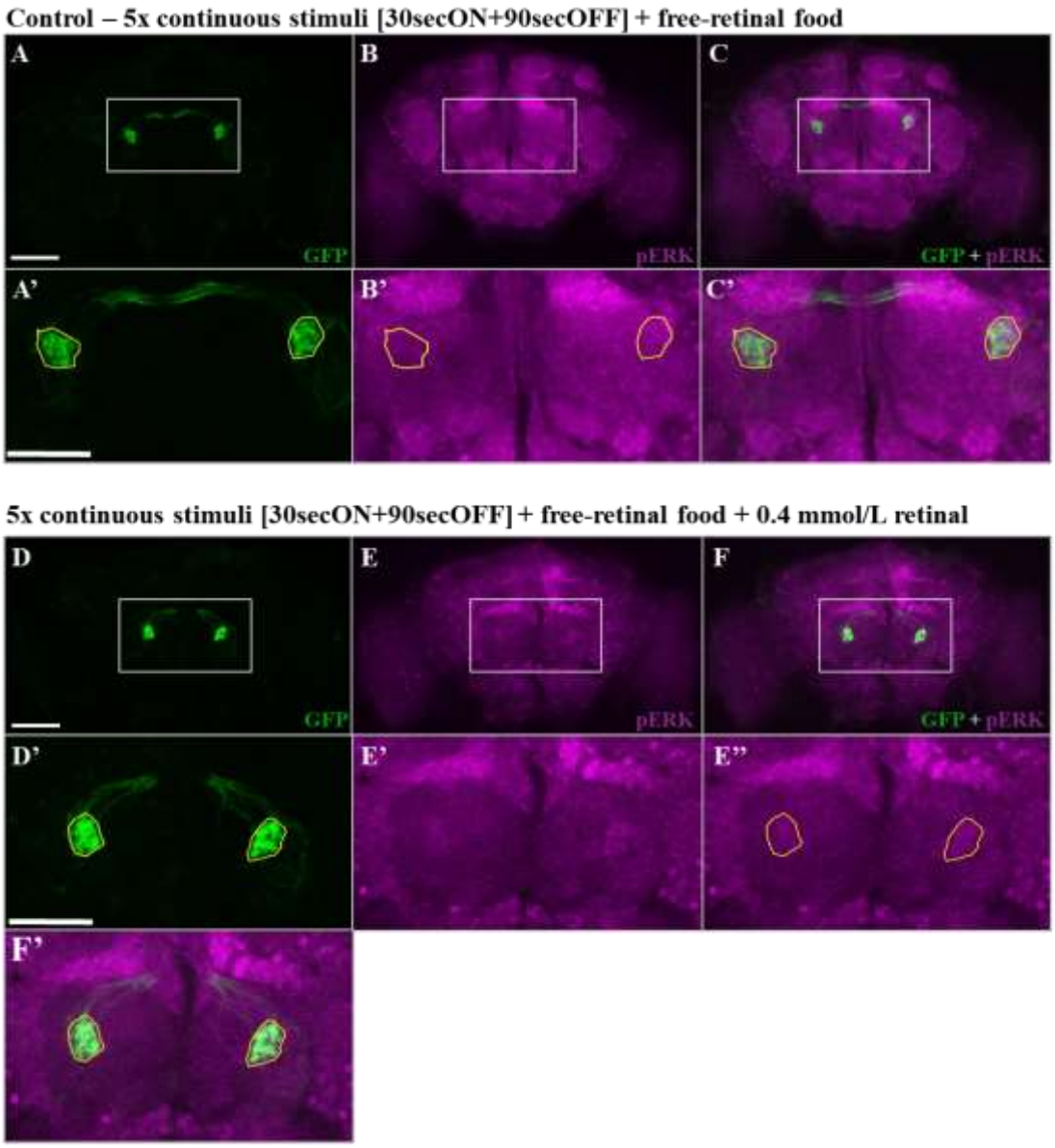

Fig. 19: 5 stimuli of continuous light to trigger Or83c neurons in the DC3 glomerulus.
(**A-C**) Control flies (n=13) were kept in free-retinal food and then exposed to the stimulation protocol (see **Table 2 and Fig. 6** in materials and methods section). (**A'-C'**) Zoomed-in images of **A-C** with a contour around the DC3 glomerulus. (**D-F**) Experimental flies (n=6) were supplemented with retinal 0.4 mmol/L for 3 days and then exposed to stimulation protocol, as previously described. (**D', E'' and F'**) Zoomed-in images of **D-F** with a contour around the DC3 glomerulus. (**E'**) Zoomed-in of **E** without the contour to clearly identify pERK expression in the glomerulus. All images are confocal ZProjections (6-12 slices, as maximum intensity projections) of fly brains stained for anti-GFP (**A-A'**, **D-D'**, in green), anti-pERK (**B-B'**, **E-E'** and **E''**, in magenta) and merge channels (**C-C'**, **F-F'**) for control and experimental brains, respectively. Scale bars represent 70 µm (**A-F**) and 26 µm (**A'-F'** and **E''** zoomed-in images).

We next performed the pERK fluorescence analysis, as shown in **Fig. 20.** The pERK fluorescence quantification was performed in experimental (**Fig. 20A** and **B**) and control (**Fig. 20C** and **D**) flies and normalized to the backgrounds 1 and 2 (see **appendix I, Fig. 6** for absolute values) in **Fig. 20E** and **F**. The average pixel intensity was not significantly different for flies exposed to the 5 stimuli of continuous light in relation to controls (Mann-Whitney U test, $p=0.9547$, $p>0.9999$, ns not significant). These results show that 5 stimuli of continuous light were also not effective to clearly activate our neurons in the DC3 glomerulus.

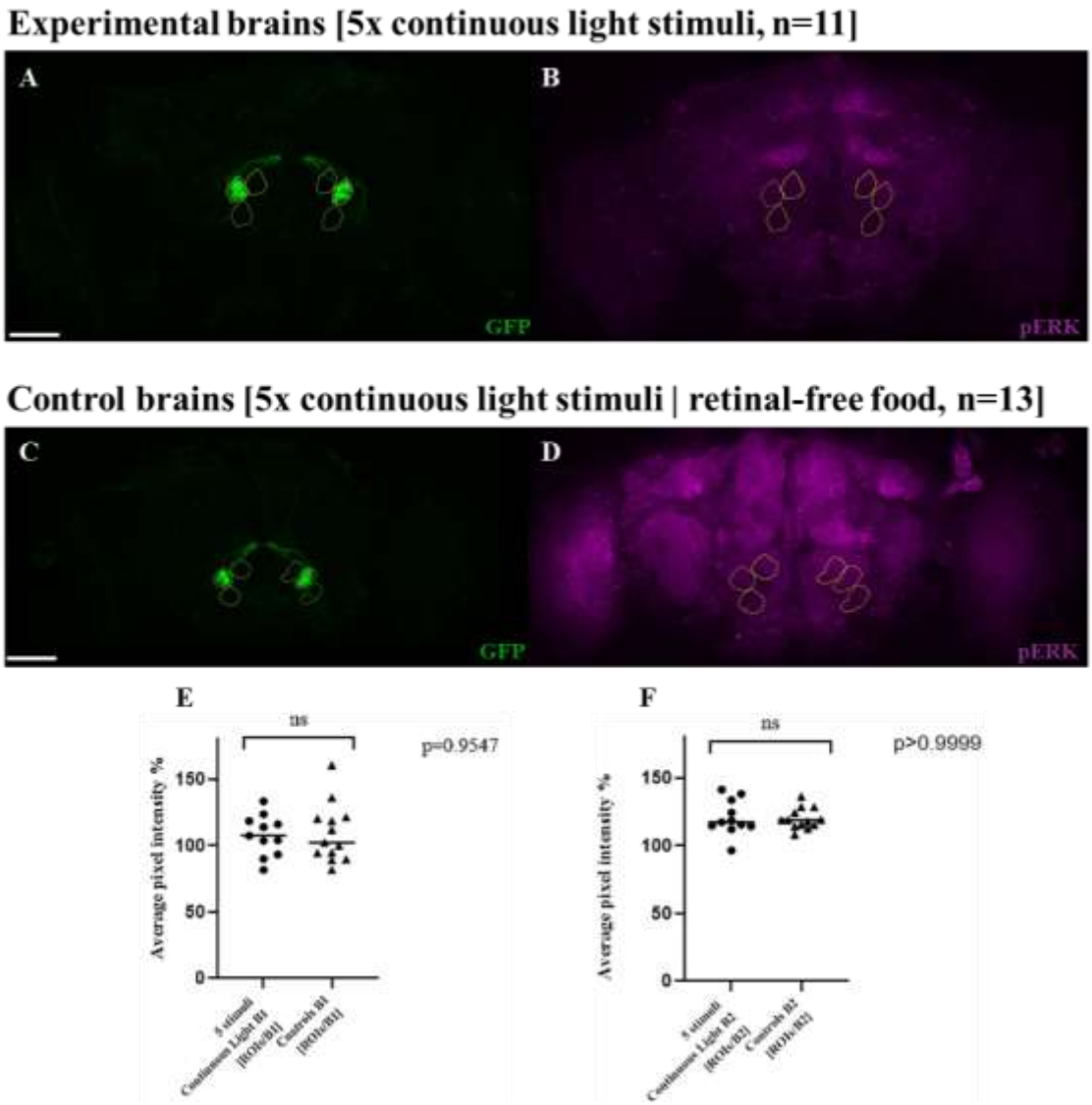

Fig. 20: 5x continuous light stimulation show no significantly higher pERK expresion in the DC3 glomerulus. We drew a contour around the DC3 glomerulus in the green channel (**A and C**) and kept the obtained ROI to the magenta channel (**B and D**) in both left and right antennal lobes of the experimental (**A-B**) and control (**C-D**) flies, respectively. The same ROI area for each glomeruli was used as a reference to the backgrounds 1 (upper B1) and 2 (bottom B2). All images are confocal ZProjections (6-12 slices, as maximum intensity projections) of fly brains stained for anti-GFP (**A** and **C**, in green) and anti-pERK (**B**, and **D**, in magenta) for experimental and control brains. Scale bars represent 70 µm. (**E-F)** Ratio of pERK fluorescence intensity in experimental and control brains, normalized to the B1 and B2, respectively. P-values result from Mann-Whitney statistical analysis. ns not significant

Main conclusions regarding the activation protocols

Taken together these results, we showed that the activation protocols were inconclusive and not efficient to induce reliable pERK expression in Or83c neurons. Regarding the visual observations, and despite the major agreement between the researchers' scores, the fluorescence analysis showed us that none of the protocols was truly successful, as we did not observe any significant difference between controls and the experimental conditions.

Discussion and Conclusions

The ability to monitor neuronal activity is vital for understanding the fundamental mechanisms of animal behavior. Several studies have shown the important role of neuronal activity for the proper formation of neuronal circuits and processes, including synaptic plasticity[2]. In flies, many efforts have emerged with sophisticated approaches to track neuronal activity in freely behaving adults. Electrophysiology recordings and Ca^{2+} imaging have been widely used in the *Drosophila* field, but the physical constraints with immobilized or in-part dissected preparations present a major disadvantage in identifying active neurons, during natural behavior. In order to overcome some of these limitations, we explored an endogenous sensor, ERK phosphorylation, as a readout of recently active neurons in the *Drosophila* brain. With an improved sensitivity in relation to immediate early genes (IEGs), pERK has been widely used to report neuronal responses in different model organisms[40,44,45], including in the olfactory system[57]. Therefore, we selected an external odor stimulus, farnesol, which is an attractive citrus compound and activates well-defined Or83c-expressing neurons in the DC3 glomerulus[69]. We were interested in studying ERK phosphorylation in Or83c neurons upon farnesol exposure and also genetically manipulate their activity to evaluate whether pERK can be used as a readout during artificial manipulation of activity.

WT flies and pERK increased levels in response to farnesol stimulus

In this first experiment, we wanted to confirm the sensitivity of pERK labeling in the Drosophila brain, and most importantly, the ability to label recently active neurons in freely behaving flies. We were focused on pERK expression in the antenna, more particularly in the antennal lobes. The blinded visual scores were very consistent and supported by the fluorescence quantification. The pERK expression was easily observed in the antennal lobe of experimental animals, in contrast with lower pERK expression levels in control brains. We were able to identify a specific region with increased pERK expression in the antennal lobes, when flies were exposed to farnesol stimulus. Our results showed a significantly higher pERK expression after farnesol exposure, which was consistent with our initial hypothesis of using pERK as a readout of neuronal activity.

Activation of Or83c neurons with increased pERK expression in response to farnesol stimulus

Next, we observed the expression pattern of DC3 neurons to confirm whether the previous identified region in WT flies was coincident with O383c-expressing neurons in the antennal lobes. We used the DC3 glomerular morphology, which allowed a more reliable comparison with background regions, with the same shape as the ROI. The pERK fluorescence

analysis showed a significant increase in pERK expression when compared to control flies, which was coherent with the results in WT flies. In summary, these initial results revealed a clear overlap between high pERK levels and Or83c active neurons in the antennal lobes upon farnesol stimulus. Hence, pERK seems to work well as a neuronal activity marker, at least for driven activity in the *Drosophila* antennal lobes.

Or83c silencing and pERK dynamics in the antennal lobe

We observed very encouraging results with the natural odor, and therefore we wanted to further investigate these observations. To confirm whether the pERK signal detected upon stimulus reflects neuronal activity, we evaluated pERK levels when the Or83c neurons were silenced. Regarding the fluorescence analysis, we would expect to see increased pERK expression in control conditions, with normalized values above 100%, in contrast to experimental condition, where we would anticipate normalized values around 100%. Consequently, if farnesol stimulation does not work for some reason, we would see fluorescence values close to 100% in all conditions. On the other hand, if silencing Or83c neurons with kir 2.1 is not successful, but the odor stimulation is, then all the conditions would show fluorescence values above 100%. Our results showed that the inhibition protocol was not enough to revert pERK levels, and so suggesting that the odor stimulus was probably successful, in contrast to the Or83c inactivation. Interestingly, we were surprised by the low levels of pERK in control conditions, since we were expecting to see higher levels of pERK upon farnesol stimulation. This fact could indicate that pERK expression is not a robust tool to track neuronal activity.

One possible future step to explore these results is to test whether total levels of ERK are affected when we silence Or83c neurons. This would allow us to see whether there are any differences between total ERK and pERK levels. In addition, previous studies described that pERK signaling can be independent of neural activity[35], and other studies reported low pERK expression in active neurons[46], which could partially explain why we could not see differences when we silence Or83c-neurons. Therefore, future experiments are required to understand whether our ion channel kir 2.1 line is working and also explore alternative genetic tools to either deactivate or suppress *Or83c* gene (knockdown) or permanently deactivate/remove the gene (knockout, KO) and investigate how pERK expression is affected in the presence of farnesol.

Or83c optogenetic activation and pERK levels in the antennal lobe

Regarding the optogenetic activation of Or83c neurons, we believe that the current study raises important questions on pERK dynamics and its complex relationship with neuronal

activity. It has been previously shown that pERK activity is dependent on the frequency and repetition of neural firing[44,76] and perhaps on the cell type[80]. We established 3 different protocols to confirm whether pERK levels were activity-dependent, considering diverse activation profiles. When we examined the pERK levels, we found no significant difference between experimental and control flies. These results suggest that possibly the activation protocol was not effective to trigger DC3 neurons and that the high levels of pERK expression may be independent of activity.

It is also worth mentioning that there was a visible overall neuronal activity, around the DC3 glomerulus region. In all activation protocols, we identified pERK expression in adjacent regions to the glomerulus, and so we wonder whether there is some sort of internal connectivity within glomerular structures. Briefly, if that is the case, we would be able to induce pERK labeling on surrounding neurons in response to a stimulus, which is challenging in terms of specificity and accuracy of this method.

Challenges with methodologies and brain image analysis

Most studies with pERK expression in flies were performed during embryonic or larval development, and therefore, the first challenging task was to establish an immunostaining protocol adapted to adult *Drosophila* brains. In our paradigm, flies were exposed to the odor stimulus and dissected after 20 minutes. We also tested different period lengths between stimulus and tissue collection (10 seconds and 5 minutes), based on previous studies that reported ERK expression within 1 to 5 minutes of activation[45,52]. However, in our experimental condition, tissue collection 20 minutes after stimulation showed a more robust and uniform expression of pERK, and so we chose this time point for all experimental protocols.

Immunohistochemical methods were combined with both qualitative observations and fluorescence quantification to determine pERK activity changes in response to the stimulus. The blinded visual scoring results were compared with a quality criterion for brain dissection (Appendix II, **Table 1** and **Fig. 7**). The partial overlap between bad brains and researchers' disagreement shows that this is a determining factor for the qualitative results (see a differently scored brain in Appendix II, **Fig. 6**). Other parameters could also work as confounders and mask the results, such as the staining quality (we observed a non-specific labeling of the anti-GFP antibody in our stainings), antibodies and laser penetrance into tissue and human manipulation of samples. Moreover, excitation light introduces some limitations in relation to photobleaching and autofluorescence. Additionally, *post-mortem* studies can limit the experiments with freely behaving animals, as they obey a defined and restricted time window. Hence, the pERK expression is conditioned to the neuronal activation pattern at a particular moment and not exactly when the animal is performing the behavior. Still, our results showed

an actual increase in pERK expression upon natural stimulus, which opens a new path to study neuronal activity in the *Drosophila* brain.

Future directions

This project has shown how neuronal activation in the *Drosophila* brain can be identified by an endogenous sensor, ERK phosphorylation, upon stimulation. Our results open a new perspective for future research in freely behaving flies and their natural behaviors, which is fundamental in understanding neuronal activity. Most of the studies are focused on creating functional tools to establish whole brain activity maps for particular behaviors. In our study, we observed a broad pERK expression in the fly brain, which supports the sensitivity aspect of the tool, but highlights the increased baseline activity, even in unstimulated brains.
Hence, it could be difficult to address activation patterns on a given behavior with pERK expression, but it can be very useful to understand the activation profile of labeled neurons.

Initially, we showed an increased pERK expression upon farnesol exposure, which is a promising result to test other stimulation paradigms in unrestrained flies. We performed both qualitative and quantitative analysis, highlighting the strength and the challenging aspects of both methods. One possible strategy to improve the accuracy of the quantification method is to perform a macro analysis (an automated input sequence). The macro analysis will allow us to randomly create multiple background areas, with the same shape as ROIs in the antennal lobes, and perform a more robust fluorescence analysis. Moreover, the macro analysis is able to register brain samples and perform a fluorescence signal comparison between ROIs and all the clearly defined glomeruli in the antennal lobes.

To confirm that pERK can be used as a neuronal activity marker, other strategies to measure neuronal activity may be used and correlated with pERK levels. TRIC[19] (a transcriptional reporter of intracellular Ca^{2+}) and Hr38[28] (an IEGs recently described in flies) are possible candidates to measure neuronal activity and evaluate pERK expression. These two reporters are non-invasive approaches, that provide stable and reproducible labeling of neurons and can be performed in freely behaving animals. TRIC can integrate changes in activity over time and allows a specific access to neurons, regarding their activity. One the other hand, Hr38 is rapidly induced and has been used to visualize and optogenetically reactivate neural circuits activated upon male courtship behavior. It would be interesting to confirm whether pERK expression is increased in previously identified neurons in courtship behavior responses. In addition to these methods, bioluminescence calcium indicators, such as GFP-Aequorin[16] (which relies on a chromophore to emit light), shows a good spatio-temporal resolution to record the activity of specific neurons in unrestrained flies. Taking advantage of the GAL4-UAS binary expression system, we could label the neurons of interest and see GFP and pERK co-localization signals in our neurons of interest.

Regarding the stimulation protocol, we could also test a different well-dissected circuitry to test neuronal activity and pERK levels. In *Drosophila*, axons of the CO_2-sensitive neurons in sensilla project to a single glomerulus in the antennal lobe (V-glomerulus), which has been previously shown to be responsive to CO_2[81,82]. Therefore, we could test whether we have pERK increased levels in the V-glomerulus, when flies are exposed to CO_2 stimulus.

A possible different strategy is to test a new live sensor of ERK activity, miniCic reporter[83], whose activity is inversely proportional to pERK expression.

We lacked a tool to measure neuronal activity in a specific subset of neurons, but now (considering some limitations), we can use pERK expression in specific neurons to test their activity responses. Recently in the laboratory, we have identified other descending neurons required for freezing behavior. It will be interesting to confirm whether these neurons show increased pERK levels when flies display the defensive response. This insight could lead us to important findings about the visual circuit and perception integration in our behavioral paradigm.

Altogether, our findings unlock a great opportunity in the *Drosophila* field and motivate further analysis to understand the extent of pERK neuronal signaling in response to external stimuli in an unrestrained and more naturalistic context.

References

1. Zhu, Y. The Drosophila visual system. *Cell Adh. Migr.* **7**, 333–344 (2013).
2. Luhmann, H. J. *et al.* Spontaneous Neuronal Activity in Developing Neocortical Networks: From Single Cells to Large-Scale Interactions. *Front. Neural Circuits* **10**, 1–14 (2016).
3. Abreu, R., Leal, A. & Figueiredo, P. EEG-Informed fMRI: A Review of Data Analysis Methods. *Front. Hum. Neurosci.* **12**, 1–23 (2018).
4. Iannaccone, R. *et al.* Conflict monitoring and error processing: New insights from simultaneous EEG–fMRI. *Neuroimage* **105**, 395–407 (2015).
5. Suter, K. J., Smith, B. N. & Dudek, F. E. Electrophysiological Recording from Brain Slices. *Methods* **18**, 86–90 (1999).
6. Cousens, G. A. & Muir, G. M. Using Extracellular Single-unit Electrophysiological Data as a Substrate for Investigative Laboratory Exercises. *J. Undergrad. Neurosci. Educ.* **4**, 68–73 (2006).
7. Svoboda, K., Denk, W., Kleinfeld, D. & Tank, D. W. In vivo dendritic calcium dynamics in neocortical pyramidal neurons. *Nature* **385**, 161–165 (1997).
8. Lin, M. Z. & Schnitzer, M. J. Genetically encoded indicators of neuronal activity. *Nat. Neurosci.* **19**, 1142–1153 (2016).
9. Wang, Y. Stereotyped Odor-Evoked Activity in the Mushroom Body of Drosophila Revealed by Green Fluorescent Protein-Based Ca2+ Imaging. *J. Neurosci.* **24**, 6507–6514 (2004).
10. Ahrens, M. B. *et al.* Whole-brain functional imaging at cellular resolution using light-sheet microscopy. *Nat. Methods* **10**, 413–420 (2013).
11. Ziv, Y. *et al.* Long-term dynamics of CA1 hippocampal place codes. *Nat. Neurosci.* **16**, 264–266 (2013).
12. Morgan, J., Cohen, D., Hempstead, J. & Curran, T. Mapping patterns of c-fos expression in the central nervous system after seizure. *Science (80-.).* **237**, 192–197 (1987).
13. Li, M., Liu, F., Jiang, H., Lee, T. S. & Tang, S. Long-Term Two-Photon Imaging in Awake Macaque Monkey. *Neuron* **93**, 1049-1057.e3 (2017).
14. Simpson, J. H. & Looger, L. L. Functional Imaging and Optogenetics in Drosophila. *Genetics* **208**, 1291–1309 (2018).
15. Yang, H. H. & St-Pierre, F. Genetically Encoded Voltage Indicators: Opportunities and Challenges. *J. Neurosci.* **36**, 9977–9989 (2016).
16. Naumann, E. A., Kampff, A. R., Prober, D. A., Schier, A. F. & Engert, F. Monitoring neural activity with bioluminescence during natural behavior. *Nat. Neurosci.* **13**, 513–520 (2010).

17. Mercier, D., Tsuchimoto, Y., Ohta, K. & Kazama, H. Olfactory Landmark-Based Communication in Interacting Drosophila. *Curr. Biol.* **28**, 2624-2631.e5 (2018).
18. Masuyama, K., Zhang, Y., Rao, Y. & Wang, J. W. Mapping neural circuits with activity-dependent nuclear import of a transcription factor. *J. Neurogenet.* **26**, 89–102 (2012).
19. Gao, X. J. *et al.* A transcriptional reporter of intracellular Ca 2+ in Drosophila. *Nat. Neurosci.* **18**, 917–925 (2015).
20. Chow, B. Y. *et al.* High-performance genetically targetable optical neural silencing by light-driven proton pumps. *Nature* **463**, 98–102 (2010).
21. Grosenick, L., Marshel, J. H. & Deisseroth, K. Closed-Loop and Activity-Guided Optogenetic Control. *Neuron* **86**, 106–139 (2015).
22. Klapoetke, N. C. *et al.* Independent optical excitation of distinct neural populations. *Nat. Methods* **11**, 338–346 (2014).
23. Bellen, H. J., Tong, C. & Tsuda, H. 100 years of Drosophila research and its impact on vertebrate neuroscience: a history lesson for the future. *Nat. Rev. Neurosci.* **11**, 514–522 (2010).
24. Hales, K. G., Korey, C. A., Larracuente, A. M. & Roberts, D. M. Genetics on the fly: A primer on the drosophila model system. *Genetics* **201**, 815–842 (2015).
25. Guzowski, J. F. *et al.* Mapping behaviorally relevant neural circuits with immediate-early gene expression. *Curr. Opin. Neurobiol.* **15**, 599–606 (2005).
26. Reijmers, L. G., Perkins, B. L., Matsuo, N. & Mayford, M. Localization of a Stable Neural Correlate of Associative Memory. *Science (80-.).* **317**, 1230–1233 (2007).
27. Liu, X. *et al.* Optogenetic stimulation of a hippocampal engram activates fear memory recall. *Nature* **484**, 381–385 (2012).
28. Fujita, N. *et al.* Visualization of Neural Activity in Insect Brains Using a Conserved Immediate Early Gene, Hr38. *Curr. Biol.* **23**, 2063–2070 (2013).
29. Takayanagi-Kiya, S. & Kiya, T. Activity-dependent visualization and control of neural circuits for courtship behavior in the fly Drosophila melanogaster. *Proc. Natl. Acad. Sci.* **116**, 5715–5720 (2019).
30. Baraban, S. C., Taylor, M. R., Castro, P. A. & Baier, H. Pentylenetetrazole induced changes in zebrafish behavior, neural activity and c-fos expression. *Neuroscience* **131**, 759–768 (2005).
31. Hussain, A. *et al.* High-affinity olfactory receptor for the death-associated odor cadaverine. *Proc. Natl. Acad. Sci.* **110**, 19579–19584 (2013).
32. Xia, Z., Dudek, H., Miranti, C. K. & Greenberg, M. E. Calcium Influx via the NMDA Receptor Induces Immediate Early Gene Transcription by a MAP Kinase/ERK-Dependent Mechanism. *J. Neurosci.* **16**, 5425–5436 (1996).
33. Cancedda, L. *et al.* Patterned Vision Causes CRE-Mediated Gene Expression in the

Visual Cortex through PKA and ERK. *J. Neurosci.* **23**, 7012–7020 (2003).

34. Pearson, G. *et al.* Mitogen-Activated Protein (MAP) Kinase Pathways: Regulation and Physiological Functions*. *Endocr. Rev.* **22**, 153–183 (2001).
35. Rosen, L. Membrane depolarization and calcium influx stimulate MEK and MAP kinase via activation of Ras. *Neuron* **12**, 1207–1221 (1994).
36. Pearson, G. *et al.* Mitogen-Activated Protein (MAP) Kinase Pathways: Regulation and Physiological Functions*. *Endocr. Rev.* **22**, 153–183 (2001).
37. Hales, K. G., Korey, C. A., Larracuente, A. M. & Roberts, D. M. Genetics on the Fly: A Primer on the Drosophila Model System. *Genetics* **201**, 815–842 (2015).
38. Liu, R.-Y., Fioravante, D., Shah, S. & Byrne, J. H. cAMP Response Element-Binding Protein 1 Feedback Loop Is Necessary for Consolidation of Long-Term Synaptic Facilitation in Aplysia. *J. Neurosci.* **28**, 1970–1976 (2008).
39. Kim, E. K. & Choi, E.-J. Pathological roles of MAPK signaling pathways in human diseases. *Biochim. Biophys. Acta - Mol. Basis Dis.* **1802**, 396–405 (2010).
40. Blum, S., Moore, A. N., Adams, F. & Dash, P. K. A mitogen-activated protein kinase cascade in the CA1/CA2 subfield of the dorsal hippocampus is essential for long-term spatial memory. *J. Neurosci.* **19**, 3535–3544 (1999).
41. Gerdjikov, T. V., Ross, G. M. & Beninger, R. J. Place Preference Induced by Nucleus Accumbens Amphetamine Is Impaired by Antagonists of ERK or p38 MAP Kinases in Rats. *Behav. Neurosci.* **118**, 740–750 (2004).
42. Atkins, C. M., Selcher, J. C., Petraitis, J. J., Trzaskos, J. M. & Sweatt, J. D. The MAPK cascade is required for mammalian associative learning. *Nat. Neurosci.* **1**, 602–609 (1998).
43. Selcher, J. C., Atkins, C. M., Trzaskos, J. M., Paylor, R. & David Sweatt, J. A necessity for MAP kinase activation in mammalian spatial learning. *Learn. Mem.* **6**, 478–490 (1999).
44. Itoh, M., Yamamoto, T., Nakajima, Y. & Hatta, K. Multistepped optogenetics connects neurons and behavior. *Curr. Biol.* **24**, R1155–R1156 (2014).
45. Ehman, E. C. *et al.* PET/MRI: Where might it replace PET/CT? *J. Magn. Reson. Imaging* **46**, 1247–1262 (2017).
46. Vanderheyden, W. M., Gerstner, J. R., Tanenhaus, A., Yin, J. C. & Shaw, P. J. ERK Phosphorylation Regulates Sleep and Plasticity in Drosophila. *PLoS One* **8**, e81554 (2013).
47. Koh, Y.-H., Ruiz-Canada, C., Gorczyca, M. & Budnik, V. The Ras1–Mitogen-Activated Protein Kinase Signal Transduction Pathway Regulates Synaptic Plasticity through Fasciclin II-Mediated Cell Adhesion. *J. Neurosci.* **22**, 2496–2504 (2002).
48. Wairkar, Y. P. *et al.* Unc-51 controls active zone density and protein composition by

downregulating ERK signaling. *J. Neurosci.* **29**, 517–528 (2009).

49. Thomas, G. M. & Huganir, R. L. MAPK cascade signalling and synaptic plasticity. *Nat. Rev. Neurosci.* **5**, 173–183 (2004).
50. Sakamoto, K., Karelina, K. & Obrietan, K. CREB: a multifaceted regulator of neuronal plasticity and protection. *J. Neurochem.* **116**, 1–9 (2011).
51. Gao, Y.-J. & Ji, R.-R. c-Fos or pERK, Which is a Better Marker for Neuronal Activation and Central Sensitization After Noxious Stimulation and Tissue Injury? *Open Pain J.* **2**, 11–17 (2009).
52. Marella, S. *et al.* Imaging Taste Responses in the Fly Brain Reveals a Functional Map of Taste Category and Behavior. *Neuron* **49**, 285–295 (2006).
53. Paulk, A. C., Zhou, Y., Stratton, P., Liu, L. & van Swinderen, B. Multichannel brain recordings in behaving Drosophila reveal oscillatory activity and local coherence in response to sensory stimulation and circuit activation. *J. Neurophysiol.* **110**, 1703–1721 (2013).
54. Ng, M. *et al.* Transmission of Olfactory Information between Three Populations of Neurons in the Antennal Lobe of the Fly. *Neuron* **36**, 463–474 (2002).
55. Wang, J. W., Wong, A. M., Flores, J., Vosshall, L. B. & Axel, R. Two-Photon Calcium Imaging Reveals an Odor-Evoked Map of Activity in the Fly Brain. *Cell* **112**, 271–282 (2003).
56. Olsen, S. R. & Wilson, R. I. Cracking neural circuits in a tiny brain: new approaches for understanding the neural circuitry of Drosophila. *Trends Neurosci.* **31**, 512–520 (2008).
57. Mirich, J. M., Illig, K. R. & Brunjes, P. C. Experience-dependent activation of extracellular signal-related kinase (ERK) in the olfactory bulb. *J. Comp. Neurol.* **479**, 234–241 (2004).
58. Vosshall, L. B. & Stocker, R. F. Molecular Architecture of Smell and Taste in Drosophila. *Annu. Rev. Neurosci.* **30**, 505–533 (2007).
59. Ha, T. S. Odorant and pheromone receptors in insects. *Front. Cell. Neurosci.* **3**, 1–6 (2009).
60. Ronderos, D. & Smith, D. Diverse signaling mechanisms mediate volatile odorant detection in Drosophila. *Fly (Austin).* **3**, 290–297 (2009).
61. Stocker, R. F. The organization of the chemosensory system in Drosophila melanogaster: a rewiew. *Cell Tissue Res.* **275**, 3–26 (1994).
62. Shanbhag, S. ., Müller, B. & Steinbrecht, R. . Atlas of olfactory organs of Drosophila melanogaster. *Arthropod Struct. Dev.* **29**, 211–229 (2000).
63. Vosshall, L. B., Wong, A. M. & Axel, R. An Olfactory Sensory Map in the Fly Brain. *Cell* **102**, 147–159 (2000).
64. Benton, R., Vannice, K. S., Gomez-Diaz, C. & Vosshall, L. B. Variant Ionotropic

Glutamate Receptors as Chemosensory Receptors in Drosophila. *Cell* **136**, 149–162 (2009).

65. Coulson, J. M. Transcriptional Regulation: Cancer, Neurons and the REST. *Curr. Biol.* **15**, R665–R668 (2005).
66. Masse, N. Y., Turner, G. C. & Jefferis, G. S. X. E. Olfactory Information Processing in Drosophila. *Curr. Biol.* **19**, R700–R713 (2009).
67. Zacarias, R., Namiki, S., Card, G. M., Vasconcelos, M. L. & Moita, M. A. Speed dependent descending control of freezing behavior in Drosophila melanogaster. *Nat. Commun.* **9**, 3697 (2018).
68. Ferreira, C. H. & Moita, M. A. Safety in numbers is mediated by motion cues and depends on lobula columnar neurons in Drosophila melanogaster. *bioRxiv* 629311 (2019) doi:https://doi.org/10.1101/629311.
69. Ronderos, D. S., Lin, C.-C., Potter, C. J. & Smith, D. P. Farnesol-Detecting Olfactory Neurons in Drosophila. *J. Neurosci.* **34**, 3959–3968 (2014).
70. Brand, A. H. & Perrimon, N. Targeted gene expression as a means of altering cell fates and generating dominant phenotypes. *Development* **118**, 401–415 (1993).
71. Burr, A. A., Tsou, W.-L., Ristic, G. & Todi, S. V. Using membrane-targeted green fluorescent protein to monitor neurotoxic protein-dependent degeneration of Drosophila eyes. *J. Neurosci. Res.* **92**, 1100–1109 (2014).
72. Baines, R. A., Uhler, J. P., Thompson, A., Sweeney, S. T. & Bate, M. Altered Electrical Properties in Drosophila Neurons Developing without Synaptic Transmission. *J. Neurosci.* **21**, 1523–1531 (2001).
73. Ehman, E. C. *et al.* HHS Public Access. **46**, 1247–1262 (2017).
74. Hodge, J. J. L. L. Ion channels to inactivate neurons in Drosophila. *Front. Mol. Neurosci.* **2**, 1–10 (2009).
75. Inagaki, H. K. *et al.* HHS Public Access. **11**, 325–332 (2014).
76. Wu, M. C. *et al.* Optogenetic control of selective neural activity in multiple freely moving Drosophila adults. *Proc. Natl. Acad. Sci. U. S. A.* **111**, 5367–5372 (2014).
77. Awata, H. *et al.* The neural circuit linking mushroom body parallel circuits induces memory consolidation in Drosophila. *Proc. Natl. Acad. Sci. U. S. A.* **116**, 16080–16085 (2019).
78. Kogan, J. H. *et al.* Spaced training induces normal long-term memory in CREB mutant mice. *Curr. Biol.* **7**, 1–11 (1997).
79. Naqib, F., Sossin, W. S. & Farah, C. A. Molecular Determinants of the Spacing Effect. *Neural Plast.* **2012**, 1–8 (2012).
80. Ha, S. & Redmond, L. ERK mediates activity dependent neuronal complexity via sustained activity and CREB-mediated signaling. *Dev. Neurobiol.* **68**, 1565–1579

(2008).

81. Bräcker, L. B. *et al.* Essential role of the mushroom body in context-dependent CO2 avoidance in drosophila. *Curr. Biol.* **23**, 1228–1234 (2013).

82. Kwon, J. Y., Dahanukar, A., Weiss, L. A. & Carlson, J. R. The molecular basis of CO2 reception in Drosophila. *Proc. Natl. Acad. Sci. U. S. A.* **104**, 3574–3578 (2007).

83. Moreno, E., Valon, L., Levillayer, F. & Levayer, R. Competition for Space Induces Cell Elimination through Compaction-Driven ERK Downregulation. *Curr. Biol.* **29**, 23-34.e8 (2019).

Appendix I

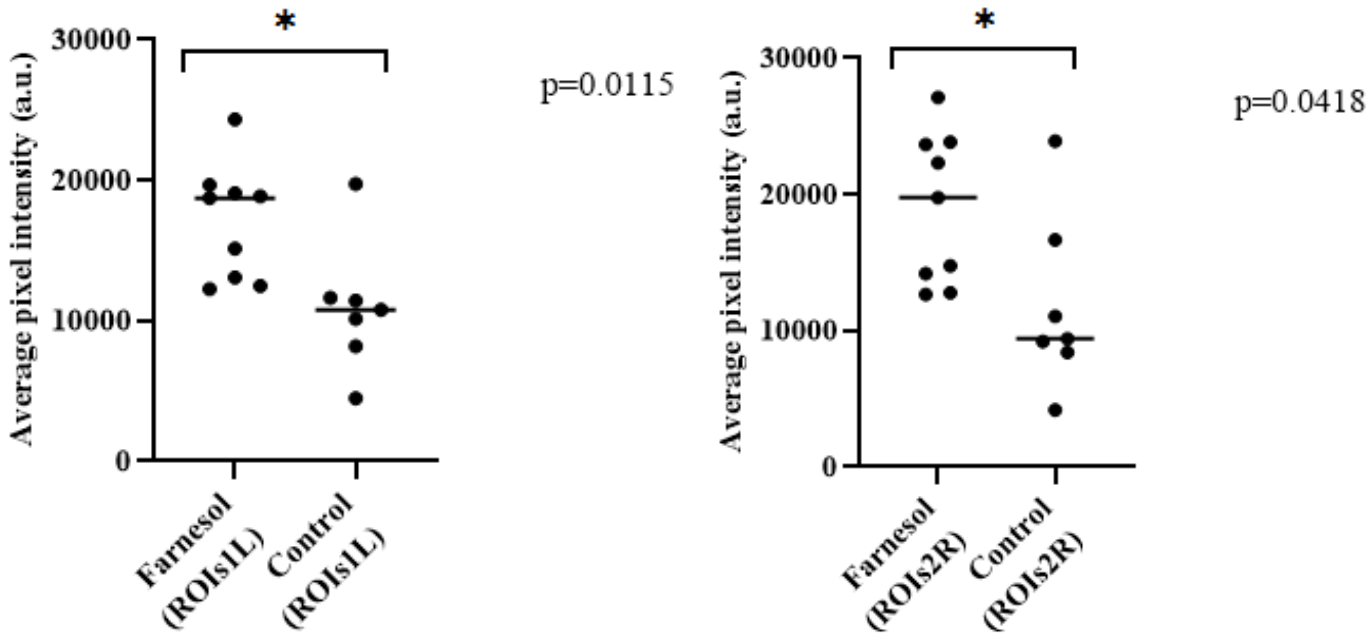

Fig. 1 – pERK average pixel intensity (a.u) in experimental and control WT brains in left and right antennal lobes. (Mann-Whitney U test, * denotes p= 0.0115, * denotes p=0.0418, respectively).

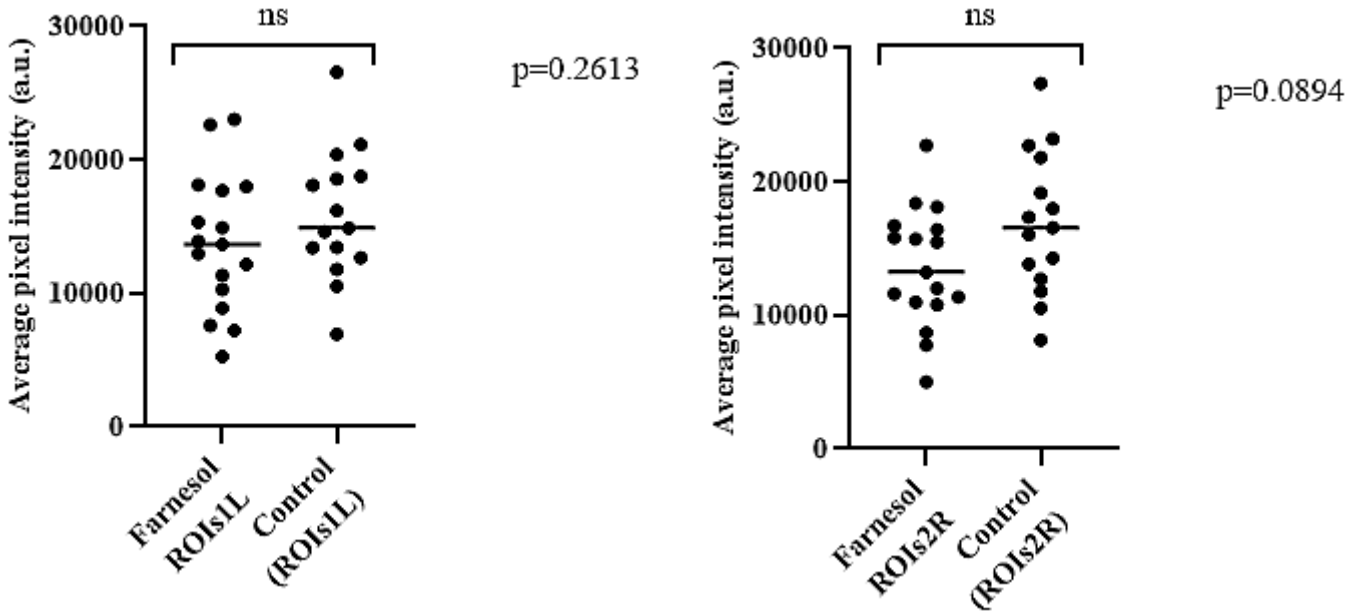

Fig. 2 – pERK average pixel intensity (a.u) in experimental and control Or83c-Gal4;UAS-CD8::GFP brains in left and right antennal lobes. (Mann-Whitney U test, p=0.2613, p=0.0894, respectively). ns not significant.

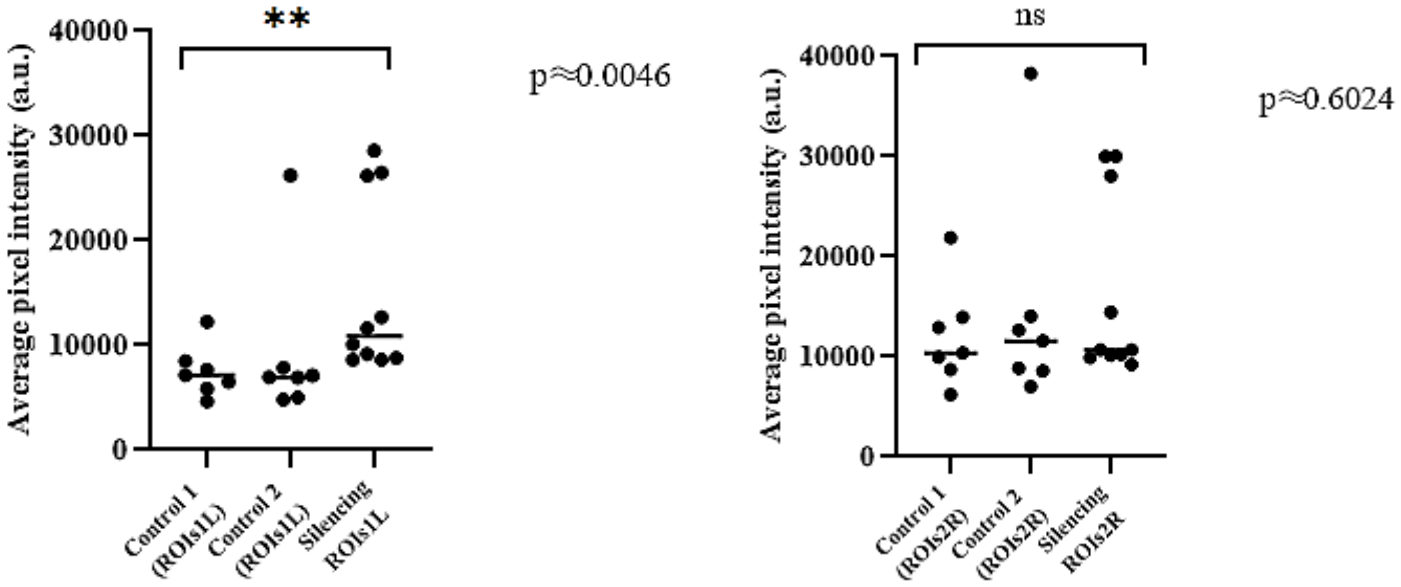

Fig. 3 – pERK average pixel intensity (a.u) in control and experimental Or83c-Gal4;10xUAS-Kir2.1::EGFP brains in left and right antennal lobes. (Kruskal-Wallis test, p≈0.0046, ** denotes p≈0.6024, respectively). ns not significant.

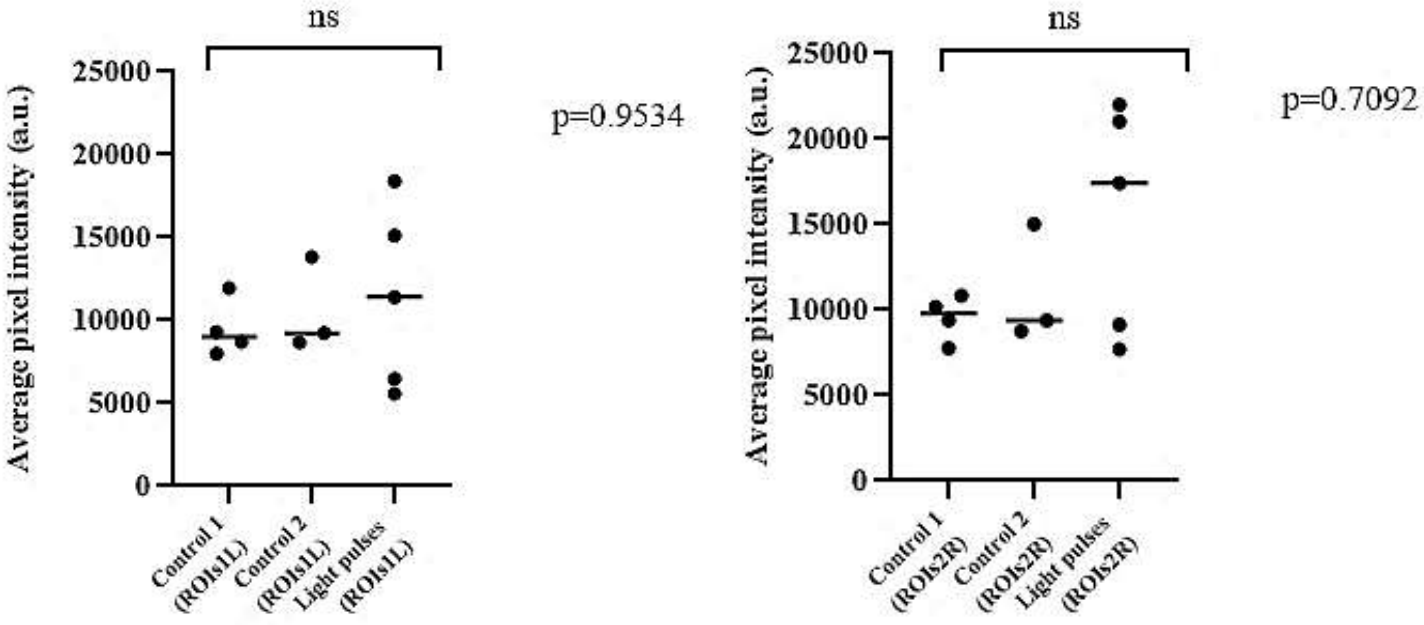

Fig. 4 – pERK average pixel intensity (a.u) in control and experimental Or83c-Gal4;UAS-Chrimson::mVenus brains in left and right antennal lobes. (Kruskal-Wallis test, p=0.9534, p=0.7092, respectively). ns not significant.

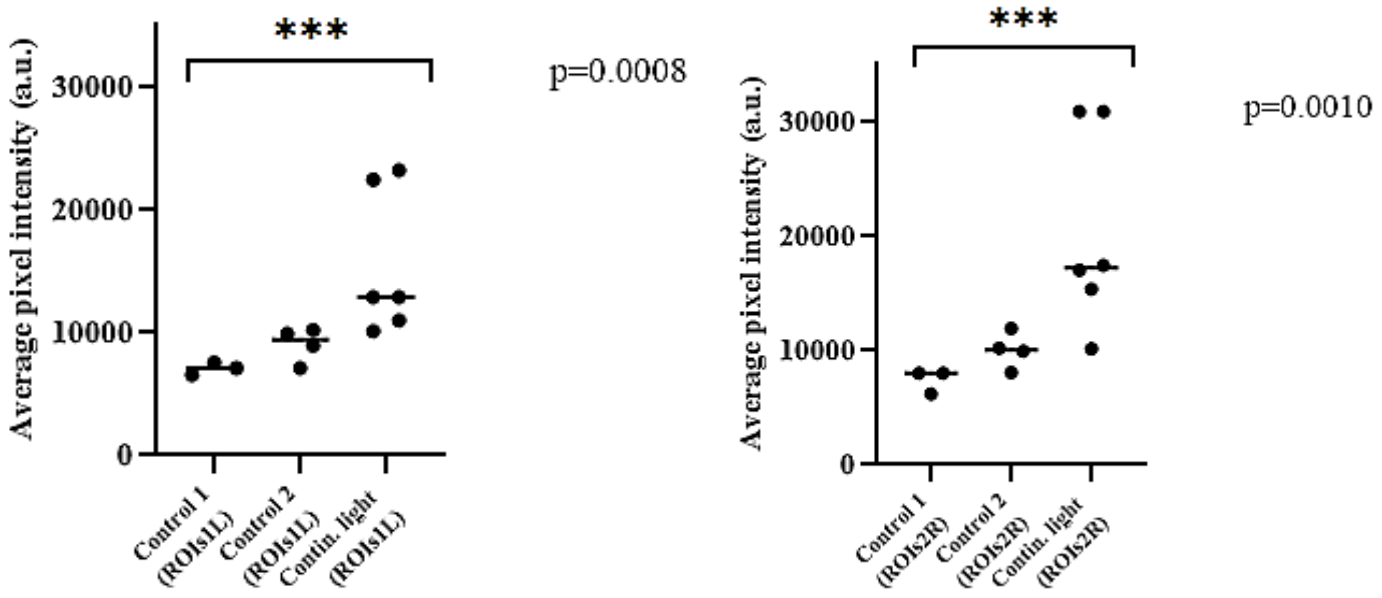

Fig. 5 – pERK average pixel intensity (a.u) in control and experimental Or83c-Gal4;UAS-Chrimson::mVenus brains in left and right antennal lobes. (Kruskal-Wallis test, *** denotes p=0.0008, *** denotes p=0.0010, respectively).

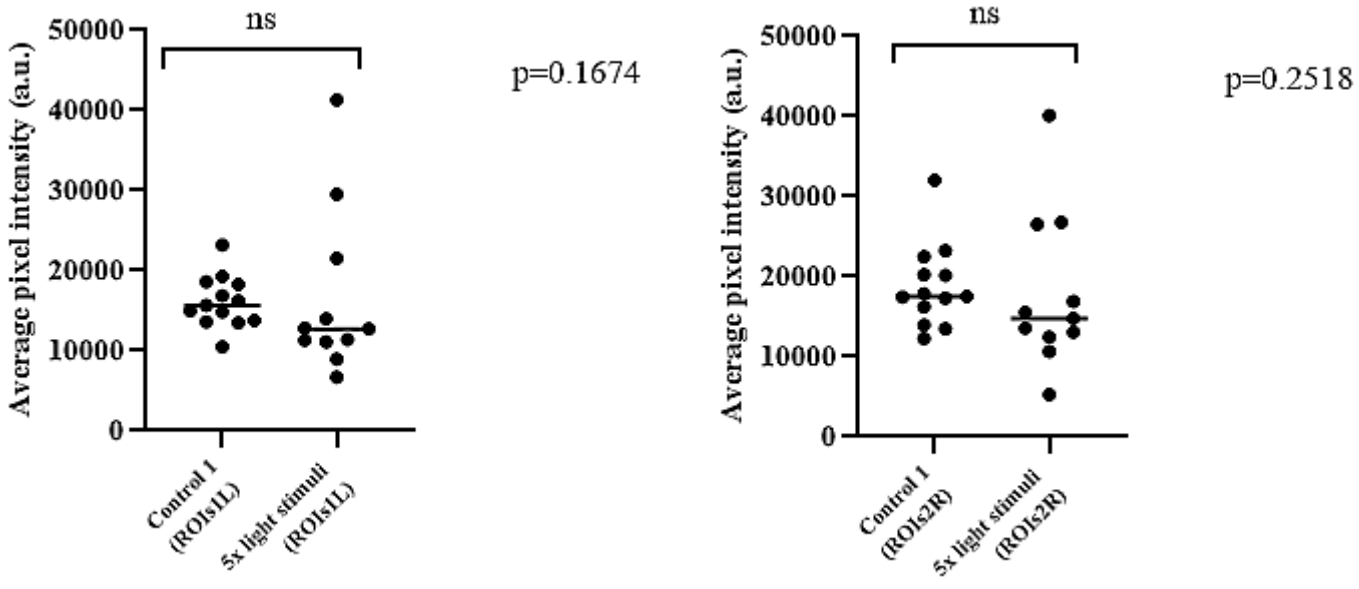

Fig. 6 – pERK average pixel intensity (a.u) in control and experimental Or83c-Gal4;UAS-Chrimson::mVenus brains in left and right antennal lobes. (Mann-Whitney U test, p=0.1674, p=0.2518, respectively). ns not significant.

Appendix II

A

Distilled water	Investigator 1 (co-staining GFP+pERK)	Investigator 2 (co-staining GFP+pERK)	Investigator 3 (co-staining GFP+pERK)
Brain #1	0	0	0
Brain #2	0	0	0
Brain #3	0	0	0
Brain #4	0	0	1
Brain #5	0	0	0
Brain #6	0	0	0
Brain #7	0	0	0
Brain #8	0	0	0
Brain #9	NA	0	0
Brain #10	0	0	0
Brain #11	0	0	0
Brain #12	0	NA	0
Brain #13	NA	0	0
Brain #14	0	0	0
Brain #15	0	0	0

0 = no
1 = yes

B

Farnesol stimulation	Investigator 1 (co-staining GFP+pERK)	Investigator 2 (co-staining GFP+pERK)	Investigator 3 (co-staining GFP+pERK)
Brain #1	1	1	1
Brain #2	1	1	1
Brain #3	1	1	1
Brain #4	0.5	1	1
Brain #5	0	0	NA
Brain #6	0	1	1
Brain #7	1	0	1
Brain #8	0	0	0
Brain #9	NA	0	0
Brain #10	0	1	0
Brain #11	0	0	0
Brain #12	0	0	0
Brain #13	1	1	1
Brain #14	1	0	1
Brain #15	0	0	0
Brain #16	1	1	1
Brain #17	0	0	0

0 = no
1 = yes

A1

Or83c-Gal4xUAS-CD8::GFP male brains (4-6 days old) Control (n=15)	% of brains with co-labeling (DC3 glomerulus)
Investigator 1	0%
Investigator 2	0%
Investigator 3	6.7%
Mean	**2.2%**

B1

Or83c-Gal4xUAS-CD8::GFP male brains (4-6 days old) Farnesol (n=17)	% of brains with co-labeling (DC3 glomerulus)
Investigator 1	46.9%
Investigator 2	50%
Investigator 3	56.3%
Mean	**51.1%**

C

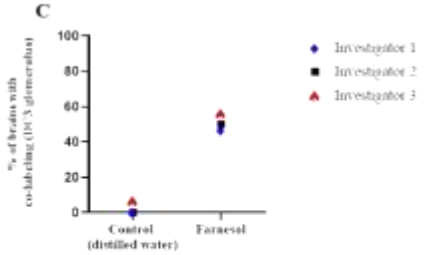

D

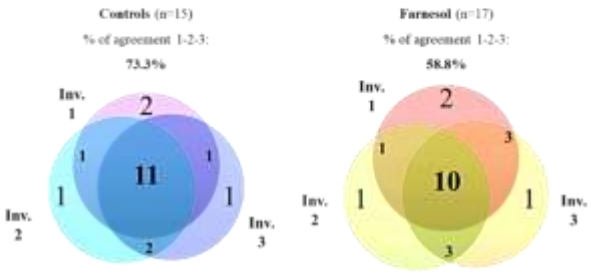

Fig. 1 - Farnesol stimulus increases pERK expression in the DC3 glomerulus. Blinded visual scoring from 3 impartial investigators for the absence (scored as 0) or presence (scored as 1) of co-localization between GFP and pERK signals in the DC3 glomerulus (**Tables A and B**). Brains scored as 0.5 were considered half positives as having only one antennal lobe with GFP+pERK co-labeling. **Tables A1** and **B1** show the percentage of brains scored as having co-expression of GFP+pERK in the DC3 glomerulus by each individual observer, in both control and experimental situations, respectively. Control flies (n=15) were exposed to distilled water, as previously described (**Fig. 1**) and only 2.2% of the brains were classified as 1s by the observers (**Table A1**). Experimental flies (n=17) were exposed to farnesol solution (see **Fig. 1**) and 51.1% of the brains have co-labeling between GFP and pERK in the glomerulus, according to the investigators (**Table B1**). (**C**) Graph of the percentage of brains with GFP and pERK co-staining in the DC3 glomerulus in both control and farnesol experimental conditions, scored by the investigators. All brains classified as NA (non-applicable) by the investigators (**Tables A** and **B**) were removed from the statistical analysis. Red-highlighted brain numbers (**Tables A** and **B**) show the different scores. (**D**) Venn diagrams show the relationship between all investigators in control and farnesol experimental conditions. All investigators show 73.3% of agreement in control brains and 58.8% of agreement in farnesol condition. NA brains (**Tables A and B**) were included in the ratio of agreement analysis.

A

Controls (Farnesol)	Investigator 1 (pERK expression)	Investigator 2 (pERK expression)	Investigator 3 (pERK expression)
Brain #1	1	0	0
Brain #2	0	0	0
Brain #3	0	0	0
Brain #4	0	0	0
Brain #5	0	0	0
Brain #6	1	0	0
Brain #7	0	0	0
Brain #8	0	0	0
Brain #9	0.5	0	0
Brain #10	1	0	0
Brain #11	0	0	0
Brain #12	0	0	0
Brain #13	0.5	0	0
Brain #14	0	0	0
0 = no			
1 = yes			

B

Or83c-Gal4 x 10xUAS-kir::2.1::EGFP (Farnesol)	Investigator 1 (co-staining GFP+pERK)	Investigator 2 (co-staining GFP+pERK)	Investigator 3 (co-staining GFP+pERK)
Brain #1	0	1	0
Brain #2	0	0	0
Brain #3	0	0	1
Brain #4	0	0	0
Brain #5	0	1	1
Brain #6	0	0	1
Brain #7	0	0	1
Brain #8	1	1	0
Brain #9	1	1	1
Brain #10	0	0	0
0 = no			
1 = yes			

A1

Or83c-Gal4xUAS-10xUAS-Kir2.1::EGFP male brains (4-6 days old) Controls	% of brains with pERK expression
Investigator 1	28.6%
Investigator 2	0%
Investigator 3	0%
Mean	**9.5%**

B1

Or83c-Gal4xUAS-10xUAS-Kir2.1::EGFP male brains (4-6 days old) Farnesol (1min)	% of brains with co-labeling (DC3 glomerulus)
Investigator 1	20%
Investigator 2	40%
Investigator 3	50%
Mean	**36.7%**

C

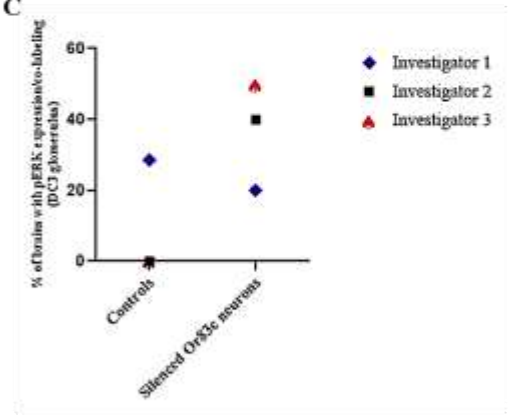

D

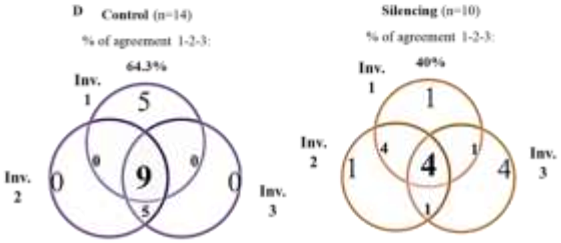

Fig. 2 – Inactivation of Or83c neurons in the DC3 glomerulus, scored by the researchers. Blinded visual scoring from 3 impartial investigators for the absence (scored as 0) or presence (scored as 1) of pERK expression and GFP+pERK co-labeling in both control and experimental conditions, respectively (**Tables A and B**). Brains scored as 0.5 were considered half positives as having only one antennal lobe with GFP+pERK co-labeling. **Tables A1** and **B1** show the percentage of control and experimental brains scored as having expression of pERK in the antennal lobes and GFP+pERK co-labeling in the DC3 glomerulus by each individual observer, respectively. Control flies (n=14) were exposed to the odor protocol (see **Fig. 1**), as well as experimental flies (n=10). 9.5% of controls brains were classified as having expression of pERK by the observers (**Table A1**), while in experimental condition we have 36.7% of brains with co-labeling between GFP and pERK, according to them (**Table B1**). (**C**) Graph of the percentage of control and experimental brains with pERK expression and GFP+pERK co-labeling, as shown in **Tables A1 and A2**. Red-highlighted brain numbers (**Tables A** and **B**) show the different scores. (**D**) Venn diagrams show the relationship between all investigators in control and experimental conditions. All investigators show 64.3% of agreement in control brains and 40% of agreement in experimental condition.

A

Control 1 (Light pulses)	Investigator 1 (co-staining GFP+pERK)	Investigator 2 (co-staining GFP+pERK)	Investigator 3 (co-staining GFP+pERK)
Brain #1	1	0	0
Brain #2	0	0	0
Brain #3	1	0	1
Brain #4	1	0	1

Control 2 (no light)	Investigator 1 (co-staining GFP+pERK)	Investigator 2 (co-staining GFP+pERK)	Investigator 3 (co-staining GFP+pERK)
Brain #1	0	0	1
Brain #2	0	0	0
Brain #3	0	0	0

0 = no
1 = yes

B

Light pulses (1min, 2 Hz)	Investigator 1 (co-staining GFP+pERK)	Investigator 2 (co-staining GFP+pERK)	Investigator 3 (co-staining GFP+pERK)
Brain #1	1	1	1
Brain #2	0.5	1	1
Brain #3	0.5	NA	1
Brain #4	0	0	0
Brain #5	0.5	1	1

0 = no
1 = yes

A1

Or83c-Gal4xUAS-Chrimson::mVenus male brains (4-6 days old) Controls 1 and 2 (n=7)	% of brains with co-labeling (DC3 glomerulus)
Investigator 1	42.9%
Investigator 2	0%
Investigator 3	42.9%
Mean	**28.6%**

B1

Or83c-Gal4xUAS-Chrimson::mVenus male brains (4-6 days old) Light pulses (n=5)	% of brains with co-labeling (DC3 glomerulus)
Investigator 1	50%
Investigator 2	75%
Investigator 3	80%
Mean	**68.3%**

C

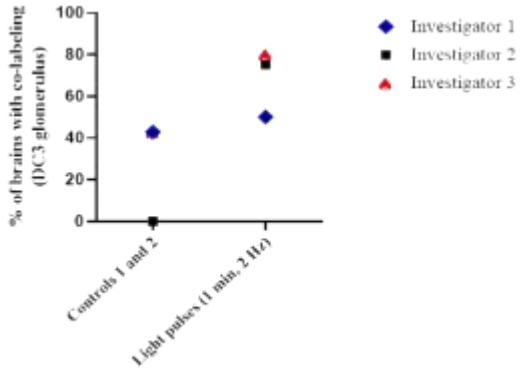

D

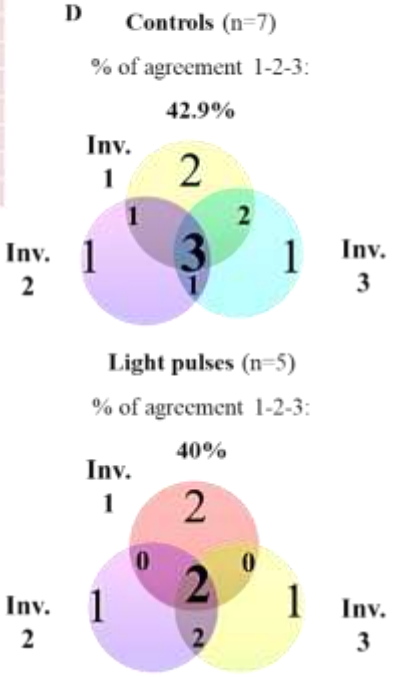

Fig. 3 – Pulsed light stimulation of Or83c neurons, scored by the investigators. Blinded visual scoring from 3 impartial investigators for the absence (scored as 0) or presence (scored as 1) of co-localization between GFP and pERK signals in the DC3 glomerulus (**Tables A and B**). Brains scored as 0.5 were considered half positives as having only one antennal lobe with GFP+pERK co-labeling. **Tables A1** and **B1** show the percentage of brains scored as having co-expression of GFP+pERK in the DC3 glomerulus by each individual observer, in both control and experimental situations, respectively. Control 1 flies (n= 4) were exposed to pulsed light, in contrast to unstimulated control 2 flies (n=3), as previously described (**Table 2, in methods**). 28.6% of controls brains were classified as 1s by the observers (**Table A1**). Experimental flies (n=5) were exposed to pulsed light (see protocol in methods, **Table 2**) and 68.3% of the brains have co-labeling between GFP and pERK in the glomerulus, according to the investigators (**Table B1**). (**C**) Graph of the percentage of brains with GFP and pERK co-staining in the DC3 glomerulus in both control and experimental conditions, as previously described in **Tables A1** and **B1**. The brain classified as NA (non-applicable) in **Tables B** was removed from the statistical analysis. Red-highlighted brain numbers (**Tables A** and **B**) show the different scores. (**D**) Venn diagrams show the relationship between all investigators in control and experimental conditions. All investigators show 42.9% of agreement in control brains and 40% of agreement in experimental condition. NA brain (Fig. **8B**) was included in the ratio of agreement analysis.

A

Control 1 (Continuous light)	Investigator 1 (co-staining GFP+pERK)	Investigator 2 (co-staining GFP+pERK)	Investigator 3 (co-staining GFP+pERK)
Brain #1	0	0	0
Brain #2	0	0	0
Brain #3	0	0	0

Control 2 (no light)	Investigator 1 (co-staining GFP+pERK)	Investigator 2 (co-staining GFP+pERK)	Investigator 3 (co-staining GFP+pERK)
Brain #1	1	1	0
Brain #2	1	0	0
Brain #3	0	0	0
Brain #4	0	1	1

0 = no
1 = yes

B

Continuous light (1min)	Investigator 1 (co-staining GFP+pERK)	Investigator 2 (co-staining GFP+pERK)	Investigator 3 (co-staining GFP+pERK)
Brain #1	0	1	1
Brain #2	0	1	1
Brain #3	0	1	1
Brain #4	1	0	1
Brain #5	1	0	1
Brain #6	0	0	0

0 = no
1 = yes

A1

Or83c-Gal4xUAS-Chrimson::mVenus male brains (4-6 days old) Controls 1 and 2 (n=7)	% of brains with co-labeling (DC3 glomerulus)
Investigator 1	28.6%
Investigator 2	28.6%
Investigator 3	14.3%
Mean	**23.8%**

B1

Or83c-Gal4xUAS-Chrimson::mVenus male brains (4-6 days old) Continuous light (n=6)	% of brains with co-labeling (DC3 glomerulus)
Investigator 1	33.3%
Investigator 2	50%
Investigator 3	83.3%
Mean	**55.5%**

C

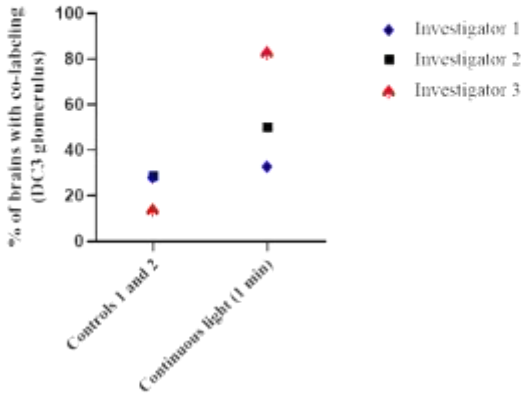

D

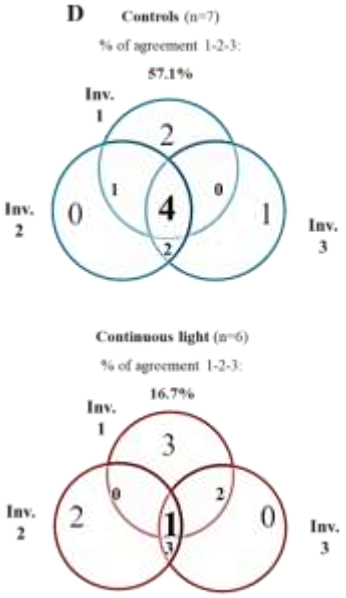

Fig. 4 – Continuous light stimulation of Or83c-expressing neurons, scored by the researchers. Blinded visual scoring from 3 impartial investigators for the absence (scored as 0) or presence (scored as 1) of colocalization between GFP and pERK signals in the DC3 glomerulus (**Tables A and B**). **Tables A1** and **B1** show the percentage of brains scored as having co-expression of GFP+pERK in the DC3 glomerulus by each individual observer, in both control and experimental situations, respectively. Control 1 flies (n =3) were exposed to pulsed light, whereas control 2 flies (n=4) had no light stimulation, as previously mentioned (**Table 2, in methods**). 23.8% of controls brains were classified as 1s by the observers (**Table A1**). Experimental flies (n=6) were exposed to continuous light (see protocol in methods, **Table 2**) and 55.5% of the brains have co-labeling between GFP and pERK in the glomerulus, according to the investigators (**Table B1**). (**C**) Percentage of brains with GFP and pERK co-staining in the DC3 glomerulus in both control and experimental conditions, scored by the investigators in **Tables A1 and A2**. Red-highlighted brain numbers (**Tables A** and **B**) show the different scores. (**D**) Venn diagrams show the relationship between all investigators in control and experimental conditions. All investigators show 57.1% of agreement in control brains and 16.7% of agreement in experimental condition.

A

Control (Continuous light)	Investigator 1 (co-staining GFP+pERK)	Investigator 2 (co-staining GFP+pERK)	Investigator 3 (co-staining GFP+pERK)
Brain #1	1	1	0
Brain #2	1	1	1
Brain #3	1	1	1
Brain #4	0	0	1
Brain #5	0	0	0
Brain #6	0	0	1
Brain #7	1	1	1
Brain #8	1	1	1
Brain #9	1	1	1
Brain #10	0	1	0
Brain #11	1	1	0
Brain #12	0	0	1
Brain #13	0	1	1
0 = no			
1 = yes			

B

Continuous light (5 stimuli 30"ON+90"OFF)	Investigator 1 (co-staining GFP+pERK)	Investigator 2 (co-staining GFP+pERK)	Investigator 3 (co-staining GFP+pERK)
Brain #1	0	0	0
Brain #2	1	1	1
Brain #3	1	0	0
Brain #4	0	0	0
Brain #5	1	1	1
Brain #6	1	1	1
Brain #7	0	0	1
Brain #8	0.5	0	1
Brain #9	0	0	1
Brain #10	1	1	1
Brain #11	0	0	0
0 = no			
1 = yes			

A1

Or83c-Gal4xUAS-Chrimson::mVenus male brains (4-6 days old) Control (n=13)	% of brains with co-labeling (DC3 glomerulus)
Investigator 1	53.8%
Investigator 2	69.2%
Investigator 3	69.2%
Mean	**64.1%**

B1

Or83c-Gal4xUAS-Chrimson::mVenus male brains (4-6 days old) 5x [30"ON+90"OFF] (n=11)	% of brains with co-labeling (DC3 glomerulus)
Investigator 1	50%
Investigator 2	36.4%
Investigator 3	63.6%
Mean	**50%**

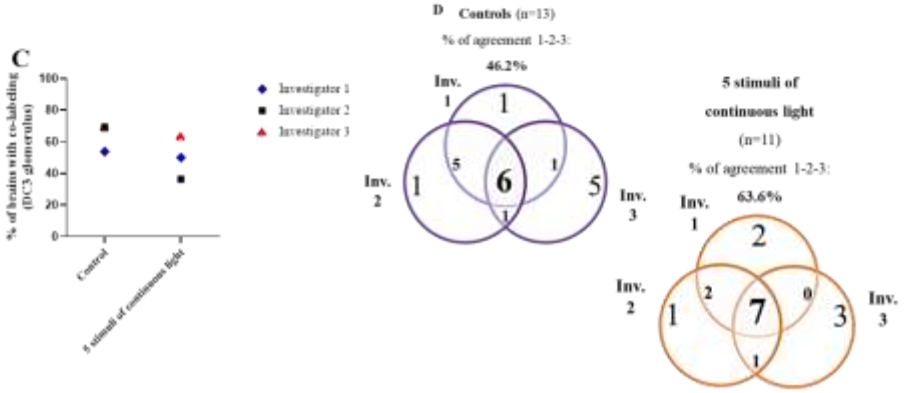

Fig. 5 – Or83c neurons response to 5 stimuli of continuous light, scored by the investigators. Blinded visual scoring from 3 impartial investigators for the absence (scored as 0) or presence (scored as 1) of co-labeling between GFP and pERK signals in the DC3 glomerulus (**Tables A and B**). Brains scored as 0.5 were considered half positives as having only one antennal lobe with GFP+pERK co-labeling. **Tables A1** and **B1** show the percentage of brains scored as having co-expression of GFP+pERK in the DC3 glomerulus by each individual observer, in both control and experimental situations, respectively. Control flies (n=13) were exposed to the stimulation protocol (see **Fig. 2** in materials section) after 3 days in retinal-free food (see **Table 2** in methods). Experimental flies (n=11) were submitted to the same protocol, after 3 days in retinal 0.4 mmol/L supplemented food. 64.1% of controls brains were classified as 1s by the observers (**Table A1**), while in experimental condition we have 50% of brains with co-labeling between GFP and pERK, according to their score (**Table B1**). (**C**) Percentage of brains with GFP and pERK in the DC3 glomerulus in both control and experimental conditions, scored by the investigators (**Table A1 and A2**). Red-highlighted brain numbers (**Tables A** and **B**) show the different scores. (**D**) Venn diagrams show the relationship between all investigators in control and experimental conditions. All investigators show 46.2% of agreement in control brains and 63.6% of agreement in experimental condition.

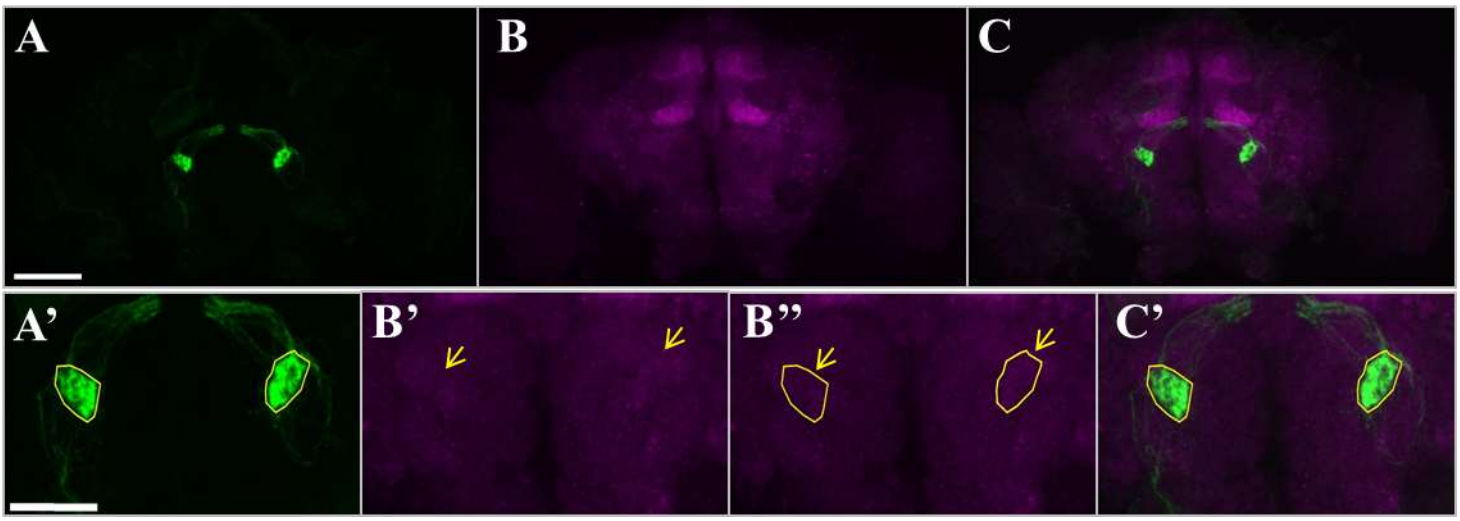

Fig. 6 – Free-retinal control brain #11 was one of the differently scored brains by the researchers. Investigators 1 and 2 considered that we have co-staining between GFP and pERK in the DC3 glomerulus, while investigator 3 classified this brain as a 0 for co-labeling between these two expressions. Control brain #11 was kept in free-retinal food and then exposed to the experimental protocol for 600 seconds, as previously mentioned in **Fig. 11** (see also **Table 2** and **Fig. 2** in methods section. (**A'**, **B''** and **C'**) Zoomed-in images of **A-C** with a contour around the DC3 glomerulus. (**B'**) Zoomed-in of **B** without the contour to openly confirm pERK expression in the glomerulus. All images are confocal ZProjections (6-12 slices, as maximum intensity projections) of fly brains stained for anti-GFP (**A-A'**, in green), anti-pERK (**B-B'** and **B''**, in magenta) and merge channels (**C-C'**). Scale bars represent 70 µm (**A-C**) and 26 µm (**A'-C'** and **B''** zoomed-in images).

Fly brains	Control 1 (discordant brain #) (bad brain #)	Control 2 (discordant brain #) (bad brain #)	Experimental condition (discordant brain #) (bad brain #)
(A) WT	#2, #3, #7 (#7)	---	#6, #8 (#6 and #8)
(B) Or83c-Gal4 x UAS-CD8::GFP	#4, #9, #12, #13 (#12)	---	#4, #5, #6, #7, #9, #10, #14 (#5, #6 and #14)*
(C) Or83c-Gal4 x UAS-Chrimson::mVenus (pulses)	#1, #3, #4 (#4)*	#1 (#1)*	#2, #3, #5 (#2, #3 and #5)
(D) Or83c-Gal4 x UAS-Chrimson::mVenus (continuous)	---	#1, #2, #4 (#2) (#4)*	#1, #2, #3, #4, #5 (#2 and #4)
(E) Or83c-Gal4 x UAS-Chrimson::mVenus (5 stimuli)	#1, #4, #6, #10, #11, #12, #13 (#1, #4, #6, #10, #11, #12, #13)	---	#3, #7, #8, #9 (#3)
(F) Or83c-Gal4 x 10xUAS-Kir2.1::EGFP	#1, #6, #9, #10, #13 (#10 and #13)	---	#1, #3, #5, #6, #7, #8 (#6)* (#7)

Table 1 - Researchers' disagreement between all scored brains seems to have a positive correlation with their dissection quality. All the numbers in black represent the brains without agreement between the researchers, while the numbers in red show which of them were considered "bad" in relation to the dissection quality. The brown numbers illustrate the brains with an intermediate dissection quality ("+/-" in **Fig. 2**) . **(A)** Control condition shows one bad brain and experimental condition show two bad brains. **(B)** Control condition shows one bad brain. Experimental condition does not show bad brains, although the investigator did not consider three of them as good dissected brains. **(C)** The control brains show no bad brains, although one brain in each of the controls was not considered as good dissected brain. The experimental condition shows three bad brains. **(D)** In control brains, we have one bad brain and one brain with intermediate dissection quality. In experimental condition, two brains were classified as bad in terms of dissection quality. **(E)** All control brains were classified as bad for dissection quality, whereas under experimental condition we have only one bad brain. **(F)** Two control brains were classified as bad regarding the dissection quality. In experimental condition, we have one bad brain and one dissected brain with intermediate dissection quality.

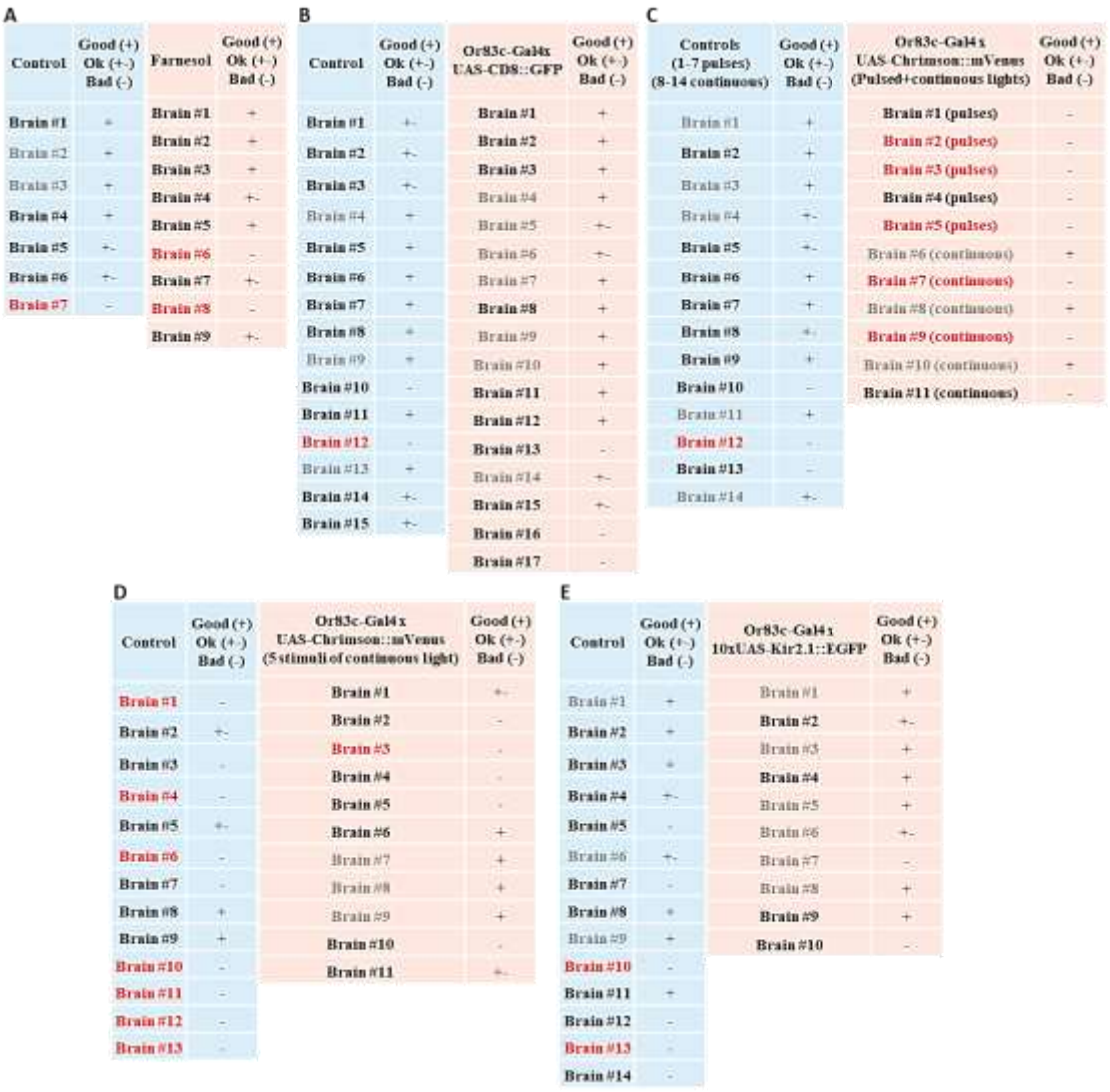

Fig. 7 – Evaluation of brain dissection quality by one of the most experienced researchers. This qualitative visual evaluation [Good (+), Ok (+-) and Bad (-)] took into account the quality of the dissection in structural and anatomical terms of the brains, with special emphasis on the region of interest (antennal lobes). All brains highlighted in gray and red (bad brains) were scored differently by the researchers. There may be some confounding factors, such as the quality of staining, the confocal ZProjections, the penetration of the laser into the neuronal tissue and proper mounting on the slide.